MASSACHUSETTS INSTITUTE OF TECHNOLOGY

LINCOLN LABORATORY

INFLUENCE OF THE EARTH'S SURFACE ON RADAR

N. I. DURLACH

Group 42

TECHNICAL REPORT 373

18 JANUARY 1965

LEXINGTON MASSACHUSETTS

ABSTRACT

This report provides radar designers with background information on how the idealized free-space radar theory must be modified to take account of reflections from the earth's surface. It is primarily concerned with problems that arise in designing systems that are airborne and contains discussions of the following topics: effects of reflections from the earth on the signal received from an elevated target, implications of these effects for detection and parameter estimation, effects of surface roughness, techniques for the reduction of clutter, scattering from the ocean, and spherical-earth geometry.

Accepted for the Air Force
Stanley J. Wisniewski
Lt Colonel, USAF
Chief, Lincoln Laboratory Office

TABLE OF CONTENTS

	Abstract	iii
	Introduction	1
I.	INFLUENCE OF A SMOOTH EARTH	5
	A. Vertical-Plane Coordinates	5
	B. Complex Spherical-Earth Reflection Coefficients	6
	C. Description of Received Signal in Frequency Domain	10
	D. Description of Received Signal in Time Domain	13
	E. Relations Between Free-Space Signal and Earth-Modification Factor	14
	F. Modifications in Received Signal Due to Motion of Antenna and/or Target	16
	G. Total Received Energy and Energy Coverage Diagram	19
	H. Implications for Detection and Parameter Estimation	20
	I. Generalized Static Equation and Generalized Approach to Effects of Translation-Motion	23
II.	GENERAL REMARKS ON INFLUENCE OF A ROUGH EARTH	26
	A. Basic Effects of Surface Roughness	26
	B. "State of the Art"	27
	C. Elementary Properties of Earth Clutter	28
	D. Techniques for Reduction of Earth Clutter	29
III.	SCATTERING FROM THE OCEAN	36
	A. Experimental Data on Sea Clutter	39
	B. Concepts for Interpreting Experimental Data on Sea Clutter	51
	C. Forward Scattering from the Ocean	56
IV.	SPHERICAL-EARTH FORMULAS	60
	A. Functions to be Computed	61
	B. Functions $R_o(h_1, h_2)$, $\delta(h_1, R)$, $\alpha(h_1, R)$, $\gamma_i(h_1, h_2, R)$, and $A(h_1, R)$	62
	C. Functions $\Delta(h_1, h_2, R)$, $\vartheta(h_1, h_2, R)$, $\beta_i(h_1, h_2, R)$, and $\mathfrak{D}(h_1, h_2, R)$	63
	D. Functions $h_2(h_1, \gamma_1, R)$ and $h_2(h_1, \Delta, R)$	68

INFLUENCE OF THE EARTH'S SURFACE ON RADAR†

INTRODUCTION

The purpose of this report is to provide radar designers with background material on how the idealized free-space radar theory must be modified to take account of the earth's surface. This surface constitutes an important component of the propagation medium and plays a significant role in determining the extent to which a given design will prove successful.

For the radar designer, the presence of the earth's surface has two important implications. First, due to the convexity of the surface, for any given height of the radar antenna, a portion of the space above the earth will lie in shadow. Second, due to the reflective properties of the surface materials, a certain amount of the energy incident on the surface will be reflected and scattered back into the space above it. Both effects must be evaluated in order to predict a radar's performance.

Assuming that the earth exists in an atmosphere with a constant index of refraction (e.g., free space) so that electromagnetic rays can be drawn as straight lines, one can represent the problem imposed by the earth's convexity as shown in Fig. 1. When a target is above the horizon

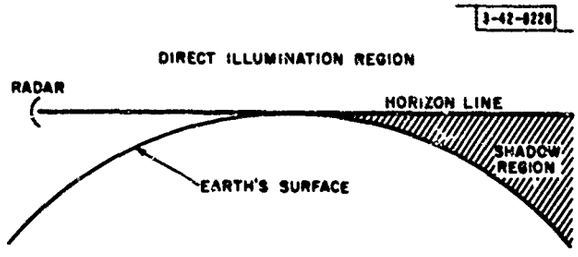

Fig. 1. Horizon limitation.

line, it will be illuminated directly. When it is below the horizon line, it will be illuminated only to the extent that diffraction takes place. Thus, if the function of the radar requires good coverage near the surface of the earth, one must either (1) try to raise the height of the radar antenna, thus extending the direct illumination region, or (2) try to take advantage of diffraction. Each of these techniques for extending low altitude coverage has certain advantages and disadvantages, and each imposes strong constraints on the choice of radar parameters. For example, to make use of diffraction, one must go to very low frequencies. On the other hand, elevating the antenna an appreciable amount limits the size of the antenna that can be employed.

†This report was originally intended for inclusion in a book. It is issued as a Technical Report because the publication of this book has been unavoidably delayed. The information on which this report is based was obtained prior to 1962 and no attempt has been made to update it.

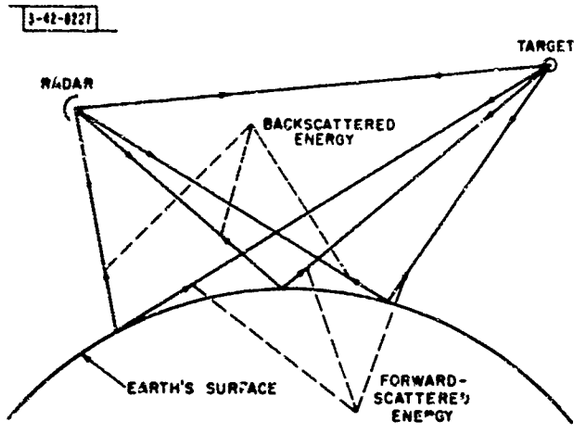

Fig. 2. Forward- and backscattered energy.

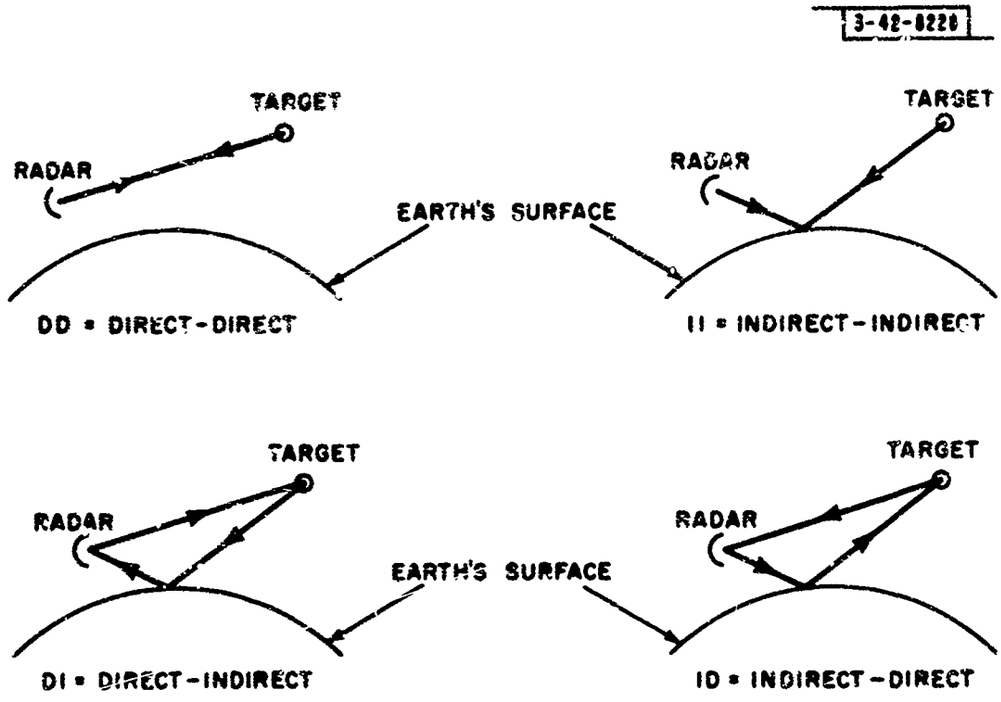

Fig. 3. Four round-trip paths.

If one takes into account the variability of the index of refraction, then a third possibility arises: (3) one can attempt to extend the low altitude coverage by making use of atmospheric bending and scattering. This again implies strong limitations on the choice of radar parameters inasmuch as one must choose parameters for which there is sufficient bending and scattering. In general, which of these techniques will be most useful will depend on the specific function for which the radar is being designed. In this report, it will be assumed that the radar's function is to detect and track aircraft at the greatest possible distances, and that these aircraft may be flying at low altitudes as well as high ones. For this function, the solution which has been found most successful is that of elevating the antenna, and it is this type of radar toward which the present discussion will be oriented. More specifically, the discussion will be limited to considerations which arise in designing an airborne early-warning and control radar, and to phenomena which occur inside the direct-illumination region. Only those problems will be considered which involve energy transmitted by the radar itself (as opposed to energy transmitted by outside sources), and special consideration will be given to the case in which the radar and target are operating over water as opposed to land. It will also be assumed that atmospheric conditions are such that the bending of the electromagnetic rays due to variations in the index of refraction can be rectified by using an equivalent earth's radius.

Within the direct illumination region, the most important phenomenon to be considered in connection with the earth's surface is that of scattering.† For many earth surface materials and many frequencies, only a small portion of the incident energy will be absorbed and most of it will be scattered back into the space above the earth. It is the existence of this scattered energy that has caused the direct-illumination region to be referred to as the "interference region." In general, at any given point on the earth's surface, this scattered energy will propagate in all directions. The only directions of importance to the radar, however, are the direction toward the target (the "forward-scattered energy") and the direction back to the radar antenna (the "backscattered energy" or "clutter"). A schematic illustration of the forward- and backscattered energy is shown in Fig. 2. As far as obtaining information on the aircraft target is concerned, whereas the forward-scattered energy is in many ways an advantage for the radar, the backscattered energy, being a form of interference, is inherently a disadvantage. The relative amounts of energy scattered backward and forward will depend upon the detailed structure of the region over which the radar is operating, the parameters of the radar system, and the geometry.

Assuming that the surface is perfectly smooth, one finds that the effect of the surface on the target signal is to create four possible round-trip paths over which the energy can travel from radar to target and back to the radar. These four paths are illustrated in Fig. 3. Making use of images (and assuming for simplicity that the earth is flat), one can interpret these four component target signals and the smooth-earth clutter signal as shown in Fig. 4. According to this interpretation, the situation is similar to one in which there are two targets and two sources in free space with the targets and sources constituting slaved pairs and with no scattering between targets. As the surface becomes rougher, the images tend to spread out.

For certain purposes, the roles of the forward- and backscattered energy in modifying the received signal can best be visualized in terms of the filter concept. Letting $X(\omega)$ and $Y(\omega)$ be the complex spectra of the transmitted and received signals, and assuming that the system consisting of the radar antenna and surrounding space can be regarded as a fixed linear filter with a transfer function $S(\omega)$, one can relate $Y(\omega)$ to $X(\omega)$ by the equation $Y(\omega) = S(\omega)\, X(\omega)$ (see Fig. 5).

† Throughout this report, the word "scattering" will be used to refer to all energy which is not absorbed.

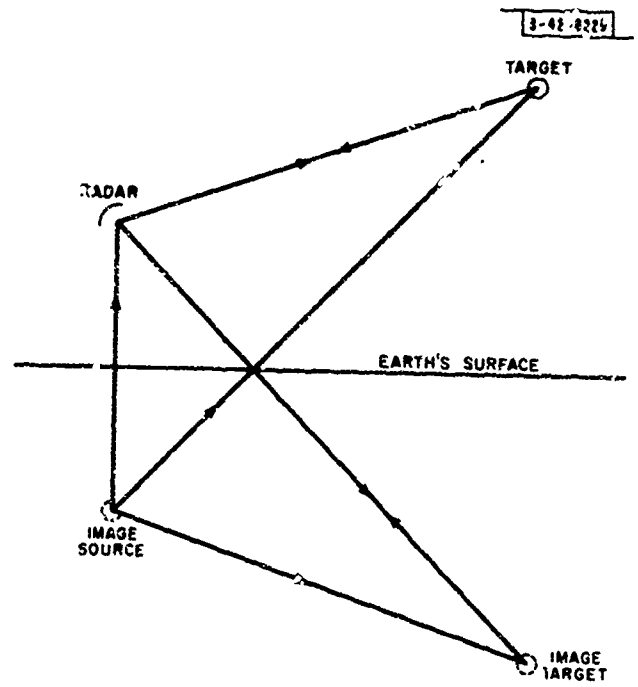

Fig. 4. Free-space interpretation.

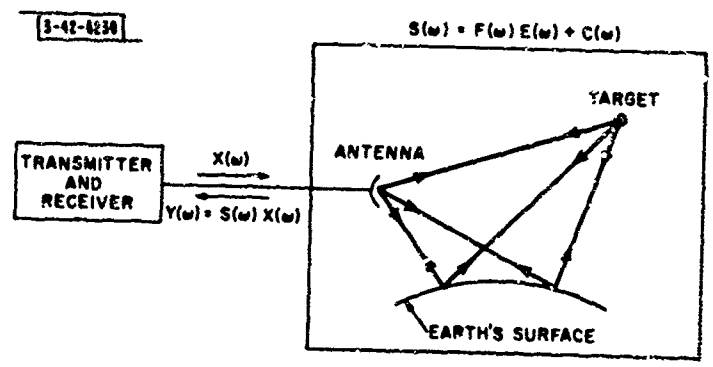

Fig. 5. Space filter.

Letting $F(\omega)$ be the space filter under the assumption that there is no earth present, and $C(\omega)$ the space filter under the assumption that there is no target present, one can write $S(\omega) = F(\omega)\,E(\omega) + C(\omega)$, where $E(\omega)$ is the earth-modification factor for the target signal. In this language, the introduction of the earth into the radar problem is equivalent to the filter transformation $F(\omega) \to F(\omega)\,E(\omega) + C(\omega)$, and the task of describing the influence of the earth on the received signal $Y(\omega)$ is equivalent to the task of describing the functions $E(\omega)$ and $C(\omega)$.

The discussion in this report will be divided into four main sections: I. Influence of a Smooth Earth; II. General Remarks on Influence of a Rough Earth; III. Scattering From the Ocean; and IV. Spherical-Earth Formulas. The main task in Sec. I will be to show how the free-space radar equation must be modified to take into account the presence of the earth's surface under the idealized assumption of specular reflection, and to point out some of the implications of this modification for various radar functions such as detection and height-finding. Inasmuch as the interference caused by the clutter signal in the smooth-earth case has no importance for the airborne early-warning problem (the source of the clutter signal being confined to the specular point directly beneath the radar), the discussion in Sec. I will be devoted exclusively to the target signal. In Sec. II, the assumption that the earth is smooth will be eliminated, and the effects of surface roughness on the radar-design problem will be considered without reference to the particular scattering characteristics of the rough surface. In Sec. III, the rough surface will be specialized to that of the ocean and a detailed description will be given of the scattering results for this surface. In both Secs. II and III, attention will be focused on the problem of backscattering, the modifications of the forward-scattered energy being considered only very briefly. Finally, Sec. IV will contain a list of formulas relating the various geometric variables whose values are needed in order to predict a radar's performance once the physical parameters of the situation have been adequately determined.

I. INFLUENCE OF A SMOOTH EARTH

As already stated, if it is assumed that the earth's surface is a smooth, homogeneous sphere, the total returned signal from an elevated target will consist of the sum of four component signals (DD, II, DI, ID), each of which corresponds to a particular round-trip path from radar to target and back to the radar again. This signal will depend upon (a) the transmitted signal, (b) the radar antenna pattern, (c) the target cross-section pattern, (d) the reflective properties of the surface, and (e) the relative locations, orientations, and motions of the antenna, target, and earth.

A. Vertical-Plane Coordinates

If the orientations of the antenna and target are held constant with respect to some fixed, arbitrary reference system, and the locations of the antenna and target are constrained to a fixed vertical plane, all the geometric variables entering into the equation for the received signal will be determined by the locations of the antenna and target within this vertical plane. Ordinarily, in order to specify these locations, one would need to use four coordinates -- two for the antenna and two for the target. However, since it has been assumed that the earth's surface is a smooth, homogeneous sphere, the returned signal will be independent of the particular portion of the surface over which the radar is operating and will thus be determined by only three coordinates. Four vertical-plane coordinate systems which are of frequent use

(see Fig. 6) are (h, H, d), (h, H, R), (h, γ, R), and (h, Δ, R), where h = radar height, H = target height, d = ground distance between radar and target, R = length of direct path, γ = angle between direct path and horizontal at radar, and Δ = pathlength difference between direct and indirect paths. Whereas the first of these systems is the most natural one from the vantage point of the earth's surface, the third and fourth are the most natural from the vantage point of the radar: all the variables h, γ, Δ, and R can be measured directly in terms of the signal returned from the target.

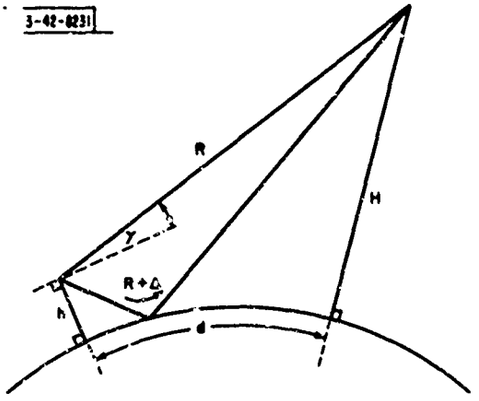

Fig. 6. Vertical-plane coordinates.

Assuming for purposes of illustration that the earth is flat, one has

$$R = [d^2 + (H-h)^2]^{1/2} \qquad \Delta = (R^2 + 4hH)^{1/2} - R$$

$$\gamma = \sin^{-1}\left(\frac{H-h}{R}\right) \qquad \frac{H^2}{(\Delta/2)^2} - \frac{d^2}{h^2 - (\Delta/2)^2} = 1 \quad . \tag{1}$$

Assuming h/d and H/d are small, one obtains the approximations

$$R = d \qquad \Delta = \frac{2hH}{R}$$

$$\gamma = \frac{H-h}{R} \qquad H = \frac{\Delta/2}{[h^2 - (\Delta/2)^2]^{1/2}}\, d \quad . \tag{2}$$

Spherical-earth relationships for these variables, as well as other variables, can be found in Sec. IV.

B. Complex Spherical-Earth Reflection Coefficients

In order to give a quantitative description of the component signals along the paths II, DI, and ID (see Fig. 3), it is necessary to compute the effect of the reflection process on the amplitude and phase of the incident rays. In general, the electromagnetic properties of the air and earth that need to be evaluated for this computation are the permittivity ϵ, the conductivity σ, and the permeability μ. In the following discussion, it will be assumed that μ, ϵ, and σ for the air are the same as for free space, and that μ for the earth is the same as for free space.

1 Plane Reflection Coefficients

Assume that the incident wave is a plane wave of wavelength γ and that the earth is flat. For any vector $\vec{z}$, let

$h(\vec{z})$ - component of $\vec{z}$ normal to plane of incidence (the plane normal to the reflecting surface which contains the incident ray)

$v(\vec{z})$ component of $\vec{z}$ in plane of incidence

$\tilde{h}\,[v(\vec{z})]$ = component of $v(\vec{z})$ parallel to reflecting surface

$\tilde{v}\,[v(\vec{z})]$ = component of $v(\vec{z})$ normal to reflecting surface.

Also, let

δ = complex dielectric constant

$= \frac{\epsilon}{\epsilon_0} - i60\lambda\sigma$ where ϵ and σ are evaluated for the earth surface material, ϵ_0 is the value of ϵ for free space, and λ is given in meters and σ in mhos/meter

$\vec{n}$ = unit propagation vector

ψ = grazing angle

$\vec{E}$ - electric field vector

$\vec{H}$ - magnetic field vector

Γ_h = reflection coefficient for horizontal polarization

Γ_v = reflection coefficient for vertical polarization.

Using the subscripts 1 and 2 to denote the incident and reflected waves, one can illustrate the cases of horizontal and vertical polarizations as shown in Fig. 7(a-b). Horizontal polarization is defined by the condition $h(\vec{E}_1) = \vec{E}_1$ and vertical polarization by $v(\vec{E}_1) = \vec{E}_1$. Making use of the above definitions and assumptions, one can show that the reflected wave will also be a plane wave of wavelength λ and that

$$\psi_1 = \psi_2$$

$$h(\vec{E}_2) = \Gamma_h(\vec{E}_1) \qquad h(\vec{H}_2) = \Gamma_v h(\vec{H}_1)$$

$$v(\vec{E}_2) = -\Gamma_v\{\vec{n}_2 \times [\vec{n}_1 \times v(\vec{E}_1)]\} \qquad v(\vec{H}_2) = -\Gamma_h\{\vec{n}_2 \times [\vec{n}_1 \times v(\vec{H}_1)]\}$$

$$\Gamma_h = \frac{\sin\psi - (\delta - \cos^2\psi)^{1/2}}{\sin\psi + (\delta - \cos^2\psi)^{1/2}} = \frac{h(\vec{E}_2)}{h(\vec{E}_1)} = \frac{\tilde{v}\,[v(\vec{H}_2)]}{\tilde{v}\,[v(\vec{H}_1)]} = \frac{-\tilde{h}\,[v(\vec{H}_2)]}{\tilde{h}\,[v(\vec{H}_1)]}$$

$$\Gamma_v = \frac{\delta\sin\psi - (\delta - \cos^2\psi)^{1/2}}{\delta\sin\psi + (\delta - \cos^2\psi)^{1/2}} = \frac{h(\vec{H}_2)}{h(\vec{H}_1)} = \frac{\tilde{v}\,[v(\vec{E}_2)]}{\tilde{v}\,[v(\vec{E}_1)]} = \frac{-\tilde{h}\,[v(\vec{E}_2)]}{\tilde{h}\,[v(\vec{E}_1)]} \quad . \tag{3}$$

Note that if $\psi = \psi_1 = \psi_2$ is small, then $\tilde{v}v = v$ so that $v(\vec{E}_2) = \Gamma_v\, v(\vec{E}_1)$ and $v(\vec{H}_2) = \Gamma_h\, v(\vec{H}_1)$. If $|\delta| \gg 1$ (which is usually the case except for very dry ground), the formulas for Γ_h and Γ_v reduce to

$$\Gamma_h = \frac{\sin\psi - \delta^{1/2}}{\sin\psi + \delta^{1/2}} \qquad \Gamma_v = \frac{\delta^{1/2}\sin\psi - 1}{\delta^{1/2}\sin\psi + 1} \quad . \tag{4}$$

Note also that

$$\lim_{\psi\to 0} \Gamma_h = \lim_{\psi\to 0} \Gamma_v = -1 \qquad \text{when } \delta < \infty$$

$$\lim_{\delta\to\infty} \Gamma_h = -1 \quad \text{and} \quad \lim_{\delta\to\infty} \Gamma_v = 1 \quad \text{when } \psi > 0 \quad . \tag{5}$$

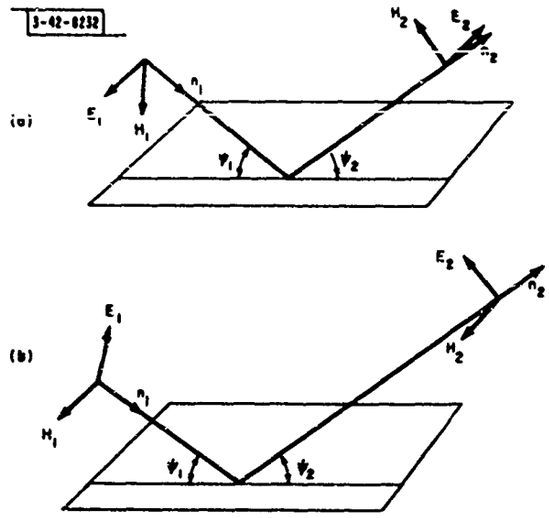

Fig. 7. Reflection of a plane wave from a plane surface: (a) horizontal polarization, (b) vertical polarization.

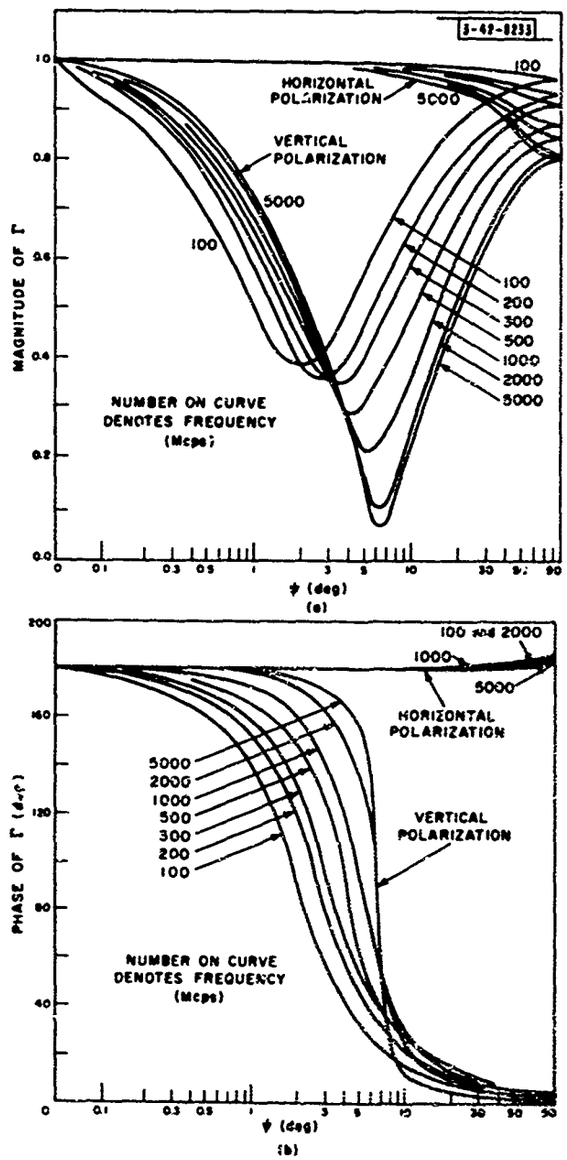

Fig. 8. Plane reflection coefficients for smooth sea water: (a) magnitude, (b) phase. (From Reed and Russell.[1])

The variations of Γ_h and Γ_v with frequency and grazing angle for the case of sea water are shown in Fig. 8(a-b). For a detailed discussion of these plane reflection coefficients, the reader is referred to Stratton.[2]

2. Divergence Factor

In the above equations for the reflection coefficients, it is assumed that a plane wave is incident on a plane surface. A more realistic assumption for propagation over the earth is that a spherical wave is incident on a spherical surface. A second-order "geometrical-optical" approximation has been worked out for this case by van der Pol and Bremmer.[3] They have shown that the reflection coefficient ρ for this case can be approximated by

$$\rho = \mathfrak{D}\Gamma \tag{6}$$

where $\mathfrak{D}$, the divergence, is a purely geometric factor which describes the extra divergence of a beam of rays due to the reflection from a spherical surface. More specifically,

$$\mathfrak{D} = \lim_{\Omega \to 0} \left(\frac{Q}{Q'}\right)^{1/2} \tag{7}$$

where Q' and Q are the corresponding curved and flat earth cross sections of the reflected beam (see Fig. 9), and Ω is the solid angle subtended by Q. Letting a denote the equivalent earth's radius, one notes that

$$\begin{aligned} &0 \leq \mathfrak{D} \leq 1 \qquad \text{for all } h,\ H,\ \psi,\ a \\ &\mathfrak{D} \to 1 \text{ as } a \to \infty \quad \text{or} \quad h \to 0 \quad \text{or} \quad H \to 0 \\ &\mathfrak{D} \to 0 \text{ as } \psi \to 0 \quad . \end{aligned} \tag{8}$$

Unless ψ is quite small, for most practical purposes, $\mathfrak{D}$ can be approximated by unity. Explicit formulas for computing $\mathfrak{D}$ can be found in Sec. IV.

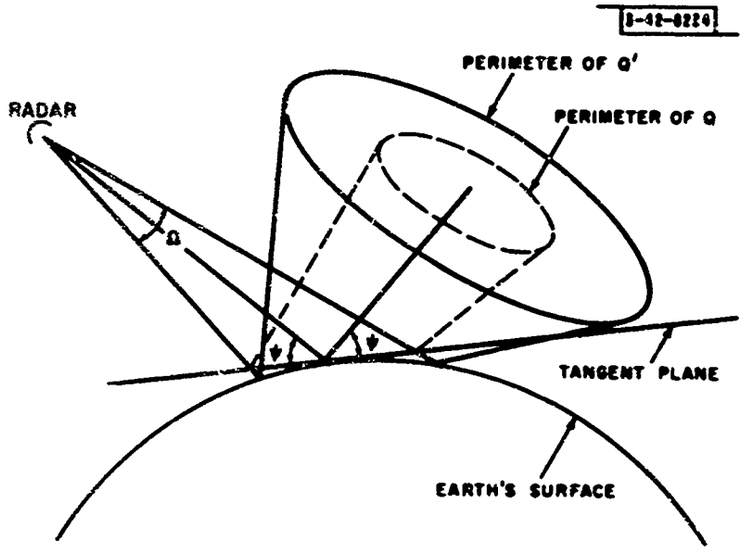

Fig. 9. Divergence factor.

C. Description of Received Signal in Frequency Domain

Assume for simplicity that (1) the transmitting and receiving antennas are identical; (2) the polarization of the antenna is pure-horizontal or pure-vertical; (3) the antenna and target are motionless; (4) the hypothesis of the reciprocity theorem is satisfied.† Let

t = time

ω = angular frequency

c = velocity of light

ℓ = direct path D or indirect path I

$g(\ell)$ = complex amplitude gain of antenna evaluated along ℓ

$s(\ell_1, \ell_2)$ = complex scattering length of target evaluated for incident wave along ℓ_1 and reflected wave along ℓ_2 (the target cross-section σ is related to s by $\sigma = 4\pi|s|^2$)

X = complex coefficient of $\exp(i\omega t)$ on transmission

Y = complex coefficient of $\exp(i\omega t)$ on reception

Y_F = free-space component of Y (i.e., component of Y resulting from path DD)

$F = Y_F/X$ = free-space factor

$E = Y/Y_F$ = earth-modification factor.

The quantities g, s, X, Y, Y_F, F, E, and ρ are all functions of the frequency ω, and all but X are also functions of the geometry. In order to simplify the notation, these dependencies will be made explicit only where necessary. Assume also that (5) $s(D, D)\, s(I, I) = s^2(D, I)$. [This assumption will be sure to be satisfied provided the angle between D and I at the target is small with respect to the angular variations in the target scattering length, for then, approximately, $s(I, I) = s(D, D) = s(D, I)$.]

Applying assumptions (1) through (5) (and assuming a reference impedance level of one ohm so that the power is given by the square of the amplitude of the voltage), one can show that

$$Y = XFE = Y_F E \tag{9}$$

where

$$F = \frac{Z}{\omega R^2} \exp\left(-\frac{2i\omega R}{c}\right) \qquad E = \left[1 + K \exp\left(-\frac{i\omega\Delta}{c}\right)\right]^2$$

and Z and K are defined by

$$Z = \frac{c}{2} g^2(D)\, s(D, D) \qquad K = \frac{R\, \rho\, g(I)\, s(D, I)}{(R + \Delta)\, g(D)\, s(D, D)} .$$

The term $K \exp(-i\omega\Delta/c)$ occurring in E is nothing more than the ratio of the complex signals corresponding to the paths I and D. The DD component Y_F of Y is obtained from the term 1 in E, the II component from the term $[K \exp(-i\omega\Delta/c)]^2$, and the DI and ID components (which are equal) from the term $2K \exp(-i\omega\Delta/c)$. When $E = 1$ (i.e., $K = 0$), Y reduces to the free-space equation $Y = Y_F$. The precise role of each of the assumptions (1) through (5) in obtaining the above equation will become apparent in Sec. I-I where this equation will be generalized.

Writing any complex number z as $|z| \exp(i\varphi_z)$ and defining q by $q = \varphi_K - \omega\Delta/c$, one finds that the quantities $|Y|^2$ and φ_Y are given by

---

†For a discussion of the reciprocity theorem, see, for example, Schelkunoff and Friis.[4]

$$|Y|^2 = |X|^2 \, |F|^2 \, |E|^2 \tag{10}$$

where

$$|F|^2 = \frac{|Z|^2}{\omega^2 R^4} \qquad |E|^2 = (1 + |K|^2 + 2\,|K|\cos q)^2$$

and

$$\varphi_Y = \varphi_X + \varphi_F + \varphi_E \tag{11}$$

where

$$\varphi_F = \varphi_Z - \frac{2\omega R}{c} \qquad \varphi_E = 2\tan^{-1}\left(\frac{|K|\sin q}{1 + |K|\cos q}\right) .$$

Assume now that the physical properties of the antenna, target, and earth, and the orientations of the antenna and target, are held fixed, and that the locations of the antenna and target are constrained to a fixed vertical plane. With this assumption, all the quantities entering into the equation for Y can be regarded as functions of h, R, Δ, and ω. If h, R, and Δ are held fixed and ω is allowed to vary, the above equations constitute a description of the frequency spectrum of the received signal for the given h, R, and Δ. Equation (9) gives the complex spectrum $Y(\omega)$, Eq. (10) gives the energy spectrum $|Y(\omega)|^2$, and Eq. (11) gives the phase spectrum $\varphi_Y(\omega)$. If ω is held fixed and h, R, and Δ are allowed to vary, the above equations constitute a description of how the received signal depends upon the positions of the antenna and target within the vertical plane for the given ω.

Assume in addition that attention is confined to a region of (h, R, Δ, ω) space in which $|K(h, R, \Delta, \omega)|$ varies slowly in comparison to $\cos[q(h, R, \Delta, \omega)]$. Within this region, the earth-modification factor E will be locally periodic in q of period 2π. Graphs of $|E(q)|^2$ and $\varphi_E(q)$ for $-\pi \leq q \leq \pi$ and various fixed values of $|K|$ are shown in Fig. 10(a-b). It is easy to show that

$$\begin{aligned}
&\max |E(q)|^2 = (1 + |K|)^4 \quad \text{occurs at } q = 2n\pi \\
&\min |E(q)|^2 = (1 - |K|)^4 \quad \text{occurs at } q = (2n + 1)\pi \\
&\text{ave } |E(q)|^2 = 1 + |K|^4 + 4\,|K|^2 \\
&|E(q)|^2 = 1 \quad \text{and} \quad \varphi_E(q) = 0 \quad \text{when } |K| = 0 \\
&|E(q)|^2 = 16\cos^4(q/2) \quad \text{and} \quad \varphi_E(q) = q \quad \text{when } |K| = 1 \\
&|E(q)|^2 \to |K|^4 \quad \text{and} \quad \varphi_E(q) \to 2q \quad \text{when } |K| \to \infty \quad .
\end{aligned} \tag{12}$$

If attention is further confined to a region of (h, R, Δ, ω) space in which $\varphi_K(h, R, \Delta, \omega)$ is slowly varying in comparison to $\omega\Delta/c$, then q, and therefore E, will be locally symmetric in ω and Δ. This implies that ω and Δ play dual roles in the modification of the free-space signal imposed by the presence of the earth. (They do not, of course, play dual roles in the total received signal Y since they do not occur symmetrically in Y_F.) Letting Δ remain fixed, E is periodic in ω of period $2\pi c/\Delta$ with a phase determined by $\varphi_K(\Delta)$. Letting ω remain fixed, E is periodic in Δ of period $2\pi c/\omega$ with a phase determined by $\varphi_K(\omega)$. This duality between ω and Δ will be referred to again below.

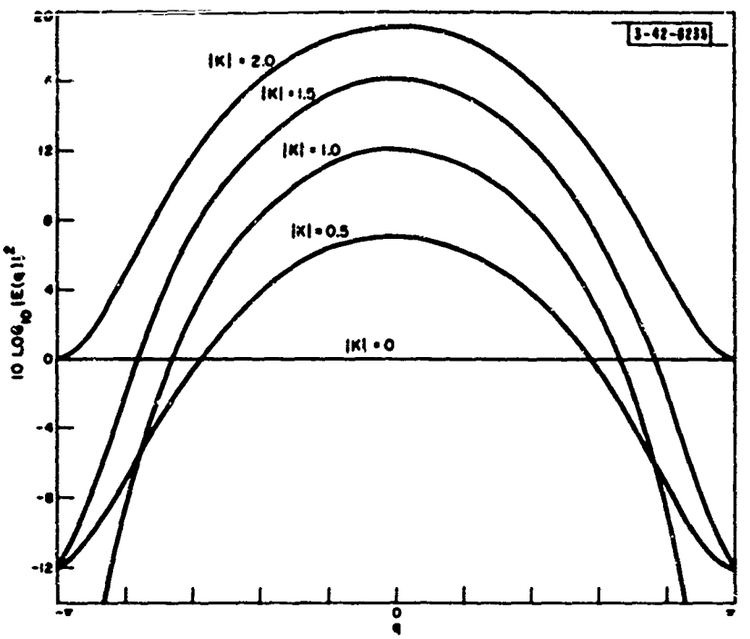

(a)

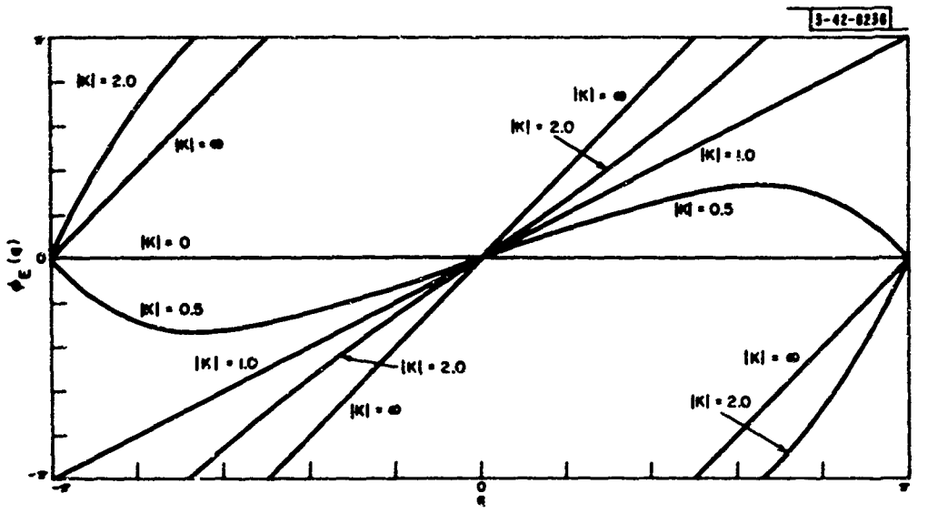

(b)

Fig. 10. Earth-modification factor E: (a) $|E(q)|^2$, (b) $\phi_E(q)$.

One important case in which K is approximately constant over a sizeable region of (h, R, Δ, ω) space, and the equation for E becomes particularly simple, is that in which (1) the polarization is horizontal, (2) the reflecting surface consists of sea water, and (3) the antenna and target both have broad vertical patterns. In this case, for a fairly large region of (h, R, Δ, ω) space, one has, approximately, $\rho = -1$, $R/(R + \Delta) = 1$, $g(I)/g(D) = 1$, and $s(D, I)/s(D, D) = 1$. Thus $K = -1$ and

$$E = \left[1 - \exp\left(-\frac{i\omega\Delta}{c}\right)\right]^2$$

$$|E|^2 = 16 \sin^4\left(\frac{\omega\Delta}{2c}\right) \qquad \varphi_E = -\frac{\omega\Delta}{c} \quad . \tag{13}$$

D. Description of Received Signal in Time Domain

Let $x(t)$, $y(t)$, and $y_f(t)$ be the time-domain counterparts of $X(\omega)$, $Y(\omega)$, and $Y_F(\omega)$; $\bar{x}(t)$, $\bar{y}(t)$, and $\bar{y}_f(t)$ be the complex representations of $x(t)$, $y(t)$, and $y_f(t)$; $\tilde{x}(t)$, $\tilde{y}(t)$, and $\tilde{y}_f(t)$ be the complex modulations of $x(t)$, $y(t)$, and $y_f(t)$ around ω_o. Thus,

$$y(t) = \frac{1}{2\pi}\int_{-\infty}^{\infty} Y(\omega)\exp(i\omega t)\, d\omega$$

$$\bar{y}(t) = \frac{1}{2\pi}\int_{0}^{\infty} Y(\omega)\exp(i\omega t)\, d\omega$$

$$\tilde{y}(t) = \frac{1}{2\pi}\int_{0}^{\infty} Y(\omega)\exp[i(\omega - \omega_o)t]\, d\omega$$

$$\bar{y}(t) = \tilde{y}(t)\exp(i\omega_o t)$$

$$y(t) = 2\,\mathrm{Re}\,[\bar{y}(t)] = 2\,|\tilde{y}(t)|\cos[\omega_o t + \varphi_{\tilde{y}}(t)] \tag{14}$$

and similarly for $x(t)$ and $y_f(t)$. Assume now that $Z(\omega)/\omega$ and $K(\omega)$ are constant across the frequency span of $X(\omega)$. Writing these constants as Z/ω_o and K, and making use of Eqs. (9) and (14), one obtains

$$\bar{y}(t) = \frac{Z}{\omega_o R^2}\left[\bar{x}\left(t - \frac{2R}{c}\right) + K^2\,\bar{x}\left(t - \frac{2R}{c} - \frac{2\Delta}{c}\right) + 2K\,\bar{x}\left(t - \frac{2R}{c} - \frac{\Delta}{c}\right)\right]$$

$$\tilde{y}(t) = \frac{Z}{\omega_o R^2}\exp\left(-\frac{2i\omega_o R}{c}\right)\left[\tilde{x}\left(t - \frac{2R}{c}\right) + K^2\,\tilde{x}\left(t - \frac{2R}{c} - \frac{2\Delta}{c}\right)\exp\left(-\frac{2i\omega_o\Delta}{c}\right)\right.$$

$$\left. + 2K\,\tilde{x}\left(t - \frac{2R}{c} - \frac{\Delta}{c}\right)\exp\left(-\frac{i\omega_o\Delta}{c}\right)\right] \quad . \tag{15}$$

The equivalent free-space equations [i.e., the equations for $\bar{y}_f(t)$ and $\tilde{y}_f(t)$] can be obtained from these equations by setting $K = 0$. If Δ is sufficiently small to allow one to ignore its effect on the modulation function $\tilde{x}(t)$ [i.e., $\exp(-i\omega\Delta/c)$ is constant across the frequency span of $X(\omega)$], then the equation for $\tilde{y}(t)$ can be simplified to

$$\tilde{y}(t) = \tilde{x}\left(t - \frac{2R}{c}\right) F(\omega_o)\, E(\omega_o) \quad . \tag{16}$$

The complex time-domain equivalents of the equations $Y(\omega) = Y_F(\omega)\, E(\omega)$ and $Y_F(\omega) = X(\omega)\, F(\omega)$ of Sec. I-C are given by the convolution products

$$\bar{y}(t) = \bar{y}_f(t) \cdot \bar{e}(t) \qquad \bar{y}_f(t) = \bar{x}(t) \cdot \bar{f}(t) \tag{17}$$

where $\bar{f}(t)$ and $\bar{e}(t)$ are the complex representations of the inverse transforms of $F(\omega)$ and $E(\omega)$. Insofar as their effects on $\bar{y}(t)$ and $\bar{y}_f(t)$ are concerned, $\bar{f}(t)$ and $\bar{e}(t)$ can be approximated by

$$\bar{f}(t) = \frac{Z}{\omega_o R^2}\, \delta\left(t - \frac{2R}{c}\right)$$

$$\bar{e}(t) = \delta(t) + K^2\, \delta\left(t - \frac{2\Delta}{c}\right) + 2K\, \delta\left(t - \frac{\Delta}{c}\right) \tag{18}$$

where $\delta(t)$ is the Dirac function.

Letting $A_{\bar{x}}(\tau)$ and $A_{\bar{y}}(\tau)$ denote the complex autocorrelation functions

$$A_{\bar{x}}(\tau) = \int_{-\infty}^{\infty} \bar{x}^*(t)\, \bar{x}(t+\tau)\, dt = \frac{1}{2\pi} \int_0^{\infty} |X(\omega)|^2 \exp(i\omega\tau)\, d\omega$$

$$A_{\bar{y}}(\tau) = \int_{-\infty}^{\infty} \bar{y}^*(t)\, \bar{y}(t+\tau)\, dt = \frac{1}{2\pi} \int_0^{\infty} |Y(\omega)|^2 \exp(i\omega\tau)\, d\omega \tag{19}$$

one can show that

$$A_{\bar{y}}(\tau) = \frac{|Z|^2}{\omega_o^2 R^4} \left[(1 + |K|^4 + 4|K|^2)\, A_{\bar{x}}(\tau) + K^2\, A_{\bar{x}}\left(\tau - \frac{2\Delta}{c}\right) + K^{*2}\, A_{\bar{x}}\left(\tau + \frac{2\Delta}{c}\right)\right.$$

$$\left. + 2K(1 + |K|^2)\, A_{\bar{x}}\left(\tau - \frac{\Delta}{c}\right) + 2K^*(1 + |K|^2)\, A_{\bar{x}}\left(\tau + \frac{\Delta}{c}\right)\right] . \tag{20}$$

The autocorrelation function $A_{\bar{y}}(\tau)$ is the complex time-domain representation of the output of a filter which is matched to the earth-modified input signal. The autocorrelation functions $A_y(\tau)$ and $A_{\tilde{y}}(\tau)$ [defined in a manner similar to $A_{\bar{y}}(\tau)$] are related to $A_{\bar{y}}(\tau)$ by the formulas

$$A_{\bar{y}}(\tau) = A_{\tilde{y}}(\tau) \exp(i\omega_o\tau) \qquad A_y(\tau) = 2\, \mathrm{Re}\, [A_{\bar{y}}(\tau)] . \tag{21}$$

E. Relations Between Free-Space Signal and Earth-Modification Factor

Let β denote the bandwidth of $Y_F(\omega)$ and T the duration of $y_f(t)$. To the extent that the target is a simple point target (i.e., the impulse response of the target is an impulse), β and T will, in most practical systems, be determined primarily by the transmitted signal X. Assuming that $K(\omega)$ is slowly varying across β, one sees that $E(\omega)$ will be locally periodic in ω of period $2\pi c/\Delta$ and the number of cycles in β will be $\beta\Delta/2\pi c$. In the event that $\Delta\beta/2\pi c \ll 1$, $E(\omega)$ will be approximately constant across $Y_F(\omega)$ and the effect of the earth will be merely to multiply $Y_F(\omega)$ by a constant. If $\beta\Delta/2\pi c \gg 1$, then $E(\omega)$ will go through many cycles within β and the effect of the earth will be to change the shape of $Y_F(\omega)$. If $Y_F(\omega)$ is such that $\beta T \approx 2\pi$ [e.g., $y_f(t)$ is a simple pulsed sinusoid], the condition $\beta\Delta/2\pi c \gg 1$ is also sufficient to ensure that $E(\omega)$ will be varying much more quickly than $Y_F(\omega)$ within β. If, on the other hand, $\beta T \gg 2\pi$ and $Y_F(\omega)$ contains fine structure within β [e.g., $y_f(t)$ is a pulse train], then in order to ensure this result

one must impose the more stringent condition $(2\pi/T)\,\Delta/2\pi c = \Delta/Tc \gg 1$. Schematic illustrations of the two extreme cases $\beta\Delta/2\pi c \ll 1$ and $\Delta/Tc \gg 1$ are shown in Fig. 11(a-b). [A precise picture of a single cycle of $E(\omega)$ has already been presented in Fig. 10.] A slight change in Δ, i.e., a change of the order of $\lambda/2 = \pi c/\omega$, will have the effect of shifting the phase of the $E(\omega)$ modulation with respect to $Y_F(\omega)$. Whereas in the $\Delta/Tc \gg 1$ case, such a phase change will be relatively unimportant, in the $\beta\Delta/2\pi c \ll 1$ case, it may be extremely important. For example, if $|K|$ is close to unity and Δ is such that $Y_F(\omega)$ is centered on a minimum of $E(\omega)$ (often referred to as a "null"), then $Y(\omega)$ will be approximately zero. Inasmuch as $\Delta \to 0$ as the target approaches the horizon, the case $\beta\Delta/2\pi c \ll 1$ will always be important if the radar is required to provide coverage at low altitudes. Inasmuch as the maximum value of Δ is $2h$, whether or not the case $\Delta/Tc \gg 1$ can occur will depend on the parameter $2h/Tc$.

The above remarks on the relation of the free-space signal to the earth-modification factor have all been stated in the frequency domain. Corresponding remarks may be made in the time domain t (the conjugate of ω) and in the pathlength-difference domain Δ (the dual of ω). In the time domain, $y(t)$ will, in general, have five different sections corresponding to five different intervals on the time axis. Assuming for simplicity that $y_f(t)$ has a rectangular envelope, one can illustrate these sections for the two extreme cases $\Delta/Tc \ll 1$ and $\Delta/Tc \gg 1$ as shown in Fig. 12(a-b). Whether or not there will be any overlapping between the pulses corresponding to the paths DD, II, and (DI, ID) depends on whether $\Delta/Tc > 1$ or $\Delta/Tc < 1$. (If $1 < \Delta/Tc < 2$, then only two of the three pulses will overlap at any one time. If $\Delta/Tc < 1$, then all three will overlap.) The value of the envelope of $y(t)$ in the overlapping sections will depend upon the frequency and phase of the carrier. If $\beta\Delta/2\pi c \ll 1$, then $y(t)$ will consist almost entirely of the result of three overlapping pulses and the envelope will be constant during this overlap, its value depending upon the precise value of Δ. If $\Delta/Tc \gg 1$, then the pulses will be widely separated and the precise value of Δ will be unimportant. If $\beta T \gg 2\pi$ and conditions are such that $\beta\Delta/2\pi c \gg 1$ and $\Delta/Tc \ll 1$ simultaneously, then the pulses will be strongly overlapping and the envelope will be modulated in the overlapping section.

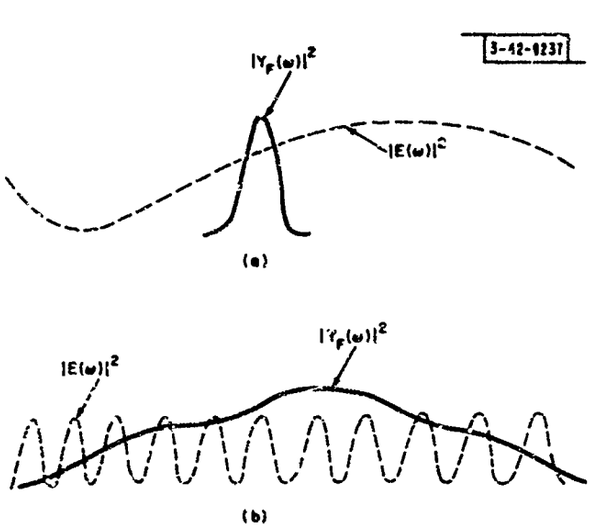

Fig. 11. Relation of $|Y_F(\omega)|^2$ to $|E(\omega)|^2$: (a) $\beta\Delta/2\pi c \ll 1$, (b) $\Delta/Tc \gg 1$.

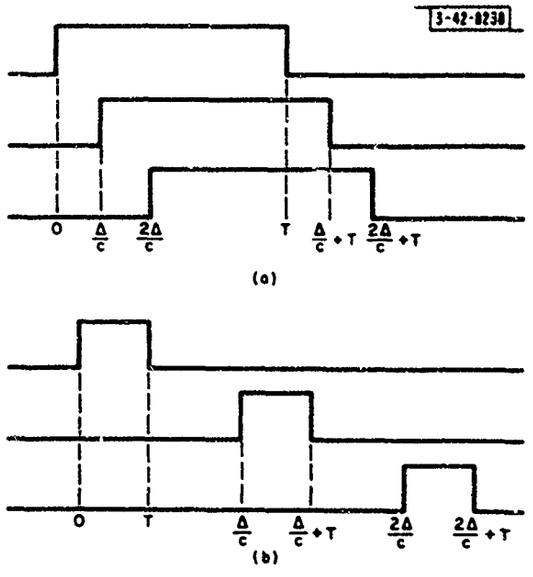

Fig. 12. Five sections of $y(t)$: (a) $\Delta/Tc \ll 1$, (b) $\Delta/Tc \gg 1$.

Turning attention to the dual domain Δ, assume now that h, R, and ω are held fixed and consider the relation between the functions $Y_F(\Delta)$ and $E(\Delta)$. The dual of the bandwidth β of $Y_F(\omega)$ is the width β' of $Y_F(\Delta)$, and the dual of the time duration T of $y_f(t)$ is the width T' of the Fourier transform of $Y_F(\Delta)$. Inasmuch as Y_F depends on Δ only through the product $g^2 s$, if s is assumed independent of Δ across the width of $g^2(\Delta)$, then β' gives the Δ-width of the square of the antenna function. Similarly, if g^2 is assumed independent of Δ across the width of $s(\Delta)$, then β' gives the Δ-width of the reflectivity pattern of the target. The dual of the assumption that $K(\omega)$ is slowly varying across β is the assumption that $K(\Delta)$ is slowly varying across β', and the duals of the parameters $\beta\Delta/2\pi c$ and Δ/Tc are the parameters $\beta'\omega/2\pi c$ and $\omega/T'c$. The parameter $\beta'\omega/2\pi c$ gives the number of cycles of $E(\Delta)$ in β', and the parameter $\omega/T'c$ determines the relation between the period of $E(\Delta)$ and the fine structure in $Y_F(\Delta)$.

Assume now for simplicity that the earth is flat and that h/H and H/R are sufficiently small to approximate Δ by $\Delta = 2h\gamma$ (see Sec. I-A). Ignoring the factor 2h, one then observes that (1) $Y_F(\Delta) \propto g^2(\Delta)\, s(\Delta)$ can be interpreted as the complex two-way antenna pattern of a hypothetical antenna; (2) β' equals the angular beamwidth of this pattern; (3) the variable conjugate to Δ (the dual of t) is the distance along the aperture of this antenna; (4) the Fourier transform of $Y_F(\Delta)$ [the dual of $y_f(t)$] is the current distribution along this aperture; (5) T' is the maximum extent of this aperture. Schematic illustrations of the two extreme cases $\beta'\omega/2\pi c \ll 1$ and $\omega/T'c \gg 1$ can be obtained from Fig. 11 by merely replacing Δ, ω, β and T by ω, Δ, β' and T', respectively. The case $\beta'\omega/2\pi c \ll 1$ corresponds to a situation in which the antenna gain pattern or the target reflectivity pattern is highly directional compared to the $E(\Delta)$ modulation, and the case $\omega/T'c \gg 1$ corresponds to a situation in which both of these patterns are broad and smooth compared to the $E(\Delta)$ modulation.

Although, in general, the existence of this duality between ω and Δ in E can be very useful, in actually applying this duality to concrete problems, it should be remembered that ω and Δ appear as duals in E only to the extent that they occur as duals in K. In the above discussion, this duality in K has been ensured by assuming that K is slowly varying over the relevant regions of ω and Δ. In a particular application, however, the assumption that K is slowly varying in ω may be valid, whereas the assumption that K is slowly varying in Δ may not be valid, and conversely.

F. Modifications in Received Signal Due to Motion of Antenna and/or Target

In the above discussion, it was assumed that the antenna and target were stationary. Attention will now be given to some of the effects introduced by relaxing this assumption. Assume first that (1) the orientations of the antenna and target are fixed; (2) the translational velocities of the antenna and target are small; (3) Δ is small. [A more precise statement of assumptions (2) and (3) will be given in Sec. I-I.] Let

$$R(t) = R + cR't \quad , \quad \text{where } R' = \frac{dR/dt}{c}$$

$$\Delta(t) = \Delta + c\Delta't \quad , \quad \text{where } \Delta' = \frac{d\Delta/dt}{c}$$

$\overline{Y}(\omega, t)$ = component of received signal corresponding to transmitted component $X(\omega)\exp(i\omega t)$

$\overline{Y}_F(\omega, t)$ = free-space component of $\overline{Y}(\omega, t)$

$\overline{F}(\omega, t) = \overline{Y}_F(\omega, t)/X(\omega)$ = free-space factor

$\overline{E}(\omega, t) = \overline{Y}(\omega, t)/\overline{Y}_F(\omega, t)$ = earth-modification factor.

It can then be shown (see Sec. I-I) that

$$\bar{Y}(\omega, t) = X(\omega)\, \bar{F}(\omega, t)\, \bar{E}(\omega, t) = \bar{Y}_F(\omega, t)\, \bar{E}(\omega, t)$$

where

$$\bar{F}(\omega, t) = \frac{Z(\omega)}{\omega R^2} \exp\left\{i\omega \left[(1 - 2R')\, t - (1 - R')\, \frac{2R}{c}\right]\right\}$$

$$\bar{E}(\omega, t) = \left\{1 + K(\omega) \exp\left[-i\omega\left(\Delta' t + \frac{\Delta}{c}\right)\right]\right\}^2$$

One sees that $2\omega R'$ is the Doppler shift along DD, $2\omega(R' + \Delta')$ is the Doppler shift along II, and $\omega(2R' + \Delta')$ is the Doppler shift along DI and ID. The term $\omega\Delta'$ is the Doppler beat between D and I.

Assuming that the Doppler shifts can be ignored in the evaluation of $Z(\omega)/\omega$ and $K(\omega)$, one finds that the complex spectrum corresponding to $\bar{Y}(\omega, t)$ is given by

$$Y(\omega) = \frac{Z(\omega)}{\omega R^2} \left\{X\left(\frac{\omega}{1 - 2R'}\right) \exp\left[-i\omega\, \frac{(1 - R')\,(2R/c)}{1 - 2R'}\right]\right.$$

$$+ K^2(\omega)\, X\left(\frac{\omega}{1 - 2R' - 2\Delta'}\right) \exp\left[-i\omega\, \frac{(1 - R')\,(2R/c) + 2\Delta/c}{1 - 2R' - 2\Delta'}\right]$$

$$\left. + 2K(\omega)\, X\left(\frac{\omega}{1 - 2R' - \Delta'}\right) \exp\left[-i\omega\, \frac{(1 - R')\,(2R/c) + \Delta/c}{1 - 2R' - \Delta'}\right]\right\} \quad . \tag{23}$$

The first term in this equation represents the signal due to DD [i.e., the free-space signal $Y_F(\omega)$], the second the signal due to II, and the third the signal due to DI and ID. As in the static case, $Y(\omega)$ can be factored into the products $Y(\omega) = X(\omega)\, F(\omega)\, E(\omega) = Y_F(\omega)\, E(\omega)$ by merely defining the free-space factor F and the earth-modification factor E by the ratios $F = Y_F/X$ and $E = Y/Y_F$.

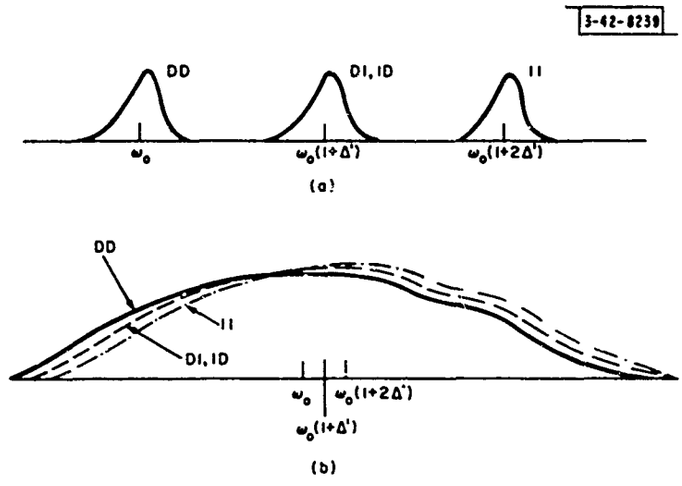

Fig. 13. Effects of translation. Relations among the energy spectra for components DD, DI, ID, and II: (a) $\omega_o\Delta'/\beta \gg 1$, (b) $\omega_o\Delta' T/2\pi \ll 1$.

Letting ω_o denote the center frequency of $Y_F(\omega)$, one can illustrate the two extreme cases $\omega_o\Delta'/\beta \gg 1$ and $\omega_o\Delta'/(2\pi/T) = \omega_o\Delta' T/2\pi \ll 1$ as shown in Fig. 13(a-b). When $\omega_o\Delta'/\beta \gg 1$, the signals along the three paths DD, II, and (DI, ID) will be separated in frequency and the energy spectrum will be given by

$$|Y(\omega)|^2 = \frac{|Z(\omega)|^2}{\omega^2 R^4}\left[\left|X\left(\frac{\omega}{1-2R'}\right)\right|^2 + |K(\omega)|^4\left|X\left(\frac{\omega}{1-2R'-2\Delta'}\right)\right|^2\right.$$

$$\left. + 4|K(\omega)|^2\left|X\left(\frac{\omega}{1-2R'-\Delta'}\right)\right|^2\right] \quad . \tag{24}$$

When $\omega_o \Delta' T/2\pi << 1$, the Doppler beat $\omega_c \Delta'$ will be small even with respect to the fine structure in $Y_F(\omega)$ and can be ignored. In this case, letting $q(\omega) = \varphi_K(\omega) - \omega\Delta/c(1-2R')$, one obtains

$$Y(\omega) = Y_F(\omega)\, E(\omega) \tag{25}$$

where

$$Y_F(\omega) = \frac{Z(\omega)}{\omega R^2} X\left(\frac{\omega}{1-2R'}\right) \exp\left[-i\omega\, \frac{(1-R')\,(2R/c)}{1-2R'}\right]$$

$$E(\omega) = \left[1 + K(\omega) \exp\left(-i\omega\, \frac{\Delta/c}{1-2R'}\right)\right]^2$$

and

$$|Y(\omega)|^2 = |Y_F(\omega)|^2\, |E(\omega)|^2 \tag{26}$$

where

$$|Y_F(\omega)|^2 = \frac{|Z(\omega)|^2}{\omega^2 R^4}\left|X\left(\frac{\omega}{1-2R'}\right)\right|^2$$

$$|E(\omega)|^2 = \left[1 + |K(\omega)|^2 + 2|K(\omega)| \cos q(\omega)\right]^2 \quad .$$

In this case, the effect of the earth on the free-space equation is identical to the . atic case except for the factor $1 - 2R'$ occurring in the function $\exp[-i\omega(\Delta/c)/(1-2R')]$. Thus, the previous discussion of E applies without change except for the contraction factor $1 - 2R'$. In many cases, the effect of this contraction factor on E can be ignored. Assuming that $Z(\omega)/\omega$ and $K(\omega)$ are constant across $X(\omega)$ (and approximating $1 - 2R'$ by 1 in the amplitude), one finds that the equation for the complex time function $\bar{y}(t)$ corresponding to Eq. (23) for $Y(\omega)$ is given by

$$\bar{y}(t) = \frac{Z}{\omega_o R^2}\left\{\bar{x}\left[(1-2R')\,t - (1-R')\,\frac{2R}{c}\right] + K^2\,\bar{x}\left[(1-2R'-2\Delta')\,t - (1-R')\,\frac{2R}{c} - \frac{2\Delta}{c}\right]\right.$$

$$\left. + 2K\,\bar{x}\left[(1-2R'-\Delta')\,t - (1-R')\,\frac{2R}{c} - \frac{\Delta}{c}\right]\right\} \quad . \tag{27}$$

Relaxing the stationarity assumptions still further, assume now that the antenna is scanning and/or the orientation of the target is changing. If these motions are slow with respect to the round-trip time $2(R + \Delta)/c$ for II, the complex time function $\bar{y}(t)$ will be given by the same formula as that shown in Eq. (27) except that $K = K(\omega_o)$ and $Z = Z(\omega_o)$ must now be replaced by $K = K(\omega_o, t)$ and $Z(\omega_o, t)$ in order to account for the time variations in the antenna factors $g(D, \omega_o)$ and $g(I, \omega_o)$ and the target factors $s(D, D, \omega_o)$ and $s(D, I, \omega_o)$. The corresponding spectrum $Y(\omega)$ can then be obtained from Eq. (23) by replacing $Z(\omega)$ and $K(\omega)$ by the Fourier transforms of $Z(\omega_o, t)$ and $K(\omega_o, t)$, and by replacing the multiplications of $X(\omega)$, $Z(\omega)$, and $K(\omega)$ by convolutions.

G. Total Received Energy and Energy Coverage Diagram

The energy $\Omega(Y)$ in the received signal Y is given by

$$\Omega(Y) = \frac{1}{2\pi}\int_{-\infty}^{\infty} |Y(\omega)|^2\, d\omega = \int_{-\infty}^{\infty} y^2(t)\, dt = A_y(0)$$

$$= \frac{1}{\pi}\int_{0}^{\infty} |Y(\omega)|^2\, d\omega = 2\int_{-\infty}^{\infty} |\bar{y}(t)|^2\, dt = 2A_{\bar{y}}(0) \quad . \tag{28}$$

Although, in general, actually computing $\Omega(Y)$ will be a rather complicated task, there are a number of important special cases in which this computation is particularly simple and the results are both practically significant and intuitively revealing. The formulas for $\Omega(Y)$ in these special cases are given by

$$\Omega(Y) \quad \Omega(Y_F)\, |E(q)|^2 = \Omega(Y_F)\,(1 + |K|^2 + 2|K| \cos q)^2$$

$$\Omega(Y) = \Omega(Y_F)\ \text{ave}\, |E(q)|^2 = \Omega(Y_F)\,(1 + |K|^4 + 4|K|^2) \tag{29}$$

where $q = \varphi_K - \omega\Delta/c(1 - 2R')$ and $|E(q)|^2$ has been described in detail in Sec. I-C. In both of these equations, it is assumed that $K(\omega)$ is constant across β. The first of these equations is valid provided that both of the following conditions are satisfied: (1) the Doppler beat $\omega_o\Delta'$ can be ignored (i.e., $\omega_o\Delta'T/2\pi << 1$); (2) $E(\omega)$ is constant across β (i.e., $\beta\Delta'/2\pi << 1$). The second of these equations is valid provided either one of the following conditions is satisfied: (3) the Doppler beat $\omega_o\Delta'$ is large (i.e., $\omega_o\Delta'/\beta >> 1$); (4) $E(\omega)$ varies much more quickly than $Y_F(\omega)$ across β (i.e., $\Delta/Tc >> 1$). The second equation can also be interpreted as giving the average energy in Y for a situation in which conditions (1) and (2) are satisfied and in which the Δ-coordinate of the target is defined probabilistically with all Δ's within a given cycle of E having the same probability.

If all the parameters in $\Omega(Y)$ are held constant except the location of the target, the locus of points which satisfy the equation $\Omega(Y) = C$ (C a constant) defines a surface in space referred to as a coverage contour. By definition, this surface has the property that whenever a target with the specified cross section is located at any point on this surface, the returned energy will be equal to the constant C. Although these contours contain no new information and are merely transformations of the energy equation from which they are derived, insofar as the radar's performance is a function of the received energy, they are useful in helping one to visualize the regions of space in which a specified performance can be expected to occur. An illustration of the effect of the earth on a vertical slice of this contour is shown in Fig. 14(a-b). The curves in Fig. 14 have been computed assuming that (1) the antenna and target are isotropic (i.e., $|g|$ and $|s|$ are independent of angle); (2) the earth is flat; (3) $\Gamma = -1$; (4) $2\pi c/\omega_o(1 - 2R') = \lambda = 10$ cm; (5) h 15,000 ft; (6) $\Omega(Y)/\Omega(Y_F)\, R^4 = 10^{-8}$ (R measured in nautical miles). The total number of lobes on one side of the antenna is given by $(\max\Delta)/\lambda = 2h/\lambda$ and, assuming that $(h + H)/d$ is small, the angular spacing between the lobes is given by $\lambda/2h$. The amplitude of the lobing modulation in this figure is given by $|K| = R/(R + \Delta) = [d^2 + (h - H)^2]^{1/2}/[d^2 + (h + H)^2]^{1/2}$ and the phase of the modulation is given by $\varphi_K = \pi$. The modulation in the received signal caused by the target's moving through these lobes is exactly the same modulation as that which has been described previously in terms of the Doppler beat $\omega_o\Delta'$.

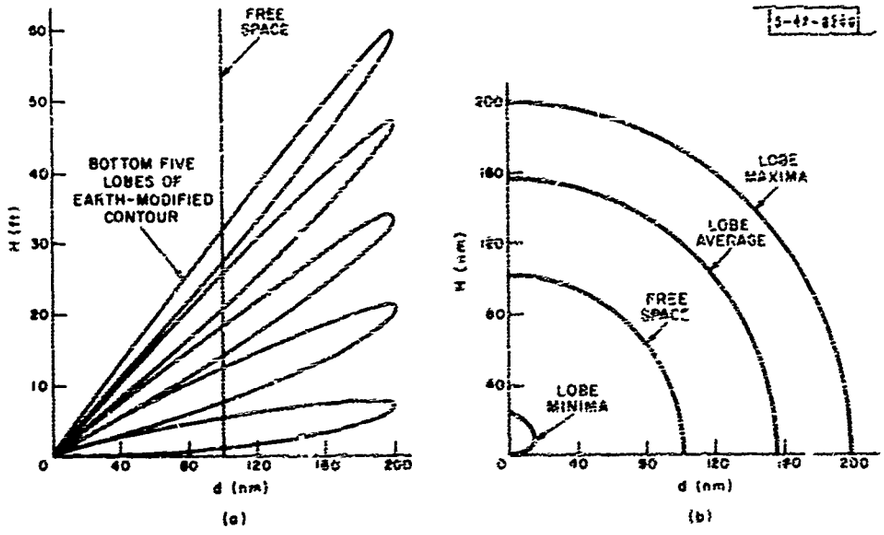

Fig. 14. Illustration of the earth's effect on the coverage diagram: (a) details of lobe structure (only five bottom lobes shown), (b) loci of lobe maxima, minima, and average.

H. Implications for Detection and Parameter Estimation

In previous sections, an analysis has been given of how the signal received from a target is modified by the presence of a perfectly smooth, homogeneous earth. In this section, a few remarks will be made on the implications of this analysis for the tasks of detection and parameter estimation. In discussing these tasks, it will be assumed that the target is a point target and reference will be made to two types of signal-processing systems: one matched to the free-space signal Y_F (denoted $\hat{Y}_F$) and one matched to the earth-modified signal Y (denoted $\hat{Y}$). In general, whereas the receiver in $\hat{Y}_F$ will consist of a filter bank of two dimensions, one for range and one for Doppler, the filter bank in $\hat{Y}$ must have additional dimensions in order to account for the factors K and Δ, as well as the Doppler beat $\omega_o\Delta'$. The application of $\hat{Y}_F$ to Y_F and to Y, and of $\hat{Y}$ to Y, will be denoted by $\hat{Y}_F \cdot Y_F$, $\hat{Y}_F \cdot Y$, and $\hat{Y} \cdot Y$, respectively. The extent of the mismatch $\hat{Y}_F \cdot Y$, and whether or not the deterioration in performance resulting from this mismatch will outweigh the additional complexities involved in the construction of $\hat{Y}$, will depend on the specific situation. In the event that $\beta\Delta/2\pi c \ll 1$ and $\omega_o\Delta'T/2\pi \ll 1$, the two systems $\hat{Y}$ and $\hat{Y}_F$ differ only by a complex constant. Inasmuch as the over-all amplitude and phase are seldom matched by the receiver in practice anyway, this difference is a trivial one. If, on the other hand, either $\beta\Delta/2\pi c \gg 1$ or $\omega_o\Delta'T/2\pi \gg 1$ so that $\hat{Y}_F$ resolves the components of Y, and $\hat{Y}_F \cdot Y$ gives the appearance of three distinct targets ($\beta\Delta/2\pi c \gg 1$ implies the components will be resolved in range and $\omega_o\Delta'T/2\pi \gg 1$ implies the components will be resolved in frequency), then the mismatch can be quite significant. One can, of course, attempt to operate further on $\hat{Y}_F \cdot Y$ by making use of one's a priori knowledge about the effects of the earth, but these further operations (whether they are automated or take place in the human brain) constitute nothing more than an attempt to extend $\hat{Y}_F$ to $\hat{Y}$ and to construct $\hat{Y} \cdot Y$.

In the event that $\beta\Delta/2\pi c \ll 1$ and $\omega_o\Delta'T/2\pi \ll 1$ (in which case $\hat{Y}$ and $\hat{Y}_F$ are essentially the same), the change in detection performance caused by the earth's presence will be determined by the energy ratio $\Omega(Y)/\Omega(Y_F) = |E|^2 = (1 + |K|^2 + 2|K| \cos q)^2$. If the indirect ray is

much weaker than the direct ray so that one can make the approximation $K = 0$, then this ratio will be approximately unity for all q. If the indirect ray is of sufficient strength compared to the direct ray to make $|K| \geq 2$ (e.g., the antenna gain is greater along I), then this ratio will be greater than unity and the detection performance will be improved for all values of q. If $0 < |K| < 2$, then whether or not this ratio is greater than unity will depend on q. In this latter case, whether or not the average detection performance will be improved will depend upon the distribution of values of q (either probabilistic or time varying), and upon which portion of the probability-of-detection (P_d)-vs-signal-to-noise-ratio (S/N) curve is being used. If the values of q can be assumed to occur uniformly so that ave $|E|^2 = 1 + |K|^4 + 4|K|^2$, and the S/N ratios for these values occur in a region of the $P_d(S/N)$ curve where the curvature is non-negative so that ave $P_d(S/N) \geq P_d(\text{ave } S/N)$, then the average detection performance will be improved for all values of $|K| > 0$. If, on the other hand, either the target tries to hide in a null of the lobe pattern by flying a path of appropriate Δ, or the S/N ratios occur in a region where the curvature of $P_d(S/N)$ is negative so that ave $P_d(S/N) < P_d(\text{ave } S/N)$, then the detection performance may deteriorate. (Note that in the case of horizontal polarization and a surface consisting of smooth sea water, the target can remain in a null by merely flying close to the surface.) Inasmuch as most $P_d(S/N)$ curves have positive curvature at low S/N ratios and negative curvature at high S/N ratios, the condition ave $P_d(S/N) \geq P_d(\text{ave } S/N)$ is likely to be relevant to early warning and the condition ave $P_d(S/N) < P_d(\text{ave } S/N)$ to high quality tracking. In order to defend against this possible deterioration in detection performance, one can make use of one or more of the following devices: (1) a high center frequency (which reduces the size of all the nulls and makes it harder for the target to hide); (2) a variable center frequency (which permits the radar "operator" to try to track the target in frequency and force it to remain in a maximum); (3) a broad-band signal (which averages out all but the lowermost lobes); (4) a shift in polarization (which shifts the phase of the lobe pattern). Which of these techniques will be the most useful will depend upon the target's tactics and upon the specific function the radar is intended to fulfill.

In the event that $\beta\Delta/2\pi c \gg 1$ or $\omega_o\Delta' T/2\pi \gg 1$ and the signals along the three paths DD, II, and (DI, ID) are resolved by $\hat{Y}_F$, it is clear that the detection performance dp for the three cases $\hat{Y} \cdot Y$, $\hat{Y}_F \cdot Y$, and $\hat{Y}_F \cdot Y_F$ will satisfy the inequality $dp(\hat{Y} \cdot Y) \geq dp(\hat{Y}_F \cdot Y) \geq dp(\hat{Y}_F \cdot Y_F)$ independent of the values of $|K|$ and ω and independent of the choice of flight path. The relation $dp(\hat{Y} \cdot Y) \geq dp(\hat{Y}_F \cdot Y)$ follows from the definition of the matched processing system, and the relation $dp(\hat{Y}_F \cdot Y) \geq dp(\hat{Y}_F \cdot Y_F)$ follows from the fact that Y_F is a component of Y which is resolved from the other components. (In order to make precise statements about the detection performance, one must, of course, specify the signal-processing systems $\hat{Y}_F$ and $\hat{Y}$ in detail and compute probability-of-detection-vs-probability-of-false-alarm curves.)

In addition to affecting the radar's ability to detect a target (i.e., to determine its existence), the presence of the earth also affects the radar's ability to estimate various characteristics of the target. According to Eq. (23), the parameters that enter into the earth-modified signal Y which do not occur in the free-space signal Y_F (and estimates of which would occur in the output of $\hat{Y}$) are the parameters Δ, Δ', and K. Looking at Eq. (9) for K, one observes that if the location of the target and the reflective properties of the surface are known, one can use Y to estimate the variable $s(D, I)/s(D, D)$ and thereby obtain information on the vertical scattering pattern of the target. In most practical cases, however, this estimate is likely to be extremely noisy (particularly when a rough reflecting surface is considered). Attention will therefore be restricted to the parameters Δ and Δ'.

With the ordinary search radar visualized in free space, the only variables describing the target's position and velocity within the vertical plane that can be measured with any degree of accuracy and reliability are the range R and the range rate R'. In order to determine further coordinates in this plane, one must employ an antenna pattern with a high degree of vertical resolution (i.e., a high frequency or a large vertical aperture). This constraint has frequently proven to be sufficiently incompatible with the search function to necessitate the construction of a completely separate radar (usually referred to as a "height-finder") whose specific function is to determine these further coordinates. If the earth's surface is taken into account, however, and the radar's antenna pattern and the reflecting properties of the surface are such that one is assured of having both a direct ray and an indirect ray, then, as mentioned above, the returned signal Y can be used not only to estimate R and R', but also Δ and Δ'. If the radar's own altitude h and rate of climb h' are known, R and Δ are sufficient to determine the target's position in the vertical plane, and R' and Δ' are sufficient to determine its velocity vector in this plane. The basic idea of these techniques is to incorporate the earth's surface as part of the antenna and thereby eliminate the need for an additional radar.

In addition to requiring that both rays be sufficiently strong, the ability to make high quality measurements of Δ and Δ' (like R and R') will depend on having a sufficiently large bandwidth β, a sufficiently long time duration T, and a sufficiently refined data-processing system. In the event that R/2h is large and the information on the target's location is required in the coordinates R and H rather than R and Δ, the measurement of Δ will have to be extremely accurate to produce an accurate measurement of H since $dH/d\Delta$ will then also be large. [For a flat earth, $H = (2\Delta R + \Delta^2)/4h$.] Note also that in order to transform the velocity coordinates R' and Δ' to R' and H', one needs to know both Δ and R, and therefore, in order to produce R' and H', one needs not only a long time duration T, but also a large bandwidth β. One makeshift technique for determining H which has been used on occasion when β has been too small to measure Δ directly and some outside intelligence is available on H', is to measure R, R', and Δ'. This technique of estimating H from a measurement of Δ' is referred to as "lobe counting." Its weakness, as compared to a direct measurement of Δ, is its dependence on outside information concerning H' (information which, under most conditions, must be very precise) and the long time duration required to measure Δ'.

So far, it has been assumed that only one target is present. In a realistic environment, the number of targets is unknown. In this case, the existence of the earth-reflected ray can lead to a variety of ambiguities. For example, if three distinct signals are received separated by equal intervals (either in Doppler or range), these signals can be interpreted as arising either from a single target with the three paths DD, II, and (DI, ID) or from three targets, each with only a single path. Similarly, if six equally spaced signals $S_1, \ldots, S_6$ are received, these signals can be identified with targets T_i in the fashion $[T_1 = (S_1, S_2, S_3),\ T_2 = (S_4, S_5, S_6)]$; $[T_1 = (S_1, S_3, S_5),\ T_2 = (S_2, S_4, S_6)]$; $[T_1 = S_1,\ T_2 = (S_3, S_4, S_5),\ T_3 = S_6]$; and so forth.

In general, the earth's presence not only introduces new target parameters to be estimated, but also affects the estimates of the old free-space parameters. In order to make precise statements about the influence of the earth on the radar's parameter-estimation ability, not only must the processing system be specified in detail, but one must select criteria for evaluating the estimates.

I. Generalized Static Equation and Generalized Approach to Effects of Translation-Motion

Before turning to the complications introduced by surface roughness, it is important to note that the previous discussion is extremely simplified even for an earth which is perfectly smooth. In this section, the previous results will be generalized in two directions. First, the static equations of Sec. I-C will be generalized by omitting assumptions (1), (2), and (5) of that section. Second, a technique will be presented for incorporating the effects of translations of the antenna or of the target which can be used to generalize the results of Sec. I-F. In both cases, the results stated previously will be derived as special cases.

1. Generalization of Section I-C

Assume now that assumptions (1), (2), and (5) of Sec. I-C are omitted. Let p denote the polarization h or v and ℓ the path D or I. Decomposing the electric vectors along D and I into the sums of their h and v components, one can write the total received signal as the sum of sixteen terms, each of which gives the received signal for a particular path-polarization combination $(p_1, p_2, \ell_1, \ell_2)$ [where "$(p_1, p_2, \ell_1, \ell_2)$" means "$p_1$ component out along ℓ_1, and p_2 component back along ℓ_2"]. Denoting the transmitting and receiving antenna functions by g_t and g_r, and inserting the polarization arguments into g_t, g_r, s, and ρ (but omitting the argument ω), define

$$Z(p_1, p_2, \ell_1, \ell_2) = \frac{c}{2}\, g_t(p_1, \ell_1)\, g_r(p_2, \ell_2)\, s(p_1, p_2, \ell_1, \ell_2)$$

$$\rho(p, \ell) = 1 \quad \text{for } \ell = D \qquad \rho(p, \ell) = \rho(p) \quad \text{for } \ell = I$$

$$L(\ell) = \text{length of } \ell \quad . \tag{30}$$

Continuing to omit the argument ω wherever possible, one then has, as the generalization of Eq. (9),

$$Y = \frac{X}{\omega} \sum_{\substack{p_1, p_2 \text{ in } \{h, v\} \\ \ell_1, \ell_2 \text{ in } \{D, I\}}} \frac{Z(p_1, p_2, \ell_1, \ell_2)\, \rho(p_1, \ell_1)\, \rho(p_2, \ell_2)\, \exp\{-i(\omega/c)\,[L(\ell_1) + L(\ell_2)]\}}{L(\ell_1)\, L(\ell_2)}$$

$$= XFE = Y_F E \tag{31}$$

where

$$F = \frac{\exp(-2i\omega R/c)}{\omega R^2} \sum_{p_1, p_2 \text{ in } \{h, v\}} Z(p_1, p_2, D, D)$$

$$E = 1 + \left[\frac{R^2 \exp(-2i\omega\Delta/c) \sum_{p_1, p_2 \text{ in } \{h, v\}} Z(p_1, p_2, I, I)\, \rho(p_1)\, \rho(p_2)}{(R + \Delta)^2 \sum_{p_1, p_2 \text{ in } \{h, v\}} Z(p_1, p_2, D, D)} \right]$$

$$+ \left[\frac{R \exp(-i\omega\Delta/c) \sum_{\substack{p_1, p_2 \text{ in } \{h, v\} \\ \ell_1 \neq \ell_2 \text{ in } \{D, I\}}} Z(p_1, p_2, \ell_1, \ell_2)\, \rho(p_1, \ell_1)\, \rho(p_2, \ell_2)}{(R + \Delta) \sum_{p_1, p_2 \text{ in } \{h, v\}} Z(p_1, p_2, D, D)} \right] .$$

Since the transmitting and receiving antennas are no longer assumed identical, the reciprocity theorem is no longer applicable and one can no longer equate the signal received over the path DI with the signal received over the path ID [i.e., $Z(p_1, p_2, \ell_1, \ell_2)$ is not necessarily equal to $Z(p_2, p_1, \ell_2, \ell_1)$]. Also, since reflection from the earth's surface (even when this surface is perfectly smooth) will depolarize any wave which is not pure-horizontal or pure-vertical [due to the differences between $\rho(h)$ and $\rho(v)$], the target scattering length s cannot be defined merely in terms of the polarization of the antenna as was done in Sec. I-C and as is usually done in the discussion of the free-space case.

If one now restores assumptions (1) and (2) of Sec. I-C, the equation for F becomes the same as in Sec. I-C and (defining K as in Sec. I-C and dropping the polarization notation) the equation for E becomes

$$E = [1 + K \exp(-i\omega\Delta/c)]^2 \left\{ 1 + \frac{K^2 \exp(-2i\omega\Delta/c)\left[\frac{s(I, I)\, s(D, D)}{s^2(D, I)} - 1\right]}{[1 + K \exp(-i\omega\Delta/c)]^2} \right\} . \qquad (32)$$

The role of assumption (5) in Sec. I-C was to reduce the second factor in this equation to unity. [Note here the asymmetry in s and g with respect to the assumptions required for writing E as the square of $1 + K \exp(-i\omega\Delta/c)$. The reason for this asymmetry is that whereas one always has $g^2(I)\, g^2(D) = [g(D)\, g(I)]^2$, the equality $s(I, I)\, s(D, D) = s^2(D, I)$ demands a special assumption.]

2. Algorithm for Generalizing Section I-F

Attention will now be turned to presenting a technique for generalizing the equations of Sec. I-F describing the effects of antenna or target translations. This technique does not take account of the effects of the motion on the various reflection processes involved or of the changes in the angles of orientation, but is merely a nonrelativistic algorithm for taking account of the time-varying nature of the travel times of the signals.

Ignoring all attenuation and distortion, one can write the received signal for a given transmitted component $\exp(i\omega t)$ and a given path (ℓ_1, ℓ_2) as $\exp\{i\omega[t - \tau(\ell_1, \ell_2; t)]\}$, where $\tau(\ell_1, \ell_2; t)$ is the delay suffered by the signal which travels along (ℓ_1, ℓ_2) and arrives back at the radar at time t. Inasmuch as $\tau(\ell_1, \ell_2; t)$ will not, in general, be linear in t, the effect of τ's dependence on t cannot be described merely in terms of a Doppler shift of ω. Also, one cannot expect $\tau(\ell_1, \ell_2; t)$ to be symmetric in ℓ_1 and ℓ_2 [since the path (D, I) will be geometrically distinct from the path (I, D)], or $\tau(\ell_1, \ell_2; t)$ to be a function merely of the relative motions of the antenna and target along D and I (since there are three bodies involved rather than only two). In order to compute $\tau(\ell_1, \ell_2; t)$, consider a single photon that travels over the path (ℓ_1, ℓ_2) and arrives back at the radar at time t, and let

t_o = time at which photon is transmitted

t_1 = time at which photon hits target

$A(\ell_1; t_1) = t_1 - t_o$ = time it takes photon to go out along ℓ_1 as a function of the time at which it hits the target

$B(\ell_2; t) = t - t_1$ = time it takes photon to get back along ℓ_2 as a function of the time at which it arrives back at the radar

$L(\ell; x, y)$ = distance along ℓ between radar at time x and target at time y.

Thus

$$A(\ell_1; t_1) = \frac{1}{c} L(\ell_1; t_o, t_1) = \frac{1}{c} L\,[\ell_1; t_1 - A(\ell_1; t_1), t_1]$$

$$B(\ell_2; t) = \frac{1}{c} L(\ell_2; t, t_1) = \frac{1}{c} L\,[\ell_2; t,\ t - B(\ell_2; t)]$$

$$\tau(\ell_1, \ell_2; t) = t - t_o = A(\ell_1; t_1) + B(\ell_2; t_2)$$

$$= A\,[\ell_1; t - B(\ell_2; t)] + B(\ell_2; t) \quad . \tag{33}$$

The first two equations are functional equations for $A(\ell_1; t_1)$ and $B(\ell_2; t)$ in terms of the arbitrary distance functions $L(\ell_1; x, y)$ and $L(\ell_2; x, y)$, and their solutions in terms of these functions can be approximated by iteration. For example, for $A(\ell_1; t_1)$ one obtains the sequence

$$A^{(1)}(\ell_1; t_1) = \frac{1}{c} L(\ell_1; t_1, t_1)$$

$$A^{(2)}(\ell_1; t_1) = \frac{1}{c} L\,[\ell_1; t_1 - A^{(1)}(\ell_1; t_1), t_1]$$

etc.

Once $A(\ell_1; t_1)$ and $B(\ell_2; t_2)$ have been determined, $\tau(\ell_1, \ell_2; t)$ can be computed by use of the third equation.

In order to see how Eq. (22) of Sec. I-F is derived from this general algorithm [and to make assumptions (2) and (3) of Sec. I-F more explicit], let $v(\ell)$ = velocity of radar along ℓ at $t = 0$, $V(\ell)$ = velocity of target along ℓ at $t = 0$, and $L(\ell; 0) = L(\ell; 0, 0)$. Assume that (a) $L(\ell; x, y)$ can be approximated by the first two terms of its Taylor series expansion around $(x = 0,\ y = 0)$; (b) $A(\ell_1; t_1)$ and $B(\ell_2; t)$ can be approximated by $A^{(2)}(\ell_1; t_1)$ and $B^{(2)}(\ell_2; t)$; (c) the terms in $v^2(\ell)/c^2$ and $V^2(\ell)/c^2$ can be ignored. With these assumptions, $\tau(\ell_1, \ell_2; t)$ can be approximated by

$$\tau(\ell_1, \ell_2; t) = \frac{1}{c} [v(\ell_1) + V(\ell_1) + v(\ell_2) + V(\ell_2)]\, t + \frac{1}{c} \left\{1 - \frac{1}{c} [v(\ell_1) + V(\ell_1)\right.$$

$$\left. + V(\ell_2)]\right\} L(\ell_2; 0) + \frac{1}{c} [1 - \frac{1}{c} v(\ell_1)]\ L(\ell_1; 0) \quad . \tag{34}$$

Since, according to this approximation, $\tau(\ell_1, \ell_2; t)$ is linear in t, the function $\exp\{i\omega [t - \tau(\ell_1, \ell_2; t)]\}$ can be rewritten as $\exp\{i\,[\omega(\ell_1, \ell_2)\, t - \varphi(\ell_1, \ell_2)]\}$, where $\omega(\ell_1, \ell_2)$ and $\varphi(\ell_1, \ell_2)$ are independent of t. Letting τ' denote the time derivative of τ, one has

$$\omega(\ell_1, \ell_2) = \omega\,[1 - \tau'(\ell_1, \ell_2; t)]$$

$$\varphi(\ell_1, \ell_2) = \omega\,[\tau(\ell_1, \ell_2; t) - \tau'(\ell_1, \ell_2; t)] \quad . \tag{35}$$

Letting ℓ_1 and ℓ_2 vary over D and I, one obtains for the frequencies $\omega(\ell_1, \ell_2)$ the usual Doppler shifted frequencies

$$\omega(D, D) = \omega\left\{1 - \frac{2}{c} [v(D) + V(D)]\right\}$$

$$\omega(I, I) = \omega\left\{1 - \frac{2}{c} [v(I) + V(I)]\right\}$$

$$\omega(D, I) = \omega(I, D) = \frac{1}{2} [\omega(D, D) + \omega(I, I)]$$

$$\omega\left\{1 - \frac{1}{c} [v(D) + V(D) + v(I) + V(I)]\right\} \quad . \tag{36}$$

Writing R = L(D;0) and Δ = L(I; 0) − L(D; 0), and assuming the validity of the approximations,

$$\frac{\omega\Delta}{c}\left[\frac{|v(\ell)| + |V(\ell)|}{c}\right] = 0$$

$$\frac{\omega R}{c}\left[\frac{|v(I) - v(D)| + |V(I) - V(D)|}{c}\right] = 0$$

one can approximate the phases $\varphi(\ell_1, \ell_2)$ by

$$\varphi(D, D) = \frac{2\omega R}{c}\left\{1 - \frac{1}{c}\left[v(D) + V(D)\right]\right\}$$

$$\varphi(I, I) = \frac{2\omega R}{c}\left\{1 - \frac{1}{c}\left[v(D) + V(D)\right]\right\} + \frac{2\omega\Delta}{c}$$

$$\varphi(D, I) = \varphi(I, D) = \frac{1}{2}\left[\varphi(D, D) + \varphi(I, I)\right]$$

$$= \frac{2\omega R}{c}\left\{1 - \frac{1}{c}\left[v(D) + V(D)\right]\right\} + \frac{\omega\Delta}{c} \quad . \tag{37}$$

Writing R' for $[v(D) + V(D)]/c$, and Δ' for $\{v(I) + V(I) - [v(D) + V(D)]\}/c$, then leads to Eq. (22) for $\bar{Y}(\omega, t)$ in Sec. I-F.

II. GENERAL REMARKS ON INFLUENCE OF A ROUGH EARTH

In Sec. I, the received signal was described under the assumption that the earth's surface constituted a smooth, homogeneous sphere. For certain types of radars, terrains, and radar problems, the results based on this assumption will constitute a useful approximation. In other cases, however, these results will be inappropriate and, at best, can only serve as a starting point for further analyses.

A. Basic Effects of Surface Roughness

For the radar designer, roughness (either in shape or in the properties of the earth surface material) has two effects: (1) it corrupts the idealized picture of forward scattering presented in Sec. I and thus further modifies the character of the signal received from the target; (2) it spreads out the source of the backscattered signal (clutter) and thus gives importance to the earth's role as a competing target. Insofar as the complexity of the earth's surface usually requires that these effects be treated statistically, to the extent that one is only interested in gathering information about the target and not about the earth's surface, both effects must be regarded as potential sources of confusion, and both must be evaluated in order to predict a radar's performance. The second effect, which leads to a form of interference, tends both to increase the total level of signal against which the target signal must compete and to introduce a new fluctuation spectrum into this signal. The first effect, which may be viewed as a statistical corruption of the earth-modification factor E discussed in Sec. I, tends to wash out the smooth-surface interference lobes (replacing them by an irregular fine structure), and to introduce a new fluctuation spectrum into the target signal. The influence of the roughness on the total received energy from the target will depend upon the specific characteristics and orientations of the antenna and target, as well as upon the specific characteristics of the surface. Of the two effects, the one which has received most attention by radar designers is the interference effect. On the whole, the corruption of the earth-reflected target signal has been regarded as an effect of the

second order. Since the clutter signal may often be as much as 50 db above the internal noise and one may not be able to see the target at all, corruption or no corruption, this attitude is quite understandable. Except for the brief description in Sec. III of forward scattering from the ocean, this report will be concerned exclusively with the clutter problem.

B. "State of the Art"

Despite the fact that a considerable amount of effort has been spent in studying scattering from the earth's surface, at present there is no unified body of knowledge which is adequate for radar design. More specifically, one finds that (1) although there is a considerable amount of experimental data available on certain aspects of the problem, many of these data are inconsistent and incomplete; (2) although there are many theoretical studies of scattering from rough surfaces, there is no theory available which starts out with a realistic description of the earth's surface and obtains results which are both consistent with the experimental data (a difficult task since the data are themselves sometimes inconsistent!) and sufficiently determinate to be of use to the radar designer.† The basic reasons for this state of affairs appear to be the following. First, the surface being considered is extremely complex. In experimental work, this complexity usually results in an inadequate measurement program for determining the surface charactertistics Thus, a substantial amount of data exists in which certain aspects of the scattered field are described in great detail, but the characteristics of the surface which has caused this field are described in no detail at all. In theoretical work, this complexity results either in equations which are unusable for concrete computations or in the replacement of the actual surface by a model which is extremely artificial. In addition, this complexity seems to have caused a great gap between theoretical and experimental work. Not only have certain theories been proposed with only token reference to the data, but many experiments appear to have been designed without regard for the results which have been obtained theoretically. Second, the systems used for measuring the scattered signal are often quite complex. Thus, one often finds experimental results in which it appears that the experimenter has been unable to obtain sufficient information on the measuring device to allow him to separate those effects which are due to the scattering properties of the surface from those which are due to the measuring device. Third, from the scientific viewpoint, the earth-scattering problem is basically uninteresting (i.e., its solution will have no implications for physical theory), and the main motivation for studying this problem has been the desire to improve radar and communication performance. Thus, very few experiments have been designed with a view toward understanding the scattering phenomenon as a whole. For example, practically no work has been done to obtain a picture of the whole scattered field. Experimenters have studied either backscattering or forward scattering (depending upon the specific application in mind), but not both. Finally, the reader should also be aware of the fact that even if there were an adequate theory for describing the scattered field, the radar designer would still be faced with the problem that there is no adequate radar-design theory for minimizing the effects of surface roughness. This question will be discussed further in Sec. II-D.

†A good introductory bibliography of theoretical papers on scattering from rough surfaces can be found in the paper by Beckmann.[3]

C. Elementary Properties of Earth Clutter

In general, the types of interference with which the target signal will have to compete are (1) internally generated noise (e.g., thermal noise in the receiver, (2) externally generated noise (e.g., other radars), and (3) clutter (e.g., birds, storms, earth). The distinguishing feature of clutter is that it represents energy transmitted by the radar and reflected from the environment, whereas the other forms of interference represent energy generated outside the radar transmitter. Accordingly, the nature of the clutter signal will, in general, be markedly different from the nature of the other interfering signals, and the techniques that will be useful for its elimination will be markedly different. For example, whereas increasing the transmitted energy is a fundamental technique for overcoming noise interference, it is an utterly useless technique for overcoming clutter interference: the target-to-clutter ratio will remain fixed. On the other hand, whereas for many forms of noise the idea of resolving the target and noise is useless because the noise is too extensive (i.e., the noise exists at all times and all frequencies), in the case of clutter, since the signal represents the return from another well-defined target with definite boundaries in range, angle, and velocity, it may be possible to resolve the target and clutter and, subsequently, to identify and suppress the clutter signal. There are certain aspects of the clutter and noise problems which, of course, are similar. For example, insofar as the target and clutter signals are not resolvable in range, angle, or velocity, one may find it useful to employ a matched filter against clutter in much the same way as one employs a matched filter against noise. In general, however, the techniques which have evolved and which are actually employed in the two cases are quite different.

Regardless of the detailed shape and electromagnetic characteristics of that portion of the earth's surface over which the radar is operating, there are certain fundamental properties of the earth target as compared with the aircraft target that are valid for most portions of the earth's surface and which lead directly to a large number of techniques for the elimination of earth clutter. Briefly, these properties are: (1) the earth target is located at a different position in space than the aircraft target; (2) the earth target has a different relative velocity than the aircraft target; (3) the earth target is much larger than the aircraft target; (4) aircraft targets which occur above the horizon line occur at different angles than the earth target; (5) the relative position and velocity of the earth target are knowable beforehand, whereas the relative position and velocity of the aircraft target are probabilistic; (6) the aircraft target is elevated above the earth and therefore may have an image below the earth's surface, whereas the earth (as a target) will not. Additional properties which may be useful for distinguishing between the earth target and the aircraft target, such as the dependence of the reflection characteristics on frequency, polarization, and incidence angle, will depend on the detailed characteristics of these targets. (It should also be noted that if the altitude of the aircraft is of the same order of magnitude as the heights of the irregularities on the surface, or if the radar has sufficient resolution to resolve individual scattering elements on the surface, then certain of the above statements will no longer be appropriate and the features that will be useful for distinguishing between the aircraft and the surface may depend even more heavily on these detailed characteristics.)

Despite the fact that many land surfaces are poorer reflectors than the surface of the ocean, the interference caused by land clutter is usually more difficult to overcome (or even to describe) than that caused by sea clutter. Not only is the total energy in the clutter signal at small grazing angles often greater for land surfaces due to the greater slopes encountered, but also, the

statistical properties of the signal are often much more complicated. The basic reasons for this added complexity are: (1) the electromagnetic properties of land surfaces tend to be less homogeneous; (2) the variety of surface irregularities tends to be greater, both in size and in shape; (3) these irregularities tend to be distributed less uniformly. Whereas in many cases the sea clutter can be treated as a simple random-noise phenomenon, the land clutter must often be treated as a multiple-signal-plus-random-noise phenomenon. Some results on the characteristics of land clutter can be found in the report by Katzin, Wolff and Katzin.[6] A description of sea clutter is given in Sec. III.

D. Techniques for Reduction of Earth Clutter

Assuming that the function of the radar being designed is to gather information on targets other than the earth's surface, one must regard the signal returned from this surface as a form of clutter and design the radar in such a way that the effects of this clutter will be minimized. In principle, for any given system of constraints imposed by the state of component technology and for any given radar function, it should be possible to determine the system which will best satisfy that function in the presence of clutter. In practice, however, the problem usually becomes so complicated that the optimum system is never actually determined. This state of affairs is due primarily to the following facts. First, as already indicated, the statistical characteristics of the clutter signal depend not only on the nature of the scattering surface, but also on a large complex of factors describing the behavior of the radar. Thus, in trying to optimize the system with respect to a given radar function, one is faced with an optimization problem in which not only must many variables be optimized over simultaneously, but one in which each variable has an effect on the interfering signal as well as on the target signal. Second, as also indicated previously, one's knowledge of how the statistics of the clutter signal vary with the various radar parameters is still very limited. Finally, these statistics will, in general, be nonstationary. Thus, for the system to be optimum, it will have to be adaptive: the basic design of the radar will have to contain a plan for sampling the clutter signal and adjusting the various radar parameters according to the results of this sampling. In general, it is clear that the problem of determining an optimum anticlutter system is very complex and that no one has yet determined such a system. On the other hand, due to the importance of the clutter problem, considerable effort has been spent in developing specific anticlutter techniques and in developing optimization theories that are valid within certain limited contexts. Roughly speaking, these efforts can be divided into two classes, according to whether or not they make use of the specific reflective characteristics of the clutter source (i.e., the clutter's dependence on frequency, polarization, and grazing angle). The purpose of the remarks in this section is to outline some of the clutter-rejection schemes which, at least in basic conception, are independent of these characteristics. Some techniques which capitalize on these characteristics for the special case of the ocean can be derived from the description of these characteristics given in Sec. III.

1. Elevated Target Indicators (ETI)

Since the target and the earth's surface will always be located at different positions in space, it is theoretically possible to eliminate the effects of clutter by designing a radar with a high degree of spatial resolution and ignoring all signals which correspond to positions on the surface.

Inasmuch as the surface will exist at all azimuths and all ranges out to the horizon range, aside from requiring that the radar have sufficient range resolution to be able to separate returns from inside and outside the horizon range, the basic resolution requirement will be on the altitude variable H, the height of the target above the surface. Any system which can be designed to filter out signals that arise from scatterers with zero elevation will be effective in eliminating the clutter signal.

The most obvious way of obtaining such a system is to employ a transmitted waveform with a high degree of range resolution and an antenna pattern with a very narrow vertical beam, and to filter out the zero-height signals by a simple gating process. A somewhat more elegant system which makes smaller demands on the vertical aperture of the antenna is to replace the narrow vertical beam by a broad vertical beam combined with an adjustable vertical null. Targets with positive altitudes can then be detected by scanning the null through the region of elevation angles corresponding to the position of the clutter and comparing the observed return with the position of the null. If no target of positive altitude is present at range R, the return from range R will be zero when the null is pointing in the direction of range R on the surface. If a target of positive elevation is present at range R, the return will not be zero. In order to be able to examine all ranges R on a single pulse, one can restrict the occurrence of the null to the receiving antenna only and, making use of phased-array techniques, perform the null scanning operation in the receiver. One disadvantage of this system, as compared with the narrow-beam system, is that whereas the narrow-beam system enables one to simultaneously eliminate the clutter and measure the target's altitude, in the null-scanning system one can only determine the target's altitude when it is at a range where there is no clutter. In order to detect a target in clutter and simultaneously measure its altitude with a null-scanning system, one needs to employ two nulls, the positions of which can be adjusted independently.

A system which makes no demands at all on the angular resolution of the vertical antenna pattern, but demands an exceedingly fine range resolution, is based on the use of the forward-scattering properties of the surface. Assuming that conditions are such that the direct and indirect rays are both sufficiently strong, and making use of the fact that the altitude H is positive if and only if the pathlength difference Δ is positive, one can filter out signals of zero altitude by filtering out signals of zero pathlength difference. One simple way of achieving this (but by no means the ideal way) is to compare the range autocorrelation function of the total received signal with the autocorrelation function of the transmitted waveform. Whereas the autocorrelation function of the clutter component will (assuming appropriate statistics) tend to be the same as the autocorrelation function of the transmitted waveform, the autocorrelation function of the target component will have additional structure due to the various paths. For example, if the transmitted waveform is a simple pulsed sinusoid of pulselength T, whereas the autocorrelation function of the clutter component will have a peak at $\tau = 0$ and will tend to vanish by the time $\tau = T$, the autocorrelation function of the target component will (assuming the distortion of E is small) have peaks at $\tau = 0$, $\tau = \pm\Delta/c$, and $\tau = \pm 2\Delta/c$. Thus, to filter out signals of zero altitude, one need merely set a threshold on the level of the autocorrelation function in a τ-region away from $\tau = 0$. Since the peaks at $\tau = \pm\Delta/c$ and $\tau = \pm 2\Delta/c$ enable one not only to detect the existence of the target, but also to measure the value of Δ, this system, like the narrow-beamwidth system, allows one to simultaneously eliminate the clutter and measure the target's altitude.

On the whole, ETI clutter-rejection techniques have received very little attention. Aside from the gross mapping-out procedures, which have been incorporated into a variety of systems, most of the work has been theoretical. Very little effort has been made to test these ideas empirically or to develop the appropriate equipment.

2. Point Target Indicators (PTI)

In the ETI techniques, the clutter is eliminated by employing a radar with sufficient spatial resolution to resolve the target from the earth's surface, and then by "gating out" the clutter. Another set of techniques for clutter elimination, based on the differences between the target and the surface with respect to their size, makes use of spatial resolution to "thin out" the clutter. If the target is a point target and the surface constitutes a more or less continuously extended source of echoes which cannot be resolved from the target, the effects of the clutter can be reduced by spreading the clutter energy out over an increased number of resolution "boxes." The most widely used technique of this sort consists of shortening the radar pulse (either directly or by pulse compression) or narrowing the beamwidth, thereby decreasing the illuminated area (i.e., that area on the surface which contributes to the received signal at a given instant of observation). As long as the size of the resolution volume remains larger than the target so that the target itself does not appear extended, a decrease in the area of illumination will, on the average, result in an increase in the target-to-clutter ratio.

Another PTI technique makes use of pulse-to-pulse frequency jumping and coherent integration. Whereas the reflective properties of a small target vary slowly with changes in frequency, the reflective properties of a large complex target like the earth's surface vary rapidly and randomly with such changes. Thus, if the frequency jumps are chosen properly, whereas the target signal will tend to integrate coherently, the clutter signal will, like noise, tend to integrate incoherently. Assuming that the source of the clutter signal can be represented as a collection of statistically independent random scatterers, one can show that the clutter signal will be sure to be decorrelated provided the frequency jump is greater than or equal to the bandwidth of the envelope of the transmitted signal.

3. Moving Target Indicators (MTI)

In addition to taking advantage of the differences in the positions of the target and the earth's surface as is done in the ETI techniques, one can attempt to eliminate the clutter by making use of the differences in their velocities. Since, in general, the target will have a nonzero velocity relative to the earth's surface, it is theoretically possible to eliminate the effects of clutter by designing a radar which is responsive to velocity differences. These velocity-discrimination techniques can be conveniently divided into two categories: Doppler MTI techniques and volume MTI techniques. In the Doppler techniques, the velocity discrimination is based on changes in the range of a target of the order of a wavelength of the transmitted frequency. In the volume techniques, the velocity discrimination is based on changes in the position of the target of the order of the dimensions of the illuminated volume. Inasmuch as the velocities are usually too small to cause the target to move from one resolution box to another between pulses, volume MTI systems must usually be based on the changes in position which occur between scans of the antenna. The Doppler systems, which have received the greater attention of the two, can be further subdivided according to whether they are coherent or incoherent and continuous or pulsed.

In the coherent systems, the discrimination is based on information concerning the Doppler-shifted frequencies themselves, and the clutter is rejected by suppressing those frequencies which correspond to the velocity of the earth relative to the radar. In the incoherent systems, the discrimination is based on information concerning the beat frequencies between the Doppler-shifted frequencies, and the clutter is rejected by suppressing those signals which do not contain the appropriate beat frequencies. Although the incoherent systems are simpler in that they do not require information on the velocity of the earth relative to the radar, they are of use only to the extent that the locations of the clutter source are predictable. (Inasmuch as the decision as to the presence of a target is based on the observation of a beat frequency between the target and clutter, if the system is used in regions where there is no clutter, it will suppress the target signal.) The pulsed systems differ from the continuous ones in that the pulsed systems only provide samples of the information provided by the continuous ones and thus are afflicted by ambiguities (leading to the so-called "blind-speed" and "fold-over" problems).

Independent of the particular type of Doppler system employed, the extent to which the system will be successful will depend on the location and extent of the clutter spectrum. In a continuous system, the ability to detect targets in clutter will depend on the relative characteristics of the clutter spectrum and the target spectrum. In a pulsed system, the performance will also depend on the relation of the clutter spectrum to the pulse-repetition frequency. In general, the fluctuations entering into the clutter signal will be of two types: those which result from variations in the scattering elements on the surface (the so-called "internal clutter process") and those which result from variations in the radar. If the radar is airborne, an important item in the latter category is the motion of the antenna. Assuming that the antenna is being both scanned and translated, one must consider not only the spectral broadening caused by the internal clutter variations, but also the broadening caused by variations in the illumination of the scattering elements and by the differential Doppler shifts associated with scattering elements at different angles.

4. Resolving the Clutter

In all the techniques previously discussed, the earth's surface has been viewed macroscopically. Another set of techniques which can be used to reject the clutter is based on the fact that, in many cases, the source of the clutter signal will not actually be continuous, but will consist of a collection of closely spaced discrete targets. If the radar's spatial resolution can be made sufficiently fine to resolve these discrete targets, and the extent of the aircraft target is sufficiently limited to permit the aircraft to fit in between these discrete targets, then the problem of determining whether or not an aircraft is present is reduced to a pure multiple-target-identification problem. Assuming that this problem cannot be solved by ETI or MTI techniques, how difficult it will be to solve will depend on the degree to which the detailed scattering properties of the aircraft target differ from those of the discrete earth targets.

5. Theoretical Work on Optimum Anticlutter Waveforms and Optimum Anticlutter Filters

In recent years, increasing thought has been given to the problem of determining the optimum waveform and the optimum filter for purposes of clutter rejection. Although these efforts have not yet culminated in a comprehensive theory of anticlutter design, some of the results are of considerable interest and should be of definite use to the radar designer.

One line of research, exemplified by Applebaum and Howells,[7] Westerfield, Prager and Stewart,[8] and Fowle, Kelly and Sheehan,[9] is based on the use of the time-frequency ambiguity function. These analyses start by assuming that the receiver consists of a bank of filters matched (in frequency and time) to an arbitrary waveform u(t) competing against white Gaussian noise. Letting τ be the delay variable and φ the Doppler shift variable, one measures the "goodness" of u(t) for purposes of clutter rejection by the extent to which the volume under the ambiguity function $\Psi(\tau,\varphi) = \left| \int u(t)\, u^*(t+\tau) \exp(-2\pi i \varphi t)\, dt \right|^2$ is prevented from overlapping the volume under the probability surface describing how the clutter energy is distributed in τ and φ. Although the maximum value of Ψ and the total volume under Ψ are independent of the waveform design and depend only on the total energy in u(t), the volume in the central spike of Ψ, and the manner in which the remaining volume is distributed in the (τ, φ) plane, are determined by the detailed structure of u(t). If the clutter energy is distributed uniformly throughout the (τ, φ) plane, then all waveforms become equivalent. If the clutter energy is concentrated in a localized region and the target of interest lies sufficiently far outside this region, then a "good" waveform is one in which all the volume under Ψ is concentrated in the central spike. If the clutter energy is concentrated in a localized region and the target lies inside this region, then a "good" waveform is one in which Ψ has a narrow central spike with as much volume as possible existing outside this region. When looked at in this way, the problem of anticlutter waveform design becomes quite similar to the problem of anticlutter antenna design. In the last case, for example, the basic idea for both antennas and waveforms is to "buy" target-to-clutter ratio at the "cost" of ambiguity. In general, this trade can be effected by the introduction of periodicity. Making the aperture periodic, i.e., chopping up the aperture and separating the pieces in space, enables one to decrease the width of the main lobe but results in strong sidelobes. Making the waveform periodic enables one to decrease the width of the central spike in Ψ but results in "blind-speed" ambiguities and "second-time-around" ambiguities. For a detailed understanding of this ambiguity-function approach and for specific quantitative results, the reader is referred to the above-mentioned references.

A second line of theoretical work oriented toward the development of a clutter-rejection theory is based on Dwork's matched filter theorem for colored Gaussian noise[10] and is exemplified by Urkowitz[11] and Manasse[12] Letting $Y(\omega)$ be the Fourier transform of the received signal and $N(\omega)$ the power spectrum of the noise, Dwork has shown that the transfer function $H(\omega)$ of the linear filter which maximizes the output peak S/N ratio is given by

$$H(\omega) = \frac{Y^*(\omega)}{N(\omega)} \exp(-i\omega T) \tag{38}$$

where T is a conveniently chosen time delay (assumed hereafter to be zero). The peak S/N ratio obtained with this filter is given by

$$\left(\frac{S}{N}\right)_{opt} = \frac{1}{2\pi} \int_{-\infty}^{\infty} \frac{|Y(\omega)|^2}{N(\omega)}\, d\omega \quad . \tag{39}$$

Assume now that (a) the duration of the signal transmitted by the radar is sufficiently short with respect to the movements of the radar, target, and clutter that everything can be regarded as fixed during the duration of the signal; (b) the signal received from the target is merely a delayed and attenuated version of the transmitted signal; (c) the statistics of the clutter signal are Gaussian and the power spectrum of the clutter (obtained from the fluctuations of the clutter

signal with range) is proportional to the energy spectrum of the transmitted signal. As will be seen in Sec. III, the last of these assumptions (the second part of which is identical to the assumption mentioned above that the autocorrelation function of the clutter is proportional to the autocorrelation function of the transmitted pulse) is reasonably well-satisfied for the case of sea clutter. With these assumptions, the above theorem implies that the linear filter which maximizes the peak signal-to-clutter-plus-noise ratio has a transfer function given by

$$H(\omega) = \frac{X^*(\omega)}{B|X(\omega)|^2 + N_o/2} \tag{40}$$

where N_o is the receiver noise power per cycle, $X(\omega)$ is the Fourier transform of the transmitted signal, and B is a constant of proportionality describing the total clutter power. The peak signal-to-clutter-plus-noise power ratio obtained with this filter is given by

$$\left(\frac{S}{C+N}\right)_{opt} = \frac{A^2}{2\pi} \int_{-\infty}^{\infty} \frac{|X(\omega)|^2}{B|X(\omega)|^2 + N_o/2}\, d\omega \tag{41}$$

where A is the amplitude of the returned target signal.

If the clutter power is zero, $H(\omega)$ reduces to the complex-conjugate filter $H(\omega) \propto X^*(\omega)$, and $[S/(C+N)]_{opt}$ becomes $[S/(C+N)]_{opt} = (S/N)_{opt} \propto (A^2/N_o) \int_{-\infty}^{\infty} |X(\omega)|^2\, d\omega$. Aside from A and N_o, the quantity $(S/N)_{opt}$ depends only on the energy in $X(\omega)$. If the noise power is zero (the case considered by Urkowitz), $H(\omega)$ reduces to the inverse filter $H(\omega) \propto 1/X(\omega)$, and $[S/(C+N)]_{opt}$ becomes $[S/(C+N)]_{opt} = (S/C)_{opt} \propto (A^2/B) \int_{-\infty}^{\infty} d\omega$. Thus $(S/C)_{opt}$ is completely independent of $X(\omega)$ and is infinite. This last result can be interpreted in more familiar terms by noting that the use of the inverse filter is theoretically equivalent to using a Dirac delta function as the transmitted signal and decreasing the illuminated area to zero. This equivalence can be demonstrated formally by representing the antenna and surrounding space as a fixed linear filter (referred to as the "space filter" in the Introduction) and reversing the order of application of this filter and the filter $H(\omega)$. Assuming that the construction of the inverse filter is limited to a finite frequency interval $\omega_1 < |\omega| < \omega_2$ and that the energy outside this interval is attenuated to zero, Urkowitz has shown that $(S/C)_{opt} \propto (\omega_2 - \omega_1)$. In other words, the ability to eliminate the clutter depends linearly on the bandwidth over which the inverse filter can be constructed.

Returning to the general case (considered by Manasse[12]) and assuming that both clutter and noise are present, one sees that $H(\omega)$ is a compromise between the complex-conjugate filter $X^*(\omega)$ and the inverse filter $1/X(\omega)$, and that $[S/(C+N)]_{opt}$ depends on both the total energy in $X(\omega)$ and on the shape of $|X(\omega)|^2$. In regions of ω where $|X(\omega)|^2 << N_o/2B$, the contribution to $[S/(C+N)]_{opt}$ is given by $(A^2/\pi N_o) \int |X(\omega)|^2\, d\omega$ and thus depends only on the total energy of $X(\omega)$ in those regions. In regions of ω where $|X(\omega)|^2 >> N_o/2B$, the contribution to $[S/(C+N)]_{opt}$ is given by $(A^2/2\pi B) \int d\omega$ and thus is entirely independent of $X(\omega)$ and depends only on the extent of those regions. It is clear, therefore, that if one wants to increase the value of $[S/(C+N)]_{opt}$ by changing the waveform (subject to a fixed total energy), one should take the superfluous energy in the $|X(\omega)|^2 >> N_o/2B$ regions and put it in the $|X(\omega)|^2 << N_o/2B$ regions. More precisely, Manasse has shown (through variational methods) that in order to maximize $[S/(C+N)]_{opt}$, the transform $X(\omega)$ should be chosen such that $|X(\omega)|^2$ is flat. If $X(\omega)$ is constrained to be zero outside the interval $\omega_1 < |\omega| < \omega_2$ and to have a total energy Ω, it will maximize $[S/(C+N)]_{opt}$ when

$$|X(\omega)|^2 = \frac{\pi\Omega}{\omega_2 - \omega_1} \quad \text{for } \omega_1 \leq |\omega| \leq \omega_2$$

$$|X(\omega)|^2 = 0 \quad \text{otherwise.} \tag{42}$$

The choice of a flat $|X(\omega)|^2$ makes the clutter power spectrum have the same shape as the noise power spectrum and eliminates the need for compromise in the optimum filter $H(\omega)$ [$H(\omega)$ now being given by $H(\omega) \propto X^*(\omega) \propto 1/X(\omega)|$. The value of $|S/(C + N)|_{opt}$ obtained with such a waveform is given by

$$\left(\frac{S}{C + N}\right)_{opt,\,opt} = \frac{2A^2\Omega}{2\pi B\Omega/(\omega_2 - \omega_1) + N_o} \tag{43}$$

Large values of Ω will have the effect of reducing the noise interference, and large values of $\omega_2 - \omega_1$ will have the effect of reducing the clutter interference. For a pulse radar which is peak power limited, this implies that the transmitted pulse should have a large time-bandwidth product (i.e., the pulse should be "coded"). Two techniques for achieving such a signal (and also satisfying the requirement for a flat energy spectrum) are to use long-duration pulses of broad-band white noise or long-duration pulses with a linearly swept carrier frequency of large deviation.

Unfortunately, although both of these approaches to the clutter-rejection problem are capable of making substantial contributions to a general anticlutter theory, at present, they both suffer from some serious limitations and, in no sense, can be regarded as constituting complete theories in themselves. Aside from the fact that both approaches disregard the specific reflective characteristics of the clutter, in neither approach is any consideration given to the problem of choosing an optimum antenna pattern. If the clutter is three dimensional, as in the case of rainstorms, the latter omission may not be too important in the sense that the total optimization process may be factorable and one may be able to optimize over the antenna pattern in a separate operation. However, in the case of earth surface clutter, where range resolution is a function both of the transmitted waveform and the vertical antenna pattern, this omission may be quite important.

In addition to these two limitations, which apply equally well to the ambiguity-function approach and the colored-matched-filter approach, the ambiguity-function approach suffers from its a priori assumption about the nature of the receiver. The optimum waveforms which can be determined through this approach are only optimum with respect to the given receiver. No optimization is performed over the receiver-waveform pair. In general, one may regard the target-in-clutter problem either as a target-in-noise problem or as a multiple-target problem. Insofar as the former philosophy is adequate, the noise against which the target signal is competing is the receiver noise plus the clutter noise and, in view of the Dwork theorem, the matched-filter bank assumed in the ambiguity-function argument is obviously not optimum. Insofar as the latter philosophy is adequate and one's objective is to detect each target and then reject the clutter targets on the grounds of certain parameter values (e.g., range and velocity), the matched-filter bank is still inadequate because it is not properly matched to the multiple-target situation. Thus, in either case, it is clear that the assumed receiver in the ambiguity-function approach is not optimum, and therefore, that the optimum waveforms which result from this approach will not really be optimum. Another limitation of this approach is that it incorporates the effects of velocity in such a way as to be valid only for narrow-band signals For signals of appreciable bandwidth, one must take account of the dependence of the Doppler shift on frequency over the bandwidth of the signal.

The colored-matched-filter approach, on the other hand, although it optimizes over both the receiver and the waveform, suffers from the fact that it totally ignores the velocity information. Moreover, the results of this approach will only be useful to the extent that the clutter can be regarded as continuous and the cross sections of the individual scatterers that constitute the source of the clutter signal can be regarded as infinitesimal in comparison to the cross section of the target. Once the clutter is resolved, the statistics of the clutter signal will no longer be Gaussian and the matched-filter theorem will no longer be applicable. Also, to the extent that the irregularities on the reflecting surface have an ordered structure and are not random, the power spectrum of the clutter will no longer be merely a replica of the energy spectrum of the transmitted signal.

In the event that the forward-scattering conditions ensure a strong reflected ray, both of the above approaches also need to be modified to include the earth-modification factor E described in Sec. I. In the ambiguity-function approach, the presence of the reflected ray implies that the receiver must consist of a multidimensional filter bank to account for K, Δ, and Δ' as well as for τ and φ, and the ambiguity function Ψ will be a function of K, Δ, and Δ' as well as of τ and φ. In the colored-matched-filter approach (still ignoring velocity), the existence of a reflected ray implies that the ideal receiver consists of a filter bank of the form $X^*(\omega)$ $E^*(\omega, K, \Delta) \exp(-i\omega T)/[N_o/2 + B|X(\omega)|^2]$, where there is a separate matched filter for each value of Δ and K.

III. SCATTERING FROM THE OCEAN

In Sec. II, the problem of surface roughness was considered without reference to the specific reflective characteristics of the surface. In the present section, attention will be devoted to the reflective properties of the ocean. This surface has been chosen for detailed consideration because (a) it is a surface of great practical importance; (b) despite its complexity, it is simpler than most other portions of the earth's surface; (c) it has received considerable attention, both experimentally and theoretically. In accordance with the fact that the clutter phenomenon is usually of greater concern to the radar designer than the corruption of the forward-scattered signal, the main concern will be with the clutter phenomenon. The discussion will be oriented toward the problem of predicting the sea-clutter signal for a narrow-band, pulsed, airborne, early-warning radar of broad vertical beamwidth and wavelength λ in the region 1 to 100 cm. Inasmuch as the early-warning function tends to focus interest on the longer ranges, special attention will be given to grazing angles α in the region 0° to 20°. A photograph illustrating the appearance of sea clutter on the PPI scope of an airborne early-warning radar is shown in Fig. 15.

In order to understand the sea clutter phenomenon and to be able to predict the properties of the clutter signal for a variety of radar configurations, it is necessary not only to make quantitative measurements of the received signal, but also to make quantitative measurements of the ocean surface responsible for this signal. If the electromagnetic properties of the sea are known and such factors as the spray and foam can be ignored (so that the sea surface actually constitutes a continuous interface between the air and the water), the scattering properties of the sea surface will be determined by specifying its shape as a function of time. Letting $z(x, y, t)$ denote the height of the surface at the point (x, y) at the time t, one can give a complete statistical description of this shape by specifying the set of probability density functions

Fig. 15. Appearance of sea clutter on PPI scope of airborne early-warning radar. Strobe is set at 135 nm, 30 nm short of horizon.

on the set of variables $\{z(x, y, t)\}_{x, y, t}$. Thus, in the ideal clutter experiment, along with the data on the received signal, data would be presented on these probability density functions describing the ocean surface. (If the spray and foam cannot be ignored, then of course, even these data would be inadequate and one would need to supplement it by a probabilistic description of various spray and foam parameters.) Unfortunately, in most of the clutter experiments reported in the literature, the amount of data on the sea surface is extremely limited. With few exceptions, the most information that is available is an estimate of wind velocity, wave height and direction, and a qualitative description of the ocean's appearance. In some cases, no data at all are available. Aside from the fact that the estimates of these parameters are often made very crudely, and the parameters being estimated are often defined very crudely, it is obvious that such a technique is basically inadequate for describing as complex a surface as that of the ocean. Although the hydrodynamic constraints on the shape of the water surface tend to reduce the randomness of the surface and thus make some of the information in the above-described probability density functions redundant, these constraints are not sufficiently strong to enable one to replace these functions by a few simple constants such as wave height and direction. Similarly, although the momentary local wind velocity will undoubtedly be correlated with certain properties of the surface (e.g., the ripple structure), it is an insufficient statistic for determining the surface as a whole. In general, the condition of the sea surface in a given area and at a given time will be a function of the history of the wind velocity over a wide region of

the ocean surface (as well as the currents, tides, and the proximity and topography of the ocean floor). For example, it is well known that the occurrence of "swells" in a given deep water area is not due to the momentary local wind velocity, but rather, to wind conditions which existed in regions far away and at an earlier time. These waves have outrun the wind which created them and are in the process of decay. As far as the waves which are generated locally are concerned, their characteristics are determined not only by the momentary local wind velocity, but also by the length of time during which the wind has been blowing and the length of ocean over which it has been blowing. In describing data on the clutter signal, the symbol "ζ" will be used to denote the "condition of the ocean surface." In the ideal experiment, ζ would consist of the set of all probability density functions previously mentioned. In practice, however, it must be interpreted as the wave height or wind velocity, or even more vaguely, as the "degree of roughness." For some detailed results on the actual characteristics of the ocean surface, the reader is referred to works of hydrodynamicists and oceanographers.[13]

The discussion in this section will be divided into three parts. In Sec. III-A, an attempt will be made to provide a brief summary of the major experimental results on the clutter signal. When considering any of the statements in this summary, the reader should be aware of the following facts. First, the data on sea clutter are inconsistent and incomplete and, in the usual sense of the word, there is no such thing as a "typical" result. Although a certain class of results may occur more frequently than any other single class, there is no class which occurs more frequently than the total of all other classes combined, unless one defines this class so generally as to be almost meaningless. Second, in view of these inadequacies, in order to present a general summary of the data, one must either (a) violate the empirical facts and ignore large portions of the available data; (b) state the summary in such vague terms as to make the summary almost meaningless; or (c) perform a massive statistical analysis of thousands of curves, weighting each curve according to the results of a comprehensive analysis of the detailed conditions under which the curve was obtained. Understandably, no one to date has performed the analysis required by (c). In this report, the writer has done his best to compromise between evils (a) and (b). The summary has been obtained by looking at a large number of experimental studies and represents a synthesis of the writer's impressions of the main results Specific references will frequently be omitted, but many of the remarks will be illustrated by concrete experimental data. In Sec. III-B, some theoretical concepts will be introduced for use in interpreting the experimental data. Since there is no unified theoretical model available which is consistent both with a realistic description of the ocean surface and with the clutter data, the best the radar designer can do in trying to predict the clutter signal for an hypothesized radar is to combine the results obtained from a study of the empirical findings with results computed from various fragmentary, phenomenological models. The concepts chosen for discussion have been selected for their popularity with researchers who have actually "dirtied their hands" in the sea-clutter problem and have been forced to make concrete recommendations on radar-design problems. In Sec. III-C, a brief summary will be given of some of the results on forward scattering from the ocean.

Those who are familiar with the subject of sea clutter will note that, with few exceptions, the results presented in Secs III-A and B represent only a very modest advance over those presented by Goldstein in the years 1946 to 1951.[14-16] This is not meant to imply that no important work has been done since that time. On the contrary, the picture of sea clutter has been extended

and refined in a variety of ways. For example, (a) data are now available at much lower frequencies; (b) more work has been done with coherent spectra; (c) the dependence on polarization has been explored more fully; (d) more careful data analysis techniques have been worked out; (e) specific theoretical models have been studied in more detail. Nevertheless, if one confines one's attention to the airborne early-warning problem, the above statement still holds: a significant portion of the knowledge which is now useful to the radar designer can be found in the writings of Goldstein.

Finally, the reader should be aware of the fact that the references cited in connection with this discussion are, in no sense, intended to constitute a bibliography. A complete bibliography on this subject would be longer than the discussion itself.

A. Experimental Data on Sea Clutter

1. Average Power

For a point target in free space, the dependence of the received power on the characteristics of the target is described through use of the target cross section $\sigma \propto |s|^2$. Aside from the characteristics of the target proper, this parameter depends only on the frequency, the polarization, and the angle of orientation; it is independent of the transmitted power, the transmitted pulselength, the antenna function, and the range. This independence has the important advantage of allowing one to extrapolate results obtained on the target characteristics with one radar configuration to those of another, provided only that the frequency, polarization, and angle are known. If one wants to achieve a similar independence for a parameter describing the backscattering properties of the ocean surface, the notion of cross section is inadequate. Since the ocean is an extended target, σ(ocean) will depend on how much of the surface is illuminated (i.e., how much of the surface contributes to the returned signal at a given instant of observation) and, therefore, will be a function of the antenna pattern, the transmitted waveform, and the range. In order to eliminate this dependence, it is necessary to determine how σ(ocean) varies with the illuminated area and, making use of this knowledge, to define a new parameter describing the properties of the ocean surface proper.

Let A denote the area of illumination and $\bar{\sigma}$ the pulse-to-pulse average of σ(ocean). It has been shown experimentally that, over a wide variety of conditions, $\bar{\sigma}$ varies linearly with A:

$$\bar{\sigma} = \sigma_o A \quad . \tag{44}$$

[These data have been obtained by (a) varying the transmitted pulselength, (b) varying the antenna pattern, and (c) varying the range or height while keeping the grazing angle constant.] Thus, a natural definition for the sought-after parameter is $\sigma_o = \bar{\sigma}/A$, the cross section per unit area. This parameter plays the same role for the ocean as the ordinary cross section σ plays for the point target; aside from the properties of the target itself, it depends only on the frequency, the polarization, and the angle of orientation. Letting Θ denote the horizontal beamwidth, Φ the vertical beamwidth, T the transmitted pulselength, and α the grazing angle, one can approximate the area of illumination A [see Fig 16(a-b)] by

$$A = R\Theta \frac{cT}{2} \sec\alpha \quad \text{when } \tan\alpha < \frac{\Phi R}{cT/2}$$

$$A = R^2 \Theta\Phi \csc\alpha \quad \text{when } \tan\alpha > \frac{\Phi R}{cT/2} \quad . \tag{45}$$

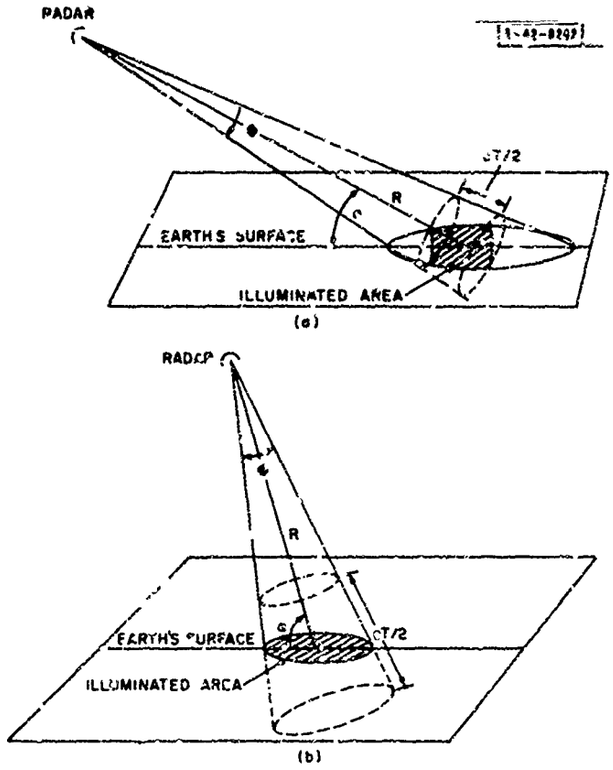

Fig. 16. Area of illumination: (a) tan $\alpha < \Phi R/(cT/2)$, (b) tan $\alpha > \Phi R/(cT/2)$.

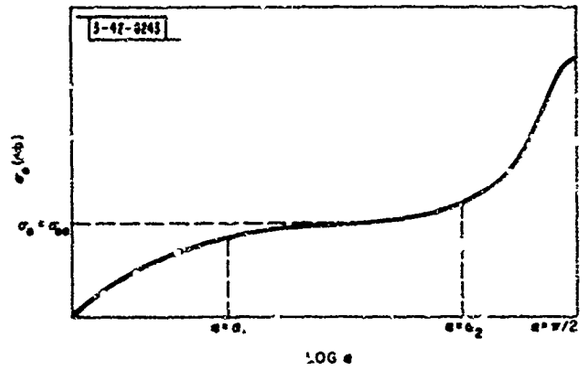

Fig. 17. Form of dependence of σ_c on α.

A brief description will now be given of the dependence of the cross section per unit area σ_o on the grazing angle α, the transmitted wavelength λ, the polarization p, the "condition of the sea surface" ζ, and the azimuth with respect to the structure on the sea surface.

For all but the calmest of seas, the form of the function σ_o(db) vs $\log\alpha$ most often encountered is that shown in Fig. 17 [σ_o(db) = 10 $\log_{10}\sigma_o$]. Starting at very small α, the parameter σ_o increases fairly rapidly with α until α equals the "critical angle" α_1. It then increases much more slowly (if at all) until the second "critical angle" α_2 is reached. Beyond α_2, it increases very rapidly until just before $\alpha = \pi/2$, whereupon it tends to flatten out again. The total range of slopes for $\log\sigma_o$ vs $\log\alpha$ (i.e., exponents for σ_o vs α) is about 0 to 20. In the region $\alpha < \alpha_1$, the slope is usually between 2 and 5, and in the region $\alpha_1 < \alpha < \alpha_2$, the slope is usually between 0 and 2. The total measurable range in σ_o from very small α to $\alpha = \pi/2$ may cover as much as 80 db with σ_o being as great as 10 to 20 db at $\alpha = \pi/2$. The actual range, of course, is infinite in decibels since σ_o must equal zero at the horizon. (The lower measurable limit on σ_o is determined by the amount of receiver noise.)

Letting σ_{oo} be the average level of σ_o between α_1 and α_2 and letting σ_o(vv) and σ_o(hh) be the values of σ_o for vertical and horizontal polarizations, one can make the following general statement about the variables α_1, α_2^{-1}, σ_{oo}^{-1}, and σ_o(vv)/σ_o(hh): they all tend to be monotonically decreasing with (a) decreasing λ and (b) increasing ζ. The variable $\sigma_o(\pi/2)$ also appears to be monotonically decreasing with increasing ζ. Presumably, the same result would hold for decreasing λ, but very few data are available on $\sigma_o(\pi/2)$ for low frequencies. The value of σ(vv)/σ(hh) is, of course, always equal to unity at $\alpha = \pi/2$ since vv and hh are identical at $\pi/2$. For all wavelengths in the region 1 cm $\leq \lambda \leq$ 100 cm and all but the smallest ζ, one finds that $\alpha_2 \geq 20°$. Typical values of σ_{oo} and α_1 for λ = 10 cm and a moderate to rough sea are σ_{oo} = -35 db and $\alpha_1 = 1°$.

Restricting attention to $\alpha \leq \alpha_2$, one finds that $\sigma_o \propto \lambda^{-n}$, $0 \leq n \leq 4$. In terms of $\alpha_1(\lambda)$ and $\sigma_{oo}(\lambda)$, the dependence of σ_o on λ can usually be described by the relations $\sigma_{oo} \propto \lambda^{-n}$, $0 \leq n \leq 2$, and $\alpha_1 \propto \lambda^n$, $0 \leq n \leq 1$. Thus the smaller n in $\sigma_o \propto \lambda^{-n}$ tend to occur when α is sufficiently large to make $\alpha > \alpha_1(\lambda)$, and the larger n tend to occur when this condition is violated. If one holds λ fixed and examines the variation of σ_{oo} and α_1 with ζ, one finds that σ_{oo} increases rapidly with ζ for relatively small ζ but then tends to "saturate," the saturation level occurring at smaller ζ for smaller λ. If one identifies ζ with the wind speed W, one finds $\sigma_{oo} \propto W^n$, $0 \leq n \leq 3$. If one identifies ζ with the wave height H, α_1 appears to vary with H as $\alpha_1 \propto H^{-n}$, $0 \leq n \leq 1$. Thus, for a fixed α, the smaller n in $\sigma_o \propto \lambda^{-n}$ tend to occur when ζ is large, and the larger n when ζ is small.

For large λ and small ζ, σ_o(vv)/σ_o(hh) is much greater than unity, sometimes reaching a value of more than 30 db. As λ is decreased or ζ is increased, σ_o(vv)/σ_o(hh) decreases; however, the rate of decrease diminishes as σ_o(vv)/σ_o(hh) decreases. At small λ and large ζ, σ_o(vv)/σ_o(hh) approaches unity and sometimes even becomes a few decibels less than unity. In general, σ_o(hh) is found to be more sensitive than σ_o(vv) to variations in ζ. Also, there is evidence that σ_o(vv)/σ_o(hh) decreases as α becomes extremely small. The cross-polarization cross sections σ_o(vh) and σ_o(hv) (which theoretically should be the same because of reciprocity) are usually smaller than either σ_o(hh) or σ_o(vv).

Finally, assuming that the direction of the wind and the wave structure on the surface are approximately the same, σ_o (upwind) is almost always a few decibels higher than either σ_o (downwind) or σ_o (crosswind), and σ_o (crosswind) is usually, but not always, a little greater than σ_o (downwind).

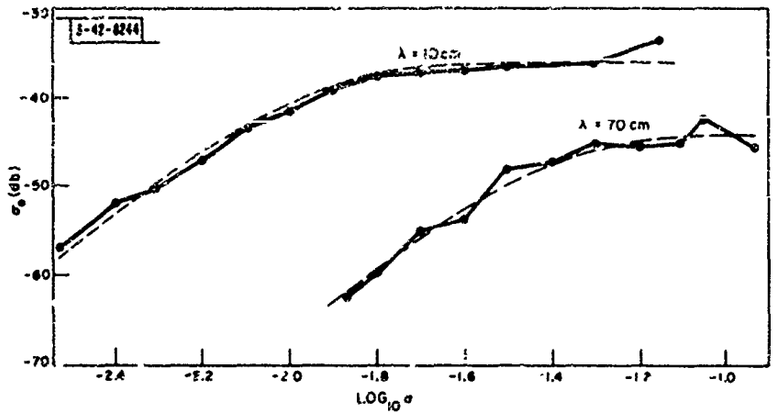

Fig. 18. $\sigma_o(\alpha,\lambda)$ data. p = hh, wave height = 4 ft, wind speed = 24 knots. (From Lincoln Laboratory experiments.[17]) Dashed curves are theoretical (see Sec. III-B-3).

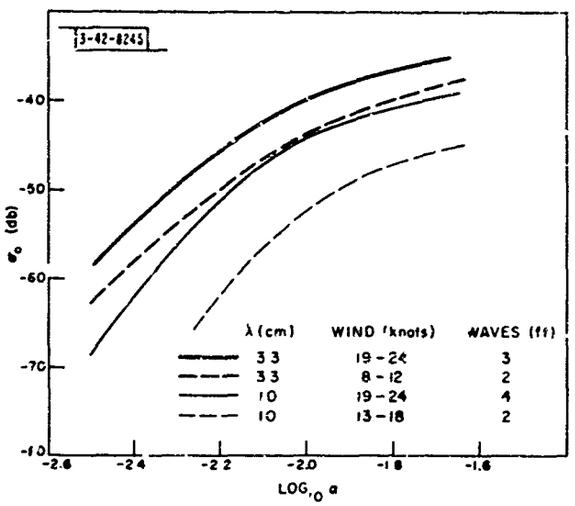

Fig. 19. $\sigma_o(\alpha,\lambda,\xi)$ data. p = hh. (Adapted from Gold and Renwick.[18])

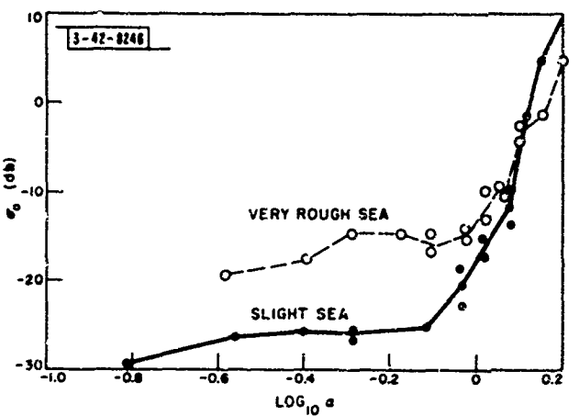

Fig. 20. $\sigma_o(\alpha,\xi)$ data. λ = 3.2 cm, p = hh. (Adapted from MacLusky and Davies.[19])

In the above remarks, the dependence of the average backscattered power on the characteristics of the surface has been described in terms of the average cross section per unit area σ_o. Another parameter which has occasionally been used and which measures the surface's deviation from perfect roughness is the parameter f_o which is defined as the ratio of the power actually observed to the power that would be observed if the surface scattered isotropically. It can be shown that f_o and σ_o are related by the equation $\sigma_o(\alpha) = 2 \sin(\alpha) f_o(\alpha)$.

Some specific results illustrating some of the above remarks are shown in Figs. 18 through 24. Figure 18 illustrates the dependence of σ_o on λ and α for small values of α. Figure 19 illustrates the dependence of σ_o on λ, α, and ζ for small values of α. Figure 20 illustrates the dependence of σ_o on α and ζ for large values of α. Figure 21 illustrates the dependence of σ_o on p, ζ, and α over a wide range of α. Figure 22 is a correlogram for the polarization ratio $\sigma_o(vv)/\sigma_o(hh)$ taken at two different λ with variable ζ. Figure 23 shows how σ_o varies with p and ζ for small α. Figure 24(a-b) shows how $f_o(\alpha) = \sigma_o(\alpha)/2 \sin\alpha$, which was observed to be constant over the region $1^\circ \leq \alpha \leq 5^\circ$, varies with λ and ζ. The smooth curves in Figs. 18 and 22 are theoretical and are discussed in Sec. III-B-3. In addition to the sources cited in connection with these figures, further data on the average backscattered power can be found in Kerr,[14] Katzin,[23] Grant and Yaplee,[24] and Wiltse, Schlesinger and Johnson[25] (as well as many others).

2. Fluctuations

In the previous section, the clutter signal was described in terms of the average power parameter σ_o. In this section, attention will be given to how the clutter signal varies (a) as a function of range within a given sweep and (b) as a function of time at a given range.

In general, there appear to be very few data on the fluctuations in range. However, whatever data there are indicate that if one confines one's samples to the small angle region $\tan\alpha < \Phi R/(cT/2)$ where the area of illumination is defined by the transmitted waveform, the autocorrelation function of the returned range sweep is approximately the same as the autocorrelation function of the transmitted waveform. In addition, it has been observed that for small α, the signal tends to resolve itself into distinct point-target-like echoes with substantial regions of zero signal occurring between these echoes. This "spikyness" tends to increase with (a) decreasing grazing angle and (b) decreasing area of illumination. Also, (c) this spikyness is much more pronounced with horizontal polarization than with vertical polarization. There is good evidence that the occurrence of these spikes is related to the occurrence of well-defined, steep-crested waves on the ocean surface.

Although there are considerably more data on fluctuations in time than on fluctuations in range, there are still fewer data than on the more easily measured σ_o. In general, it has been found that these fluctuations tend to resolve themselves into three main regions: (a) the "fast" fluctuations (presumably due to the beating of signals of different frequencies returned from different elements on the sea surface moving with different velocities); (b) the "slow" fluctuations (presumably due to the changes in amplitude caused by the changes in shape and orientation

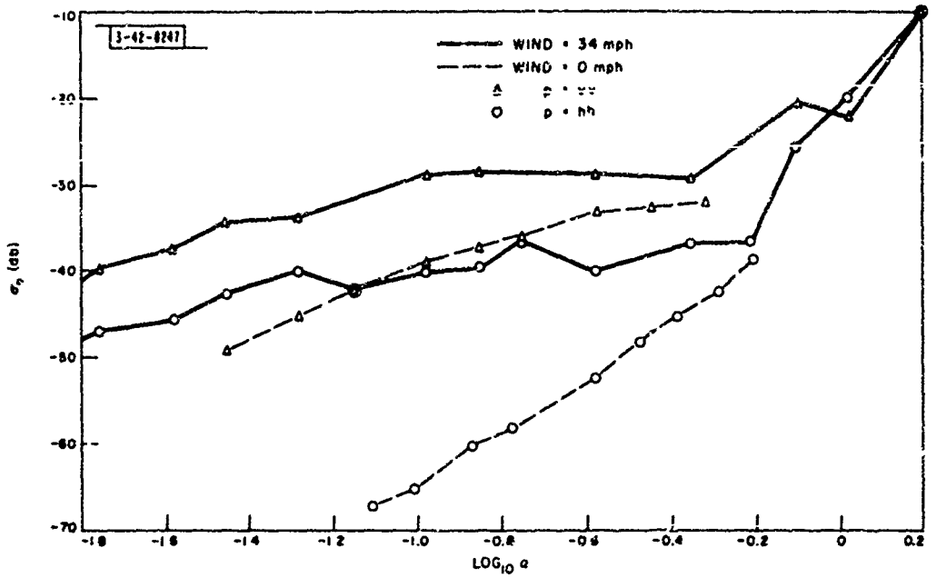

Fig. 21. $\sigma_o(\alpha, \rho, \zeta)$ data. $\lambda = 24$ cm. (After Macdonald.[20])

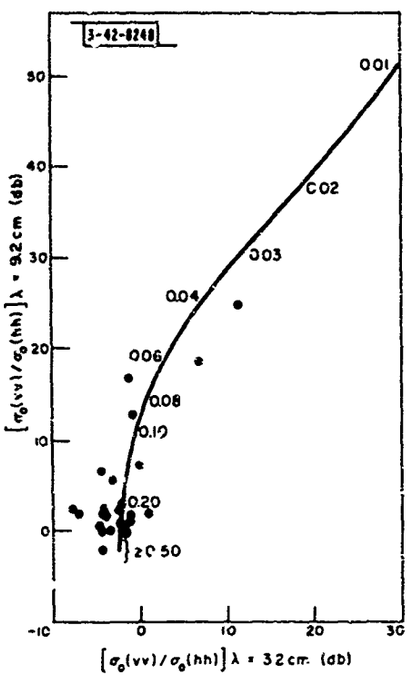

Fig. 22. $\sigma_o(\lambda, \rho, \zeta)$ data. $0.7° \leqslant \alpha \leqslant 1.3°$. (After Goldstein.[15]) Numbers on curve give $\bar{H}$ in feet (see Sec. III-B-3).

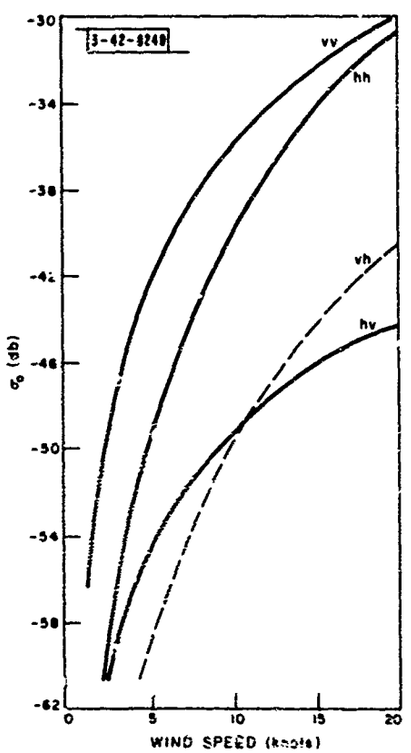

Fig. 23. $\sigma_o(\rho, \zeta)$ data. $\lambda = 4.8$ cm, $\alpha = 4°$. (After Boring, et al.[21])

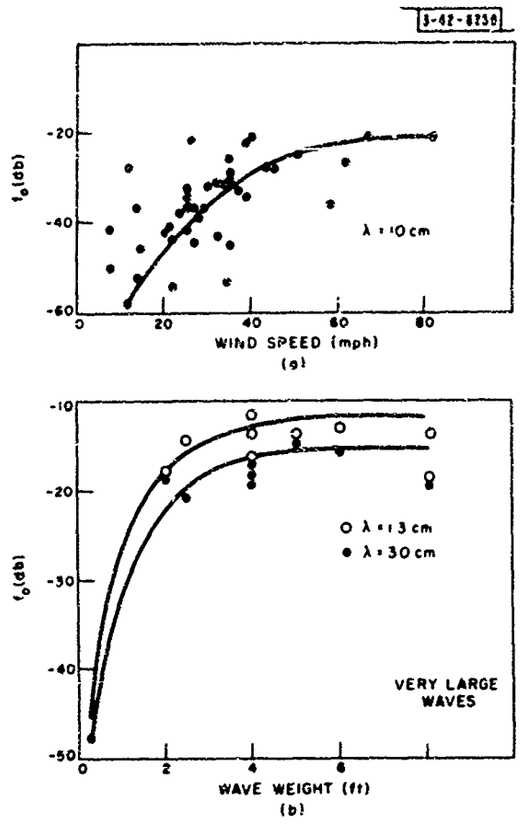

Fig. 24. $f_o(\lambda, \ell)$ data. p = hh, α in region $1.0° \leq \alpha \leq 5.0°$. (After Davies and Macfarlane.[22])

of the individual scattering elements, the passage of these elements through the area of illumination, and the growth, decay, and shadowing of these elements); (c) the "very slow" fluctuations (presumably due to changes in meteorologic and oceanographic conditions). In making measurements of σ_o, the general practice is to present results which are averages over the fast fluctuations, but not over the very slow fluctuations. The extent to which the slow fluctuations are averaged out will depend on the detailed characteristics of the device used to measure σ_o and on the amount of averaging done on these measurements before presentation of the final results. If the transmitted wavelength is sufficiently short (e.g., 10 cm), the fast and slow fluctuations are easily distinguishable; however, if the transmitted wavelength is long (e.g., 100 cm), these two regions will tend to merge.

With regard to the fast fluctuations, there are three facts on which there is more or less general agreement: (a) the first and second probability density functions are often similar to those for a narrow-band Gaussian noise process; (b) the width of the power spectrum, or equivalently, the inverse of the correlation time, varies approximately linearly with the transmitted frequency; (c) if one assumes that these fluctuations are due primarily to the relative motion of the scattering elements on the surface, the average relative velocity of these elements is of the order of 0.5 to 7.0 knots. There is considerable uncertainty as to what general statements can be made about the precise location and shape of the spectrum or exactly how the spectrum varies with polarization, grazing angle, azimuth, and sea condition. There appears to be some evidence that the width of the spectrum is independent of polarization and that it is monotonically increasing with sea roughness and grazing angle.

With regard to the slow fluctuations, about all that can be said in general is that (a) considerable energy may exist in the region 0.001 to 10 cps even for high transmitted frequencies;

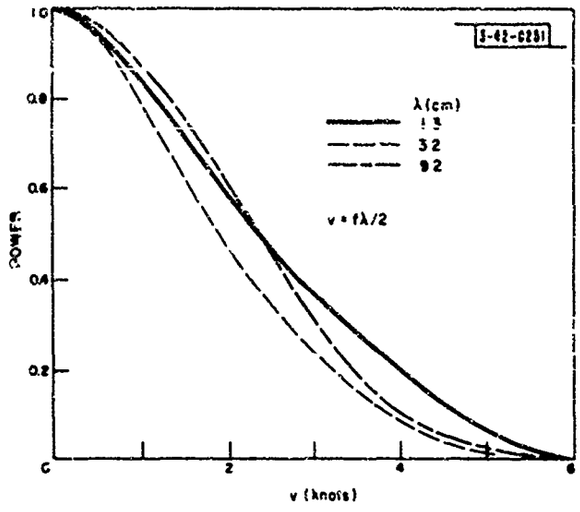

Fig. 25. Incoherent power spectrum as a function of λ. (Adopted from Goldstein.[14,16])

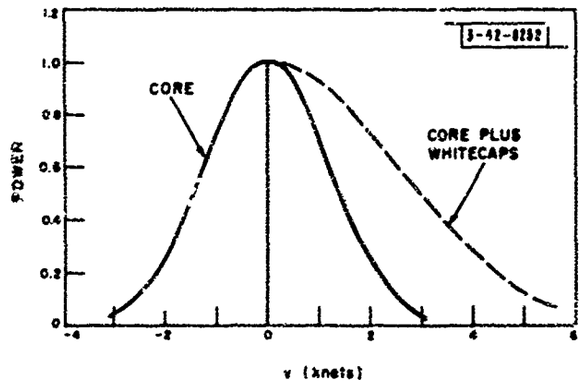

Fig. 26. Coherent power spectrum as a function of ζ. λ = 3.2 cm, ρ = hh, 2° ≤ α ≤ 8°. (After Kovaly, et al.[26])

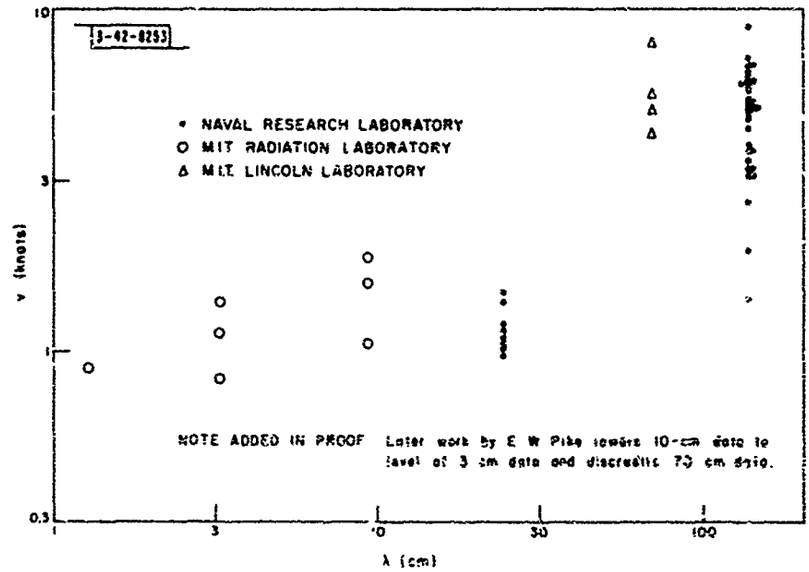

Fig. 27. Spectrum width as a function of λ. (See text for details and source of data.)

(b) the slow fluctuations often appear to be much more periodic than the fast fluctuations and the density functions often appear to be less Gaussian when slow fluctuations are included; (c) the slow fluctuations contain relatively more energy when the polarization is horizontal than when it is vertical and when the clutter is spiky than when it is continuous; (d) the slow fluctuations do not scale linearly with frequency. Frequently, the slow fluctuations, rather than being regarded as a subject for study, have been regarded as a source of error in the measurements of the fast fluctuation parameters. Practically no attention at all has been paid to the statistics of the very slow fluctuations.

Illustrations of the pulse-to-pulse fluctuation rates are shown in Figs. 25 to 28. (In Figs. 25 to 27, it has been assumed that the fluctuations are due to Doppler beats and the frequency scale is plotted in terms of scatterer velocities.) Figure 25 shows incoherent power spectra for λ = 1.3, 3.2, and 9.2 cm plotted as a function of $v = f\lambda/2$ (f = observed frequency in cycles/sec, λ = transmitted wavelength). Since these spectra are incoherent (i.e., the returned signal has not been compared to any reference signal), they contribute information only on the relative velocities of the scatterers, not the absolute velocities. Goldstein found these spectra to be roughly Gaussian in shape and to be independent of the sea condition. Figure 26 shows the coherent spectrum for λ = 3.2 cm. According to Kovaly, et al.,[26] and Hicks, et al.,[27] the core spectrum (again found to be Gaussian) was obtained for all wind directions and calm to moderate seas, and the core-plus-whitecap spectrum was obtained for upwind and downwind runs on rough sea states with whitecaps. The half-power width of the total spectrum at a grazing angle of 4° was found to vary from about 2 to about 5 knots, depending upon the sea condition. There was some evidence that the width decreased with a decrease in grazing angle. The average downwind velocity of the scatterers was found to be of the order of 0 to 7 knots. The result of convolving the core spectrum with itself to obtain the equivalent incoherent spectrum led to results consistent with those of Goldstein. Figure 27 is a summary of estimates of the root-mean-square spectral width as a function of the transmitted wavelength. These estimates were computed by Pike from pulse-to-pulse correlation data obtained at the M.I.T. Radiation Laboratory, the Naval Research Laboratory, and the M.I.T. Lincoln Laboratory.† Of the 80 data samples considered, Pike was able to fit about 50 of them to within observational errors by assuming that the corresponding power spectrum was a mixture of the following components: (a) a spike, (b) not more than two narrow-band Gaussian spectra, each centered on the frequency of the spike, and (c) white noise. Of these 50, about 30 could be fitted by white noise plus a single Gaussian component. In those cases in which two Gaussian components occurred, the energy associated with the broader component was almost always small compared to that of the narrower component. The results shown in Fig. 27 refer to the width of the main Gaussian component only. To what extent the white-noise component resulted from receiver noise and to what extent from the clutter signal itself was not determined. If one assumes that it was all receiver noise, then the chief difference between the widths plotted and the widths of the total clutter signal occurs in the elimination of the spike component, exclusion of the spike necessarily leading to greater widths. According to Pike's analysis, this spike contained relatively little energy except at 136 cm. At this wavelength, the energy in the spike

†The points at 1.3, 3.2, and 9.2 cm are based on data obtained by Goldstein and associates at the M.I.T. Radiation Laboratory; the points at 24 and 136 cm are based on data obtained by Macdonald and associates at the Naval Research Laboratory; and the points at 70 cm are based on data obtained by McGinn and associates at Lincoln Laboratory. (The Goldstein and Macdonald data were obtained by Pike and McGinn through private communication.)

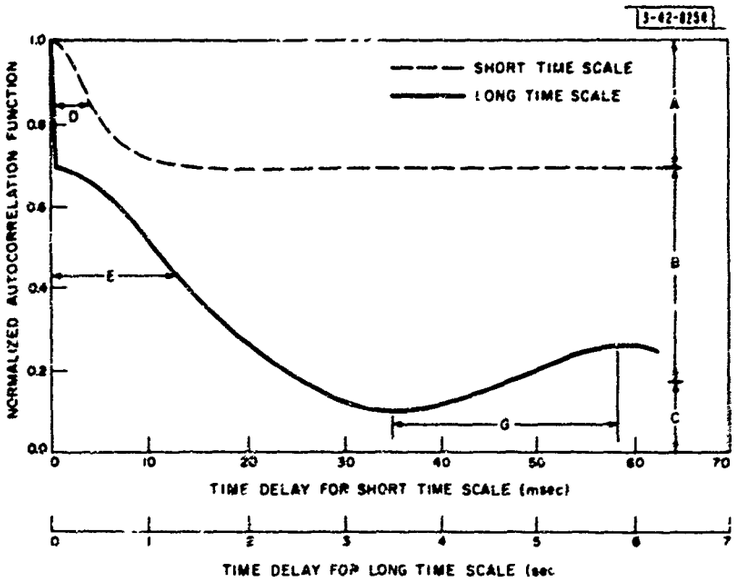

Fig. 28. Autocorrelation function for long time samples. $\lambda = 4.8$ cm, $0.5° \leq \alpha \leq 4.0°$, 10-minute samples. (After Boring, et al.[21])

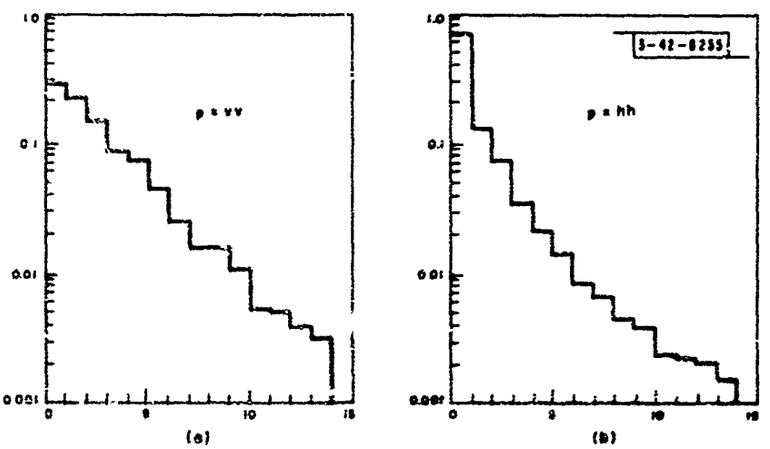

Fig. 29. First order probability density function on the power. $\lambda = 4.8$ cm, $0.5° \leq \alpha \leq 4.0°$, 10-minute samples. Abscissa gives signal power in arbitrary linear units; ordinate gives fraction of signal received in unit power range. (After Boring, et al.[21])

exceeded half the total energy in the function for about one third of the samples. The data at 1.3, 3.2, and 9.2 cm are for vertical polarization and a grazing angle of 0.6°; the data at 24 cm combine both vertical and horizontal polarization and cover grazing angles ranging from about 5° to 20°; the data at 70 cm are for horizontal polarization and a grazing angle of about 5°; and the data at 136 cm are for horizontal polarization and grazing angles in the region 1° to 14°. As a result of his analysis, Pike has concluded that, at wavelengths less than about 50 cm, the width of the main Gaussian component increases with sea roughness but is independent of grazing angle. At wavelengths greater than about 50 cm, he has concluded that this width increases with an increase in grazing angle, but is independent of sea roughness. (This observation, together with the increase in the width at about 50 cm, has led Pike to conjecture that a different scattering mechanism takes over at this wavelength.) Remembering that the spectrum widths reported by Hicks, et al.,[27] (2 to 5 knots) refer to the total width at the half-power points, one notes that the results in Fig. 27 at 3 cm are consistent with those of Hicks. The results at 136 cm are somewhat different from those reported by the Naval Research Laboratory, despite the fact that both sets of results are based on the same data. Whereas the 136-cm results in Fig. 27 vary from about 1 to 9 knots, the root-mean-square widths reported by Ament, et al.,[28] are confined to the region 1 to 4 knots. Also, unlike Pike, Ament found the spectral width to be independent of grazing angle. (In considering these differences, it should be noted that, whereas the results in Fig. 27 refer only to the main Gaussian component, the results of Ament refer to all the components mixed together, only the white noise being eliminated.) In contradistinction to the results reported by Hicks at 3 cm, Ament found the width at 136 cm to be greater for crosswind than for upwind or downwind. Figure 28 shows the appearance of the slow fluctuations for λ = 4.8 cm and α in the region 0.5° to 4.0° when long observation intervals are employed. The upper curve is an expanded version of the initial drop pictured in the lower curve and corresponds to the fast fluctuations. The width D of the fast component was found to vary inversely with frequency and wind speed, but was independent of polarization. The width E of the slow random component was found to be independent of frequency, polarization, wave height, and wind speed. The ratio B/A, measuring the relative power in the two components, was found to be ten times larger on horizontal polarization than on vertical polarization (0.7 on hh and 0.07 on vv). The periodic tail component (described by the parameters G and C) occurred mainly for large wave heights and high wind speeds. Figure 29(a-b) shows the first probability density function for the pulse-to-pulse fluctuations in power as a function of polarization for λ = 4.8 cm and long observation intervals. To the extent that the process is Gaussian, it can be shown that these histograms should be linear. The histogram for vertical polarization is typical of the results usually obtained when the observation interval is much shorter and the slow fluctuations are eliminated. The fact that the graph for horizontal polarization has a variable slope, whereas the graph for vertical polarization does not, is consistent with the fact that the slow fluctuations contain relatively more energy in the horizontal case and that the spikyness effect is more pronounced in the horizontal case. Additional data on both the first and second probability density functions of the pulse-to-pulse fluctuations can be found in Kerr.[14]

An illustration of the spikyness effect in the range fluctuation data and its strong dependence on polarization is shown in Fig. 30(a-b). These spikes were found to be correlated with the occurrence of well-defined, steep-crested, ocean waves. Some interesting results on the spikyness phenomenon can also be found in a paper by Macdonald.[29]

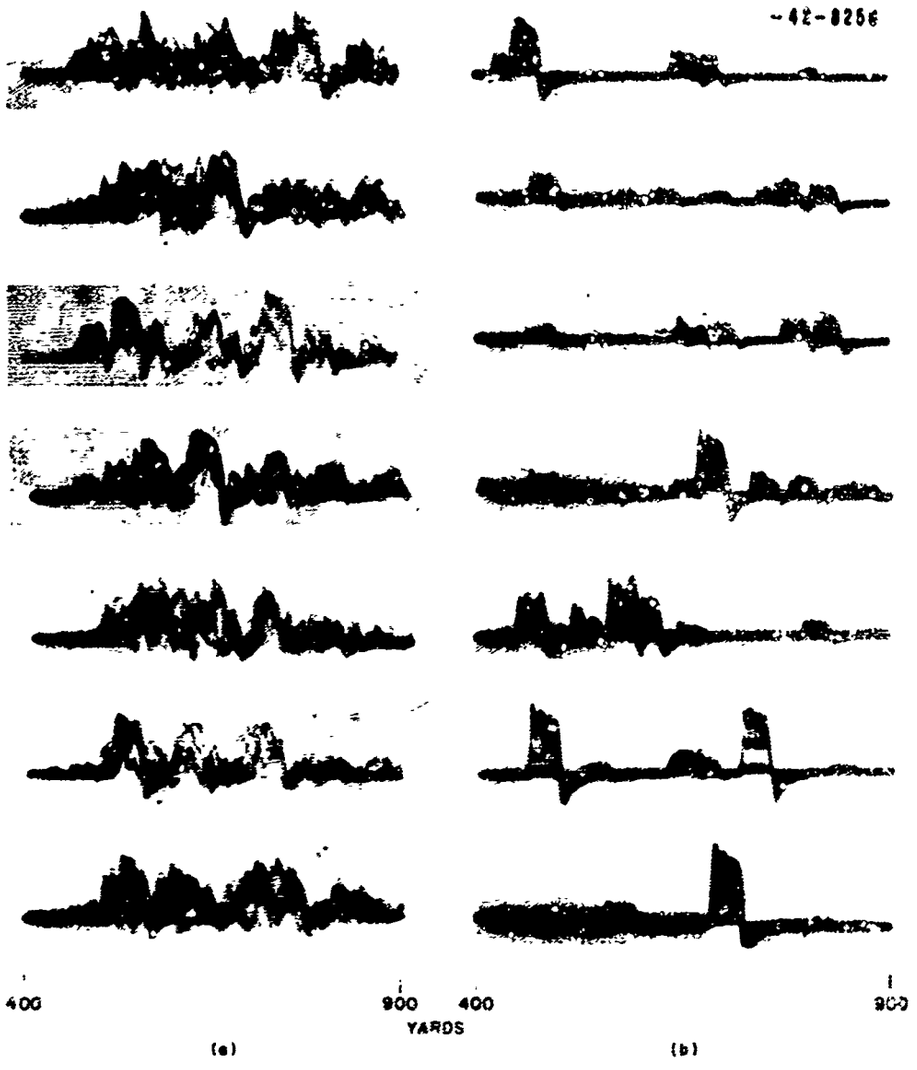

Fig. 30. Appearance of spiky clutter on the A-scope. $\lambda = 4.8$ cm, beamwidth = 2.3°, pulselength = 0.2 μsec, antenna elevation = 52 ft: (a) p = vv, pictures taken at random, (b) p = hh, pictures taken only when an echo was visible. (After Boring, et al.[23])

B. Concepts for Interpreting Experimental Data on Sea Clutter

1. Random-Scatterer Concept

One idea frequently used in interpreting the data on the clutter signal is that the source of the clutter can be regarded as a collection of a large number of random, similar, independent, uniformly distributed, point scatterers. This is the standard assumption used in phenomenological models for describing targets that are very complex and which contain no dominant reflector. Aside from greatly simplifying certain computations, this assumption leads to the predictions that (a) the probability density functions are Gaussian; (b) the average power varies linearly with the area of illumination; (c) the autocorrelation function of the fluctuations in range is equal to the autocorrelation function of the transmitted pulse. Together with the assumption of a narrow-band transmitted signal, it allows one to treat the clutter signal as narrow-band Gaussian noise. This concept will obviously be inappropriate for describing the clutter when the radar has sufficient resolution to resolve the irregularities on the ocean surface or when these irregularities are correlated over distances which are appreciable with respect to the dimensions of the illuminated area. For discussions of clutter signals as narrow-band Gaussian noise processes, the reader is referred to Kerr,[14] Lawson and Uhlenbeck,[30] Kelly and Lerner,[31] and McGinn and Pike.[32] For a general background in relevant statistical theory, the reader is referred to Cramér,[33] Davenport and Root[34] and Bendat[35]

2. Doppler-Image Concept

A concept which frequently has been used for interpreting the data on pulse-to-pulse fluctuation rates (already employed in presenting the data in Sec. III-A) is that the pulse-to-pulse frequency spectrum of the clutter can be interpreted as the Doppler image of the velocity spectrum of the scatterers. If u denotes the velocity spectrum of the scatterers, f the fluctuation rate (in cycles per second) of the clutter signal, and λ the transmitted wavelength, the fluctuation spectrum $U(f)$ is given, according to this assumption, by $U(f) = u(f\lambda, 2)$. The fact that the spectrum of the fast fluctuations scales linearly with the transmitted frequency at the higher frequencies would appear to lend strong support to th s interpretation for the fast fluctuations at these frequencies. However, in view of the fact that (a) at small grazing angles, the irregularities on the ocean surface which backscatter most effectively at one wavelength are not likely to constitute the most effective scatterers for other wavelengths,† and (b) different irregularities are likely to travel with different velocities, this confirmation of the Doppler-image interpretation must be regarded with considerable skepticism. In general, although the Doppler-image interpretation of the fast fluctuation spectrum may be correct for a wide range of transmitted frequencies, one has no right to assume that this spectrum will scale linearly with the transmitted frequency unless one can show that the important scattering elements at the different frequencies travel with the same velocity. In this connection, it is important to note that the Doppler-image concept has frequently led (along with other considerations) to the belief that, at the higher frequencies, the scattering motions are similar to the orbital motions suffered by a small particle of water (see, for example, Hicks, et al.[27]) and, at the lower frequencies, these

†At small grazing angles, where no portion of the surface is normal to the incoming energy, irregularities which are large with respect to the transmitted wavelength will reflect the energy forward. On the other hand, irregularities which are small with respect to the transmitted wavelength will cause little scattering in any direction. Thus the irregularities which will be most effective at small grazing angles (per irregularity) will be those whose size is of the order of the transmitted wavelength.

motions are similar to the phase velocities of the ocean waves (see, for example, Ament, et al.[28]). At extremely low frequencies (13 to 25 Mcps), the identification of the clutter spectrum with the phase velocities has received strong support from the work of Crombie[36] and Stutt, Fricker, Ingalls and Stone[37] (see diffraction-grating concept in Sec. III-B-5.)

3. Interference Concept —

Another concept which frequently has been used to interpret certain aspects of the clutter data is that the rough ocean surface can be regarded as a smooth ocean surface with scatterers elevated above it. Insofar as the return from each scatterer can then be thought of as consisting of a direct and reflected ray as discussed in Sec. I, this concept has proved useful in interpreting the results on the average power at small grazing angles, as well as the occurrence of spikyness at small grazing angles. According to this concept, the variation of σ_o with α, λ, and p is interpreted in terms of the variation of the interference pattern with these variables, and the variation of σ_o with t is interpreted in terms of the height distribution of the scatterers. Thus, for example, assuming that the polarization is horizontal (so that the reflection coefficient $\Gamma \approx -1$), the critical angle α_1 below which σ_o falls off rapidly with decreasing α is interpreted as the angle at which the bottom lobe in the interference pattern becomes too far removed from the surface to be averaged out by the height distribution of the scatterers. The fact that α_1 increases with λ then follows directly from the fact that the height of the bottom lobe increases with λ. The differences between horizontal and vertical polarization are interpreted in terms of the differences in the interference patterns implied by the differences in the reflection coefficients for the two polarizations. In general, the return on vertical polarization tends to be stronger because the phase lag of the reflection coefficient is such that more energy exists at points close to the surface. As λ decreases or the scatterers are raised higher above the surface (corresponding to an increase in sea roughness), more of the interference pattern tends to be averaged out and its value at points close to the surface becomes less crucial. For very small λ or very rough seas, the phase of the interference pattern (determined by the phase of the reflection coefficient) becomes irrelevant and σ_o depends only on the average field strength (determined by the magnitude of the reflection coefficient). Finally, the spikyness effect which occurs at small grazing angles (where the area of illumination is actually the largest) is explained by the fact that when the bottom lobe is sufficiently far removed from the surface, only those scatterers with exceptional height will be illuminated.†

In Goldstein's original discussion[14] of possible theories for explaining the behavior of σ_o, he considered the interference concept only in connection with the assumption that the scattering elements were droplets of water actually separated from the water surface. This theory (the so-called "droplet theory") proved useful for explaining the polarization and grazing angle dependence of σ_o, but failed when the frequency dependence was considered unless it was assumed that the drops were comparable in size to the transmitted wavelength. (Goldstein also pointed out that the polarization dependence was greatest in calm weather when the drops were least likely to occur.) In the opinion of many workers in this field, it is possible to retain the forward-scattering postulate without assuming that the scattering elements are drops. There is no reason

†To the extent that the reduction in sea clutter achieved by using horizontal polarization and large λ can be explained by the interference concept, these clutter-rejection techniques should be regarded as special cases of the ETI concept discussed in Sec. II-D. According to the interference concept, these techniques are effective in rejecting the clutter because they null-out targets at very small altitudes.

to believe that forward scattering does not play an important role even when the scattering elements are irregularities on the surface itself. A more serious problem, perhaps, independent of the scatterers' identity, is the assumption that the forward-scattered energy can be represented in the same way as for a surface which is smooth. This is obviously an extremely artificial assumption and, at best, represents only a very crude approximation. (In defense of this approximation, however, it should be noted that in most of the models which constitute serious attempts at constructing real physical theories, the question of multiple reflections is ignored entirely.)

In order to illustrate the application of this concept to the experimental data, assume that (a) the scatterers are statistically independent and statistically identical; (b) the scatterers are distributed uniformly over the illuminated area with a density η; (c) the earth-modification factor E and the cross section σ of a single scatterer are independent. Denoting the ensemble average by a bar and making use of Eq. (9) for E, one can show that

$$\sigma_0 = \sigma_0' \overline{|E|^2} \tag{46}$$

where

$$\sigma_0' = \eta \overline{|\sigma|^2}$$

$$\overline{|E|^2} = \overline{|1 + K \exp(-i\omega\tfrac{\Delta}{c})|^4}$$

$$= 1 + \overline{|K|^4} + 4\overline{|K|^2} + 2\mathrm{Re}\left[\overline{K^2 \exp(-2i\omega\tfrac{\Delta}{c})} + \overline{2K(1 + |K|^2)\exp(-i\omega\tfrac{\Delta}{c})}\right] .$$

Assuming furthermore that (d) K and Δ can be approximated by $K \approx \Gamma$ and $\Delta \approx 2\alpha H$ (H being the height of the scatterer), one can rewrite the equation for $\overline{|E|^2}$ as

$$\overline{|E|^2} = 1 + |\Gamma|^4 + 4|\Gamma|^2 + 2\mathrm{Re}\left[\Gamma^2 \overline{\exp(-4i\xi)} + 2\Gamma(1 + |\Gamma|^2)\overline{\exp(-2i\xi)}\right] \tag{47}$$

where $\xi = \omega\alpha H/c = 2\pi\alpha H/\lambda$ and the averaging operation applies to the variable H. Assume now that the set of probability density functions $\{p_\gamma(H)\}_\gamma$ on H corresponding to the set of sea conditions γ is a one-parameter family in which each member p_γ is determined by the mean value $\overline{H}$, and the higher order moments $\overline{H^n}$ are related to $\overline{H}$ by equations of the form $\overline{H^n} = B_n \overline{H}^n$ with B_n independent of γ. Then $\overline{|E|^2}$ will depend on λ, α, and γ only insofar as they determine the product $\bar{\xi} = 2\pi\alpha\overline{H}/\lambda$.† This dependence can be described explicitly by expanding $\exp(-4i\xi)$ and $\exp(-2i\xi)$ in power series, averaging each term with respect to H, and then replacing $\overline{H^n}$ by $B_n \overline{H}^n$. Assuming that $\bar{\xi}$ is small and that the scatterers are close to the surface with respect to variations in the interference pattern, one can approximate $\overline{|E|^2}$ by the first few terms of this series. Going to the other extreme and assuming that $\bar{\xi}$ is large and that the scatterer heights cover a number of lobes, one obtains $\overline{|E|^2} \approx 1 + |\Gamma|^4 + 4|\Gamma|^2$. Assuming that $\Gamma \approx -1$ (horizontal polarization), one has

†Note that the variable $\bar{\xi}$ is nothing more than the classical Rayleigh roughness parameter often used for deciding whether or not a surface is "rough."

$$\overline{|E|^2} = 6 + 2\,\overline{\cos 4\xi} - 8\,\overline{\cos 2\xi} \tag{48}$$

$$\overline{|E|^2} = 6 \qquad \text{when } \bar{\xi} \text{ is large}$$

$$\overline{|E|^2} = 16\,B_4\bar{\xi}^4 \qquad \text{when } \bar{\xi} \text{ is small}$$

$$\overline{|E|^2} = \frac{384\bar{\xi}^4}{(1 + 4\bar{\xi}^2)(1 + 16\bar{\xi}^2)}$$

$$\text{when } p_\zeta(H) = \frac{1}{\bar{H}} \exp\left(-\frac{H}{\bar{H}}\right) \qquad 0 \leqslant H \leqslant \infty \quad . \tag{49}$$

$$\overline{|E|^2} = 2\left[3 - 4\exp(-\pi\bar{\xi}^2) + \exp(-4\pi\bar{\xi}^2)\right]$$

$$\text{when } p_\zeta(H) = \frac{2}{\pi\bar{H}} \exp\left(-\frac{H^2}{\pi\bar{H}^2}\right) \qquad 0 \leqslant H \leqslant \infty \quad . \tag{50}$$

Returning to a general Γ for use in vertical polarization and assuming that $p_\zeta(H) = (1/\bar{H}) \exp(-H/\bar{H})$, $0 \leqslant H \leqslant \infty$, one obtains

$$\overline{|E|^2} = 1 + |\Gamma|^4 + 4|\Gamma|^2 + \frac{2|\Gamma|^2(\cos 2\varphi_\Gamma + 4\bar{\xi}\,\sin 2\varphi_\Gamma)}{1 + 16\bar{\xi}^2}$$

$$+ \frac{4|\Gamma|(1 + |\Gamma|^2)(\cos\varphi_\Gamma + 2\bar{\xi}\,\sin\varphi_\Gamma)}{1 + 4\bar{\xi}^2} \quad . \tag{51}$$

If attention is restricted to horizontal polarization and the variation of σ_o' with λ, α, and ζ is ignored, these results imply that σ_o is a function of $\bar{\xi} = 2\pi\alpha\bar{H}/\lambda$. For small $\bar{\xi}$, one obtains $\sigma_o \propto \bar{\xi}^4$. For large $\bar{\xi}$, one has $\sigma_o \propto \bar{\xi}^0$. These results are substantially consistent with the data except for (a) the behavior of σ_o above the critical angle α_2 and (b) the behavior of σ_o with λ and ζ above the critical angle α_1 before "saturation." In addition to these two major discrepancies, the first of which is important only if one is interested in grazing angles $\alpha \geqslant 20°$, one should also note that (c) whereas these results predict that $\alpha_1 \propto (\lambda/\bar{H})^n$, $n = 1$, the data indicate that n may be anywhere between 0 and 1, and (d) whereas these results predict that $\sigma_o \propto \alpha^n$, $n = 0$, for $\alpha > \alpha_1$, the data indicate that n may be anywhere between 0 and 2. In general, there are two attitudes which one may assume toward these discrepancies: one can conclude that these results are inappropriate or one can regard these discrepancies as constituting data on σ_o'. On the whole, those who have been concerned with this concept have assumed that the discrepancies constitute data on σ_o'.

In the discussion of the experimental data, $\sigma_o(\alpha)$ for $\alpha < \alpha_2$ was characterized by the plateau level σ_{oo} and the critical angle α_1. An equivalent characterization can be effected in terms of the interference concept by use of the parameters σ_o' and $\bar{H}$. In general, the most effective way of characterizing a $\sigma_o(\alpha)$ curve in terms of these parameters is to overlay the $\overline{|E|^2}$ curve and

to evaluate σ_o' and $\bar{H}$ by sliding the $\overline{|E|^2}$ curve along the abscissa and ordinate until one obtains a best fit. The results of applying this procedure [using Eq. (50)] to the data in Fig. 18 are shown on Fig. 18 by the smooth curves. (These fits are better than average.) Similar fits [using Eq. (49)] were obtained by Goldstein.[14] A slightly different technique, but one which constitutes an essentially equivalent test of the interference mechanism, has been employed by Katzin.[23] The values of σ_o' and $\bar{H}$ obtained from the fits shown in Fig. 18 are given by $\bar{H}(\lambda = 70\,cm) = 4.9\,ft$, $\bar{H}(\lambda = 10\,cm) = 2.4\,ft$, $\sigma_o'(\lambda = 70\,cm) = -52\,db$, and $\sigma_o'(\lambda = 10\,cm) = -44\,db$. Inasmuch as $\overline{|E|^2} \to 6$ for large $\bar{\xi}$, one finds that σ_o' is related to σ_{oo} by $\sigma_o' = \sigma_{oo}/6$. The relation of $\bar{H}$ to α_1 will depend on the precise definition of α_1. Defining the normalized critical angle $\bar{\xi}_1$ in the $\overline{|E|^2}$ curve by $\bar{\xi}_1 = 0.5$, one obtains $\alpha_1 = 0.08\lambda/\bar{H}$ (corresponding in Fig. 18 to $\log \alpha_1 = -1.4$ for the 70-cm curve and $\log \alpha_1 = -1.9$ for the 10-cm curve). In general, in the writer's experience, the values of $\bar{H}$ obtained from this fitting process are related to the reported wave height $\tilde{H}$ by the inequality $0.2 \leq \bar{H}/\tilde{H} \leq 2$. Inasmuch as the observed exponents in the relations $\alpha_1 \propto \lambda^n$ and $\alpha_1 \propto (1/\tilde{H})^n$ are sometimes less than unity, $\bar{H}$ will sometimes exhibit a small dependence on λ, increasing with an increase in λ, and the variation of $\bar{H}$ with $\tilde{H}$ will sometimes be less than linear. According to the model, one would expect that, in general, $\bar{H}$ would be correlated with the distribution of the heights of the large waves and the characteristics of the macrostructure, whereas σ_o' would be correlated with the state of the fine structure superimposed on these waves and with the momentary local wind conditions.

The theoretical curve in Fig 22, originally computed by Goldstein, is obtained from the above model by assuming that σ_o' is independent of polarization and computing the ratio $\sigma_o(vv)/\sigma_o(hh) = \overline{|E(vv)|^2}/\overline{|E(hh)|^2}$ as a function of $\bar{H}$ [using Eq. (51)]. Considering the scatter in the data, the fit is reasonably good. Although the values of $\bar{H}$ required to fit these data appear unreasonably small in comparison to the values of $\bar{H}$ obtained from the critical angle data, it should be noted that all values of the theoretical polarization ratio are approximately the same for $\bar{H} \geq 0.5\,ft$. Unfortunately, if one attempts to make the same sort of comparison using Macdonald's data, the results are not nearly so satisfying. Specifically, one finds that the values of $\bar{H}$ required to fit the polarization ratio data (a) increase with a decrease in grazing angle, (b) increase with an increase in wavelength, and (c) are, without question, considerably smaller than those required to fit the critical angle data on horizontal or vertical polarization taken alone. (The increase of $\bar{H}$ with λ obtained from these data appears to occur at approximately the same rate as the increase of $\bar{H}$ with λ obtained from the critical angle data.) The problem implied by the relative smallness of $\bar{H}$ and the increase of $\bar{H}$ with a decrease in grazing angle can be restated as follows: if the values of σ_o above the critical angle α_1 are the result of the scatterers being distributed over a whole lobe of the interference pattern so that the interference effect is averaged out, then why are the results on vertical polarization still greater than the results on horizontal polarization when the grazing angle is larger than the critical angles for both polarizations? If there is any difference at all between the two polarizations above the critical angles, the results on vertical polarization should be smaller. As far as the writer knows, these limitations in the interference concept for explaining the polarization-ratio data were first pointed out by Macdonald.

One further point concerning the interference concept involves its relation to the pulse-to-pulse fluctuation data. According to the interference assumption, one component in these fluctuations should arise from the Doppler beats between the direct and indirect rays. Inasmuch as

the rates of these beats will be proportional to α, these rates should be slow for small α and increase as α increases. Also, to the extent that the identity of the scatterers is independent of frequency, one would expect these rates to scale linearly with frequency. The results by Boring, et al.,[21] which indicate that the width of the slow fluctuation component is independent of frequency at small grazing angles implies that this source of fluctuations is relatively unimportant.

4. Facet Concept

In the three concepts mentioned above, no attention was paid to the problem of specifying the detailed reflective properties of the scatterers. Thus, the above concepts are, at best, only capable of providing a framework for interpreting the data. Some work on σ_o which takes account of the interference concept and goes on to consider a specific model for the scattering elements themselves is contained in the work of Katzin.[23] Assuming that the ocean can be regarded as a collection of flat plates (or "facets") of varying sizes and slopes, Katzin draws the following conclusions. At small grazing angles, where none of the facets are normal to the incoming wave, the facets which backscatter most effectively are those having a perimeter of about $\lambda/2$ and the backscattering of a facet increases about as the square of its slope (thus making the wave crests of special importance). At large grazing angles, the facets which backscatter most effectively are those which are normal to the incoming wave and which are large, the angular variation of σ_o' being determined primarily by the slope distribution of the facets. When the grazing angle is small, σ_o' is proportional to wind speed, but when the grazing angle is large, σ_o' is inversely proportional to wind speed. At small grazing angles, the frequency dependence of σ_o' is determined by the size distribution of the facets. As far as the writer knows, Katzin has examined the implications of this model only for the average power in the clutter signal. Some results relating the facet concept to irregularities actually occurring on water surfaces can be found in the papers by Schooley.[38]

5. Diffraction-Grating Concept

One further concept, based on the Doppler-image notion, which has proved extremely useful for interpreting the frequency shift in the coherent clutter spectrum at extremely low frequencies (13 to 25 Mcps) is the diffraction-grating concept first applied by Crombie[36] and later applied by Stutt, et al.[37] Assuming that the wave trains which will contribute most strongly to the clutter signal are those which are traveling toward or away from the radar and have a spacing L equal to one-half the electromagnetic wavelength λ, they have been able to predict the Doppler shift in the returned signal to a high degree of precision by use of the classical hydrodynamic formula $v = (gL/2\pi)^{1/2}$ relating the velocity v of a gravity wave to its wavelength l. (g being the acceleration due to gravity). According to this model, the Doppler beat frequency between the transmitted and received signals is given by $f = 2v/\lambda = (g/\pi\lambda)^{1/2}$. More recently, Ranzi[39] has shown that this concept is applicable to frequencies as high as 415 Mcps, but as one would expect, is not applicable at a frequency of 6800 Mcps.

C. Forward Scattering from the Ocean

According to the previous discussion, the radar designer needs to concern himself with the effects of surface roughness on forward scattering for two reasons: (1) in order to be able to

incorporate these effects into the earth-modification factor E needed for describing the signal returned from a target, and (2) in order to be able to incorporate these effects into various models used for describing the clutter signal (such as the "interference concept" described in Sec. III-B-3). Inasmuch as the height of a clutter backscatterer above the mean surface is orders of magnitude smaller than the height of an elevated aircraft target, the effects in the two cases may be radically different. Unfortunately, to the writer's knowledge, there are no data available which can be used with confidence in the clutter models. Aside from the usual difficulties encountered in scattering experiments, in this case one is faced with the additional problem of having to explore the scattered field at heights above the surface which are of the same order of magnitude as the heights of the irregularities themselves.

As far as the effects of surface roughness on the target signal are concerned, although a certain amount of relevant data exists, much of it suffers from the same sorts of inadequacies as one finds in the clutter data (e.g., inadequate specification of the sea surface). In addition, since most of the forward-scattering experiments employ only one-way propagation, to the extent that one is concerned with the radar problem and not the communication problem, one is faced with the further difficulty of having to convert the statistics of the one-way signal to those of the two-way signal. Although, theoretically, all the information which is needed for describing the two-way signal can be obtained from the statistics of the one-way signal, in actual practice, the amount of information available on the one-way signal is often insufficient for this purpose. For example, even if one assumes that the polarization of the antenna is pure-horizontal or pure-vertical, since the slope of the ocean surface is variable, in order to obtain sufficient information through a one-way experiment to describe the two-way signal, one will have to take data on all four polarization combinations hh, vv, hv, and vh.† In addition to this need for increased polarization information, one is also faced with a need for increased statistical information in the form of higher order moments. For example, in order to obtain the average value of the target signal, since the II path involves two reflections, data are required on the average value of the square of the reflection coefficient as well as on the average value of the reflection coefficient itself.

Aside from the problems encountered in trying to determine the two-way signal from the results of one-way experiments, the forward-scattering situation differs from the clutter situation in that, whereas the clutter problem can be treated as a random noise problem [see the "random-scatterer concept" (Sec. III-B-1)], the forward-scattering problem must be treated as a signal-plus-noise problem. Thus, in the forward-scattering case, the statistics tend to become more complicated.

Until the last few years, the usual means for describing the effects of roughness on the forward-scattered energy was to assume that this roughness could be accounted for by replacing the smooth surface reflection coefficient Γ by an "effective reflection coefficient" $\tilde{\Gamma}$ and evaluating $|\tilde{\Gamma}|$ by measuring the amplitude of adjacent maxima and minima in the interference pattern. Defining K by $K = R\Gamma g_r(I)g_t(I)/(R + \Delta)g_r(D)g_t(D)$, and $\tilde{K}$ by $\tilde{K} = (\tilde{\Gamma}/\Gamma)K$, one can

†C. I. Beard, in a private communication to the writer, has pointed out that an experiment by the University of Texas at X-band showed the cross-polarized components to be down from the similarly aligned components by more than 20 db. If this result is valid for all frequencies and all sea conditions, then one can probably ignore the cross-polarized components.

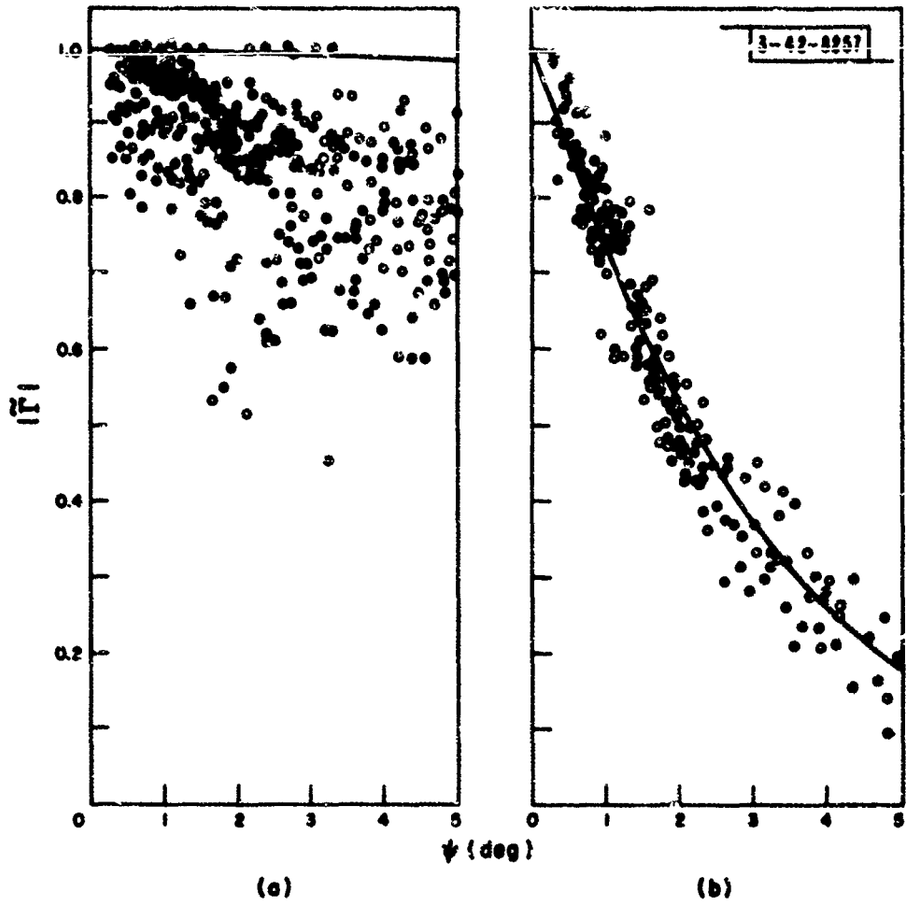

Fig.31. Amplitude of effective reflection coefficient. λ = 10 cm: (a) horizontal polarization, (b) vertical polarization. Curves are theoretical curves for a smooth sea. (After Kerr.[14])

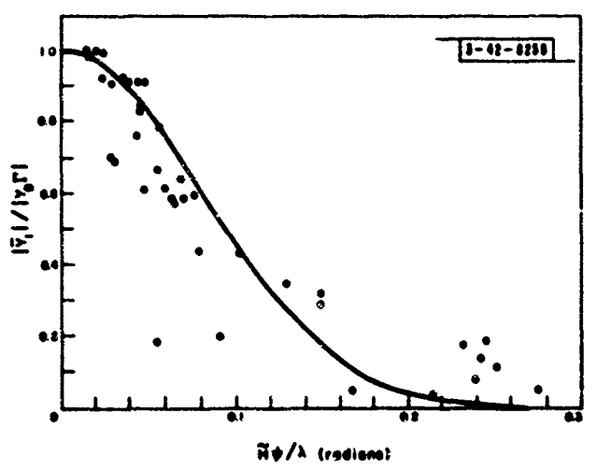

Fig. 32. Normalized coherent component. (After Beard.[40]) Curve is theoretical.

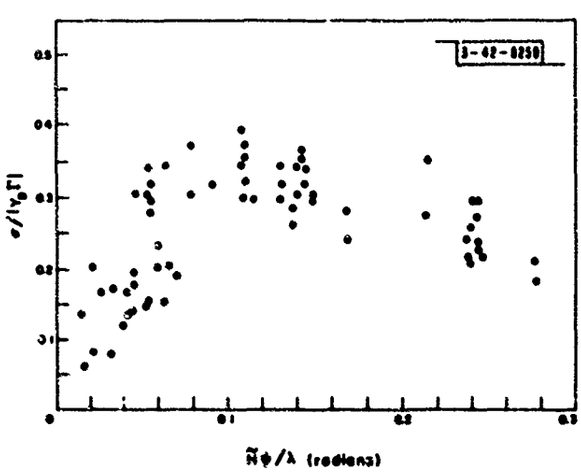

Fig. 33. Normalized incoherent component. (After Beard.[40])

evaluate $|\tilde{\Gamma}|$ from measurements of the one-way rough surface earth-modification factor $\tilde{E} = 1 + \tilde{K}\exp(-i\omega\Delta/c)$ by the equations $|\tilde{K}| = (|\tilde{E}|_{max} - |\tilde{E}|_{min})/(|\tilde{E}|_{max} + |\tilde{E}|_{min})$ and $|\tilde{\Gamma}| = |\Gamma||\tilde{K}|/|K|$. The results obtained in this manner show the following characteristics. For very smooth seas, the results on both horizontal and vertical polarization follow the smooth surface theory to within experimental error. As the sea becomes rougher, however, whereas the results on vertical polarization still cluster around the theoretical curve for a smooth surface and evidence only a mild degree of scatter, the results on horizontal polarization fall below the theoretical curve (i.e., below unity) and exhibit a high degree of scatter. A typical result illustrating these characteristics is shown in Fig. 31(a-b). For a summary of this earlier work, the reader is referred to Kerr.[14] Results similar to those shown in Fig. 31 have been obtained more recently by Macdonald for a wavelength of 24 cm (unpublished data).

In the last few years, substantial advances have been made in this field through the efforts of the Applied Physics Laboratory (APL) at Johns Hopkins University and the Electrical Engineering Research Laboratory (EERL) at the University of Texas. This work has been well summarized by Beard[40] and will be discussed here only briefly.

Let

Y_D = complex modulation of signal received along direct path
Y_I = complex modulation of forward-scattered signal
$Y_T = Y_D + Y_I$ = total received signal
$\bar{Y}_I$ = average value of Y_I
$2\sigma^2 = \overline{|Y_I - \bar{Y}_I|^2}$ = power in the fluctuations
$\tilde{H}$ = root-mean-square wave height
ψ = grazing angle
λ = transmitted wavelength.

The model used by APL and EERL for processing their data assumes that the components of the fluctuating signal $Y_I - \bar{Y}_I$ are statistically independent random variables with Gaussian density functions of mean zero and variance σ^2. (In other words, the statistics of the forward-scattered signal are assumed to be equivalent to those which would arise if one took the backscattered signal as described by the random-scatter concept mentioned in Sec. III-B-1 and added a sine wave.) The steady signal $\bar{Y}_I$ is referred to as the coherent component and the fluctuating signal $Y_I - \bar{Y}_I$ (assumed, like the clutter signal, to arise from a large number of independent random scatterers) is referred to as the incoherent component.

The results obtained on the normalized coherent and incoherent terms $|\bar{Y}_I|/|Y_D\Gamma|$ and $\sigma/|Y_D\Gamma|$ are shown in Figs. 32 and 33, respectively. These graphs contain data for both horizontal and vertical polarization and for wavelengths of 5.3, 3.2 and 0.9 cm. Some of these data were obtained by measuring the total field Y_T and extracting information on Y_I through the use of the maxima and minima in the interference pattern, and some by measuring the forward-scattered field Y_I directly through the use of antenna patterns with a high degree of vertical resolution. The distance between the transmitting and receiving antennas was 5425 ft and the range of values of $\tilde{H}$ encountered (obtained from step-gauge recordings) was 0.12 to 0.73 ft. The curve in Fig. 32 is the "classical" coherent theoretical curve

$$y = \exp(-8\pi^2\tilde{H}^2\psi^2/\lambda^2) \quad .$$

This curve is based on the assumption of a Gaussian distribution for the height of the water surface

and has been derived by many writers (some of whom are referred to in the paper by Beckmann[5]). It takes account merely of the phase differences in the indirect rays caused by variations in the height of the surface. (The more general results which have been obtained frequently include this result as a multiplicative factor.) Assuming that the data on the coherent term are obtained from a total field measurement, one sees that these data differ from those shown in Fig. 31 as follows: whereas in Fig. 31 the data were obtained by measuring $\overline{|Y_D + Y_I|}_{max}$ and $\overline{|Y_D + Y_I|}_{min}$, the data in Fig. 32 were obtained by measuring $|Y_D + \overline{Y}_I|_{max}$ and $|Y_D + \overline{Y}_I|_{min}$. Apparently, when the processing is done according to the latter procedure, the difference in the effects of roughness on the two polarizations tends to disappear.

One should also note the approximate equivalence of the following three angles: (1) the angle at which the theoretical coherent curve begins to fall below the coherent data; (2) the angle at which the experimental incoherent curve reaches its maximum; (3) the critical angle α_1 in the backscattering cross-section data (see Secs. III-A and -B). The equivalence of the first two angles led Beard to suggest that a common mechanism was responsible for the changes in behavior which occur at this angle in both the coherent and incoherent terms of the forward-scattered energy and that multiple reflections might be important. The equivalence of both these angles with the critical angle α_1 in the backscattering data, and the success of the interference concept in explaining this critical angle, lend strong support to this statement. Assuming that the independent-random-scatterer model is correct for both the incoherent forward-scattered energy and the backscattered energy (all of which is incoherent), one sees that the only difference between them should result from the angular variation in the power cross section of an individual scatterer. If one assumes that the interference concept can be applied to the incoherent forward-scattered energy in the same manner as it has been applied to the backscattered energy (i.e., assume the incoherent forward-scattered energy arises from a configuration consisting of random scatterers elevated above a smooth reflecting surface), then the data on the incoherent forward-scattered energy can be processed (after appropriate normalization) in exactly the same way as the data on the backscattered energy. The differences in the power cross section of an individual scatterer in the forward and backward directions will result in differences in the value of σ_0'.

One very surprising result obtained on the incoherent forward-scattered energy is that this energy, like the coherent energy, appears to come mainly from the first Fresnel zone. Inasmuch as the Fresnel zones are defined in terms of phase differences and the incoherent energy results form a random phase addition, this result constitutes a remarkable coincidence.

In addition to the data on $|\overline{Y}_I|$ and $|Y_I - \overline{Y}_I|^2$, this project also obtained considerable data on the power spectrum of the fluctuations in $|Y_T| = |Y_D + Y_I|$. Two important results obtained on this spectrum were (1) the spectrum was independent of polarization and (2) the spectrum was very closely correlated with the spectrum of the ocean waves.

For further details on this work, the reader is referred to the paper by Beard[40] and to the references cited in his paper.

IV. SPHERICAL-EARTH FORMULAS

In predicting or evaluating the performance of airborne radars, one is frequently faced with a problem in which the earth's curvature is a significant fact that cannot be ignored without introducing serious errors. It has often been assumed that just because the altitudes of the radar

and target are small with respect to the radius of the earth, this curvature is of minor importance and need not be considered. Actually, of course, no matter how small the altitudes are, there will always be a horizon, and the curvature will always be important in regions near that horizon.

A. Functions to be Computed

Assume that the energy scattered forward to the target can be represented by a single indirect ray reflected at the point of specular reflection. Let the variables h_1, h_2, R, M_1, M_2, d_1, d_2, r_1, r_2, h'_1, h'_2, β_1, β_2, γ_1, γ_2, δ, ψ, α, Θ_1, and Θ_2 be defined as in Fig. 34, and let $\Delta = M_1 + M_2 - R$, $r = r_1 + r_2$, $d = d_1 + d_2$, $\Theta = \Theta_1 + \Theta_2$, a = modified earth's radius, $\mathcal{D}$ = divergence, A = area of illumination, and R_o = horizon range. Assume also that the locations of the radar antenna and target are constrained to a fixed vertical plane and that their orientations are fixed. The variables which need to be evaluated in order to describe the total received signal are then R, Δ, β_1, γ_1, β_2, γ_2, ψ, $\mathcal{D}$, δ, α, A, and R_o. The first eight are needed in order to describe the target signal, the next three in order to describe the clutter signal, and the last in order to determine the range at which the geometric situation becomes degenerate. The two vertical-plane coordinate systems which are most frequently used for specifying the relative locations of the radar, target, and earth, and which serve as independent variables for this evaluation, are (h_1, h_2, d) or (h_1, h_2, R). Inasmuch as R and d are related by the relatively simple (a ' exact) formula

$$R^2 = (a + h_1)^2 + (a + h_2)^2 - 2(a + h_1)(a + h_2)\cos\left(\frac{d}{a}\right) \tag{52}$$

which of these coordinate systems is actually used for this purpose is of little importance. In

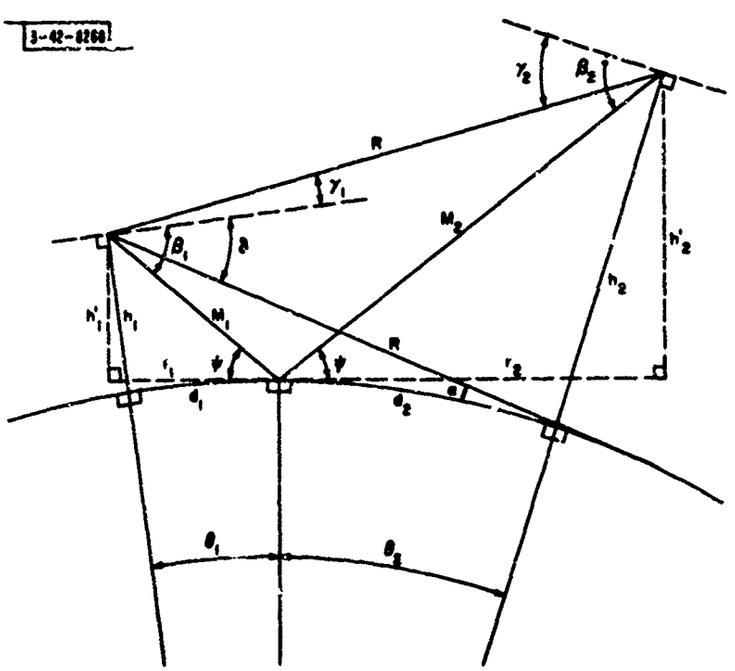

Fig. 34. Spherical-earth parameters.

addition to these functions, all of which are required in order to describe the received signal in terms of the relative locations of the radar, target, and earth, one may also need to evaluate certain functions in order to describe the location of a target in terms of the received signal. Two functions of potential interest in this category are the height-finding functions $h_2(h_1, \gamma_1, R)$ and $h_2(h_1, \Delta, R)$.

B. Functions $R_o(h_1, h_2)$, $\delta(h_1, R)$, $\alpha(h_1, R)$, $\gamma_1(h_1, h_2, R)$, and $A(h_1, R)$

The exact equations for these functions are as follows:

$$R_o(h_1, h_2) = (2ah_1 + h_1^2)^{1/2} + (2ah_2 + h_2^2)^{1/2} \tag{53}$$

$$\delta(h_1, R) = \sin^{-1}\left[\frac{h_1}{R} + \frac{R^2 - h_1^2}{2R(a + h_1)}\right] \tag{54}$$

$$\alpha(h_1, R) = \sin^{-1}\left[\frac{h_1}{R} - \frac{R^2 - h_1^2}{2Ra}\right] \tag{55}$$

$$\gamma_i(h_1, h_2, R) = (-1)^{i+1} \sin^{-1}\left[\frac{2(h_2 - h_1)a + h_2^2 - h_1^2 + (-1)^i R^2}{2R(a + h_1)}\right] \tag{56}$$

$$A(h_1, R) = \cos^{-1}\left[1 - \left(\frac{1 - \cos\Theta}{\cos^2\delta}\right)\right]\left(\frac{a}{a + h_1}\right)\left(\frac{RcT}{2} + \frac{c^2T^2}{8}\right) . \tag{57}$$

In this last equation, Θ denotes the horizontal beamwidth of the antenna in the direction of the clutter, c denotes the velocity of light, and T denotes the transmitted pulselength. This equation assumes that A is defined by the pulselength rather than the vertical beamwidth and that the illuminated region consists of a section of a lune. The first factor is the projection of Θ on the surface of the earth.

For many purposes, Eqs. (53) to (57) can be replaced by the following approximations:

$$R_o(h_1, h_2) = (2ah_1)^{1/2} + (2ah_2)^{1/2} \qquad h_i/a \text{ small} \tag{58}$$

$$\delta(h_1, R) = \frac{h_1}{R}\left(1 + \frac{R^2}{2ah_1}\right) \qquad h_1/a\ ,\ h_1/R \text{ small} \tag{59}$$

$$\alpha(h_1, R) = \frac{h_1}{R}\left(1 - \frac{R^2}{2ah_1}\right) \qquad h_1/a\ ,\ h_1/R \text{ small} \tag{60}$$

$$\gamma_i(h_1, h_2, R) = (-1)^{i+1}\left(\frac{h_2 - h_1}{R}\right)\left[1 + \frac{(-1)^i R^2}{2a(h_2 - h_1)}\right] \qquad h_i/a\ ,\ |h_2^2 - h_1^2|/R^2 \text{ small} \tag{61}$$

$$A(h_1, R) = R\Theta\,\frac{cT}{2}\sec\alpha \qquad h_1/a\ ,\ R/a\ ,\ cT/4R,\ \Theta,\ \alpha \text{ small} . \tag{62}$$

C. Functions $\Delta(h_1, h_2, R)$, $\psi(h_1, h_2, R)$, $\beta_i(h_1, h_2, R)$, and $\mathfrak{D}(h_1, h_2, R)$

These functions, all of which involve the indirect ray to the target, are much more difficult to compute than those considered in Sec. IV-B. A number of approaches to these functions will be considered.

1. Exact Equations

Letting $B_i = 1 + \frac{h_i}{a}$ and $C_i = (a^2 \sin^2\psi + 2ah_i + h_i^2)^{1/2}$, one can derive the following exact equations:

$$d_i = a\Theta_i \qquad d = a\Theta \tag{63}$$

$$h_i' = (a + h_i)\cos\Theta_i - a \tag{64}$$

$$r_i = (a + h_i)\sin\Theta_i \tag{65}$$

$$M_i = (r_i^2 + h_i'^2)^{1/2} \tag{66}$$

$$\Delta = [r^2 + (h_1' + h_2')^2]^{1/2} - [r^2 + (h_1' - h_2')^2]^{1/2} \tag{67}$$

$$\psi = \tan^{-1}\left(\frac{h_i'}{r_i}\right) = \tan^{-1}\left(\frac{h_1' + h_2'}{r}\right) \tag{68}$$

$$\beta_i = \Theta_i + \psi \tag{69}$$

$$\mathfrak{D} = \left\{\frac{(a + h_1)(a + h_2)\sin\Theta}{a(M_1 + M_2)\cos\psi}\left[1 + \frac{2M_1M_2}{a(M_1 + M_2)\sin\psi}\right]\right\}^{-1/2} \tag{70}$$

$$\begin{aligned} &4B_1^2B_2^2\cos^4\Theta_1 - (4B_1B_2^2 + 4B_1^2B_2\cos\Theta)\cos^3\Theta_1 + (B_1^2 + B_2^2 + 2B_1B_2\cos\Theta \\ &\quad -4B_1^2B_2^2)\cos^2\Theta_1 + (4B_1B_2^2\cos^2\Theta + 2B_1B_2^2\sin^2\Theta + 4B_1^2B_2\cos\Theta)\cos\Theta_1 \\ &\quad + (B_1^2B_2^2\sin^2\Theta - B_2^2\cos^2\Theta - B_1^2 - 2B_1B_2\cos\Theta) = 0 \end{aligned} \tag{71}$$

$$\Theta_2 = \cos^{-1}\left\{\frac{B_1^2\sin^2\Theta_1 + (B_1\cos\Theta_1 - 1)[B_2^2(B_1^2 + 1 - 2B_1\cos\Theta_1) - B_1^2\sin^2\Theta_1]^{1/2}}{B_2(B_1^2 + 1 - 2B_1\cos\Theta_1)}\right\} \tag{72}$$

$$M_i = C_i - a\sin\psi \tag{73}$$

$$\beta_i = \sin^{-1}\left(\frac{C_i}{a + h_i}\right) \tag{74}$$

$$R = (M_1^2 + M_2^2 + 2M_1M_2\cos 2\psi)^{1/2} \tag{75}$$

$$\tan\Theta_i = \frac{h_i'r}{(h_1' + h_2')(a + h_i')} \tag{76}$$

Equations (52) and (63) to (71) are sufficient to compute Δ, ψ, β_i, and $\mathfrak{D}$ to any desired accuracy. Starting with h_1, h_2, and R, one must solve (52) for d, $d = a\Theta$ for Θ, (71) for Θ_1, $\Theta = \Theta_1 + \Theta_2$ for Θ_2, (64) to (66) for h_i', r_i, and M_i, $r = r_1 + r_2$ for r, and finally, (67) to (70) for Δ, ψ, β_i, and $\mathfrak{D}$. In general, this procedure will be very laborious since (71) is a quartic in $\cos\Theta_1$. A much simpler procedure which can be used if one does not need to evaluate Δ, ψ, β_i, and $\mathfrak{D}$ at a specific point (h_1, h_2, R) but only to plot a curve of these functions for variable (h_1, h_2, R), is to start off by choosing (h_1, h_2, Θ_1), compute Θ_2 by (72), Θ by $\Theta = \Theta_1 + \Theta_2$, d by $d = a\Theta$, R by (52), and then continue as before. A second such method, based on the parameter ψ, is to begin by choosing (h_1, h_2, ψ), compute M_i, β_i, and R by (73) to (75), Δ by $\Delta = M_1 + M_2 - R$, d by (52), Θ by $d = a\Theta$, and $\mathfrak{D}$ by (70).

2. Approximations Based on Cubic in d_1

Assuming that h_i/a, d_i/a, and h_i/d_i are small, one can replace Eqs. (52), (64) to (68), and (70) to (72) by

$$R = d \tag{77}$$

$$h_i' = h_i - \frac{d_i^2}{2a} \tag{78}$$

$$r_i = d_i \tag{79}$$

$$M_i = d_i \tag{80}$$

$$\Delta = \frac{2h_1h_2}{d}\left(1 - \frac{d_1^2}{2ah_1}\right)\left(1 - \frac{d_2^2}{2ah_2}\right) \tag{81}$$

$$\psi = \tan^{-1}\left(\frac{h_i}{d_i} - \frac{d_i}{2a}\right)$$

$$= \tan^{-1}\left[\frac{h_1 + h_2}{d}\left[1 - \frac{d_1^2 + d_2^2}{2a(h_1 + h_2)}\right]\right] \tag{82}$$

$$\mathfrak{D} = \left(1 + \frac{2d_1d_2}{ad\psi}\right)^{-1/2} \tag{83}$$

$$2d_1^3 - 3dd_1^2 + (d^2 - 2ah_1 - 2ah_2)\,d_1 + 2ah_1\,d = 0 \tag{84}$$

$$d_2 = \frac{d_1^2 - 2ah_1}{2d_1} + \left[\frac{(d_1^2 - 2ah_1)^2}{4d_1^2} + 2ah_2\right]^{1/2} . \tag{85}$$

If $h_1 \geq h_2$, Eq. (84) has the solution

$$d_1 = \frac{d}{2} - p\cos\left(\frac{\varphi + \pi}{3}\right) \tag{86}$$

where

$$p = \frac{2}{3^{1/2}}\left[a(h_1 + h_2) + \left(\frac{d}{2}\right)^2\right]^{1/2}$$

$$\varphi = \cos^{-1}\left[\frac{2ad(h_2 - h_1)}{p^3}\right] \quad .$$

In the remaining discussion, whenever an equation based on (84) is considered, it will be assumed that $h_1 \geq h_2$. When $h_1 < h_2$, the appropriate equations can be derived by interchanging 1 and 2.

These approximations are essentially the same as those used at the Radiation Laboratory, and a considerable amount of work has been done with them by many people. (See, for example, Fishback in Kerr[14] and, also, Burrows and Attwood.[41]) Not only have a number of transformations been found which normalize the variables in such a way that the amount of computing is considerably reduced, but much of this computing has already been done and is available in graphical form. For example, Burrows and Attwood have used the transformation

$$b = (d_1 - d_2)/(d_1 + d_2) \tag{87}$$

$$c = (h_1 - h_2)/(h_1 + h_2) \tag{88}$$

$$m = d^2/4a(h_1 + h_2) \tag{89}$$

to transform (84) into the simple cubic

$$c = b + bm(1 - b^2) \tag{90}$$

and have plotted a graph relating b, m, and c (see Fig. 35). The curved contour on the right side of this graph is determined by the horizon and represents the intersection of $c = b + bm(1 - b^2)$ and $c = 2mb$. In order to compute Δ, ϕ, β_1, and $\mathfrak{D}$, one now need only to compute m and c by Eqs. (88) and (89), obtain b from Fig. (35), obtain d_1 and d_2 by Eq. (87) and $d = d_1 + d_2$, obtain Δ, ϕ, and $\mathfrak{D}$ by (81), (82), and (83), and obtain β_i by $d_i = a\Theta_i$ and (69). All these operations can be performed quite rapidly. Burrows and Attwood have also used the transformation

$$s = \frac{d_1}{d} \qquad u = \frac{h_2}{h_1} \qquad v = \frac{d}{(2ah_1)^{1/2}}$$

and have plotted graphs of $s(u, v)$, $\Delta(u, v)$, and $\mathfrak{D}(u, v)$. Fishback, on the other hand, has used the transformation

$$T = \left(\frac{h_2}{h_1}\right)^{1/2} \qquad S = \frac{d}{(2ah_1)^{1/2} + (2ah_2)^{1/2}} \qquad S_i = \frac{d_i}{(2ah_i)^{1/2}} \quad . \tag{91}$$

Letting

$$J(S, T) = (1 - S_1^2)(1 - S_2^2) \tag{92}$$

$$K(S, T) = \frac{[1 - S_1^2 + T^2(1 - S_2^2)]}{1 + T^2} \tag{93}$$

one can rewrite Eqs. (81), (82), and (83) as

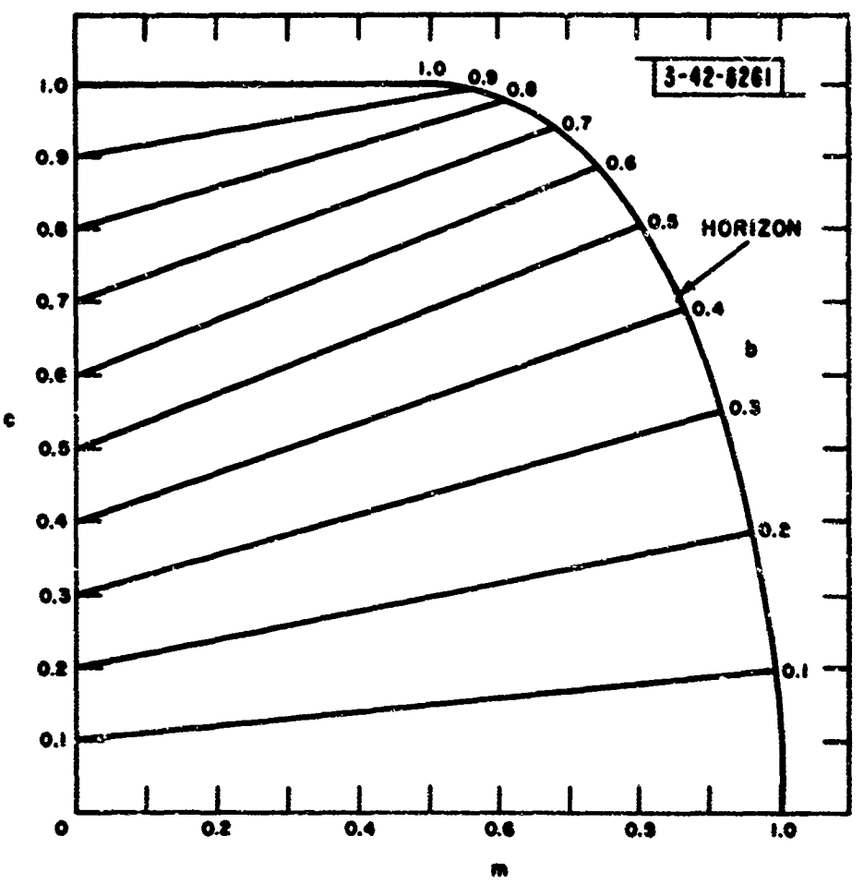

Fig.35. Graphical solution of cubic. (After Burrows and Attwood.[41])

$$\Delta = \frac{2h_1h_2}{d} J(S, T) \tag{94}$$

$$\phi = \tan^{-1}\left[\frac{h_1 + h_2}{d} K(S, T)\right] \tag{95}$$

$$\mathfrak{D} = \left[1 + \frac{4S_1^2S_2T}{S(1 - S_1^2)(1 + T)}\right]^{-1/2} \tag{96}$$

Graphs of J(S, T), K(S, T), and $\mathfrak{D}$(S, T) are available both in Kerr[14] and in Fishback.[42]

3. Approximations for Small h_2/h_1

Another set of approximations to Δ, ϕ, β_1, and $\mathfrak{D}$ which is of use when considering targets very close to the surface is the following. Assume that h_1/a, d_1/a, h_1/d_1, and h_2/h_1 are small. Then

$$\phi = \alpha = \beta_2 = \frac{h_1}{R}\left(1 - \frac{R^2}{2ah_1}\right) \tag{97}$$

$$\beta_1 = \delta = \frac{h_1}{R}\left(1 + \frac{R^2}{2ah_1}\right) \tag{98}$$

$$d_2 = -\alpha a + (\alpha^2 a^2 + 2ah_2)^{1/2} \tag{99}$$

$$\Delta = 2\alpha\left(h_2 - \frac{d_2^2}{2a}\right) \tag{100}$$

$$\mathfrak{D} = \left(1 + \frac{2d_2}{a\alpha}\right)^{1/2} . \tag{101}$$

In the event that $h_2 \ll \alpha^2 a$, then d_2 reduces to $d_2 = h_2/\alpha$, and Δ and $\mathfrak{D}$ can be approximated by $\Delta = 2\alpha h_2$ and $\mathfrak{D} = 1$.

4. Series Expansion of h_i' in r/a

One further method for approximating these functions is based on the expansion of h_i' in the variable r/a:

$$h_i' = \sum_{n=0}^{\infty} a_n^{(i)}(h_1, h_2, a)\left(\frac{r}{a}\right)^n .$$

Assuming h_i/a is small, replacing $\cos\theta_i$ by $(1 + \tan^2\theta_i)^{-1/2}$ in (64), expanding $(1 + \tan^2\theta_i)^{-1/2}$ in a power series in $\tan^2\theta_i$, and applying (76) to eliminate $\tan\theta_i$, one is lead to the expression

$$h_i' = h_i - \frac{a}{2}\left(\frac{h_i'}{h_1'^2 + h_2'^2}\right)^2\left(\frac{r}{a}\right)^2 + \frac{3}{8}a\left(\frac{h_i'}{h_1'^2 + h_2'^2}\right)^4\left(\frac{r}{a}\right)^4 + \cdots . \tag{102}$$

Replacing h_i' on both sides of this expression by the above series and computing the first five coefficients $a_n^{(i)}$, one obtains the approximation

$$h_i' = h_i \left[1 - \frac{h_i r^2}{2a(h_1 + h_2)^2} - \frac{[h_1^2 + h_2^2 - h_i(h_1 + h_2)]\, h_i r^4}{2a^2(h_1 + h_2)^5} \right] . \tag{103}$$

The closer one comes to the horizon, the more terms that will be needed for a given degree of accuracy. The corresponding approximations to $\tan\phi$ and $\cos\Theta_i$ [using (64) and (68)] are given by

$$\cos\Theta_i = 1 - \frac{h_i^2 r^2}{2a^2(h_1 + h_2)^2} - \frac{[h_1^2 + h_2^2 - h_i(h_1 + h_2)]\, h_i^2 r^4}{2a^3(h_1 + h_2)^5} \tag{104}$$

$$\tan\phi = \frac{h_1 + h_2}{r} \left[1 - \frac{(h_1^2 + h_2^2)\, r^2}{2a(h_1 + h_2)^3} + \frac{h_1 h_2 (h_1 - h_2)^2 r^4}{2a^2(h_1 + h_2)^6} \right] . \tag{105}$$

If $(h_1' + h_2')/r$ is small so that (67) can be replaced by $\Delta = 2h_1'h_2'/r$, Δ can be written

$$\Delta = \frac{2h_1 h_2}{r} \left[1 - \frac{r^2}{2a(h_1 + h_2)} + \frac{h_1 h_2 r^4}{4a^2(h_1 + h_2)^4} \right] . \tag{106}$$

Expressions for other variables can be derived similarly.

5. Approximations for Small ϕ

Using Eqs. (73), (75), and $\Delta = M_1 + M_2 - R$, and assuming that ϕ and $|(C_1 - C_2)\tan\phi|/(C_1 + C_2 - 2a\sin\phi)$ are small, one can approximate R and Δ by

$$R = C_1 + C_2 - 2a\phi \tag{107}$$

$$\Delta = (R\phi^2/2)\,[1 - (C_1 - C_2)^2/R^2] . \tag{108}$$

If, in addition, h_i/a and $\phi^2 a/h_i$ are small, then

$$R = (2ah_1)^{1/2} + (2ah_2)^{1/2} - 2a\phi + (a^2\phi^2/2)\,[(2ah_1)^{-1/2} + (2ah_2)^{-1/2}] \tag{109}$$

$$\Delta = \frac{R\,[(2ah_1)^{1/2} + (2ah_2)^{1/2} - R]^2}{8a^2} \left\{ 1 - \left[\frac{(2ah_1)^{1/2} - (2ah_2)^{1/2}}{R} \right]^2 \right\} . \tag{110}$$

Equations (107) and (108) are accurate over a wide range of interest. Equations (109) and (110) are of use only in regions extremely close to the horizon.

D. Functions $h_2(h_1, \gamma_1, R)$ and $h_2(h_1, \Delta, R)$

1. $h_2(h_1, \gamma_1, R)$

The exact equation for this function is given by

$$h_2 = -a + [(a + h_1)^2 + R^2 + 2R(a + h_1)\sin\gamma_1]^{1/2} . \tag{111}$$

If h_1/a, h_1/R and $[R^2 + 2a(h_1 + R\sin\gamma_1)]/a^2$ are small, then

$$h_2 = h_1 + R\sin\gamma_1 + R^2/2a . \tag{112}$$

2. $h_2(h_1, \Delta, R)$

Referring to the transformation (91) and defining S' by $S' = d/(2a h_1)^{1/2}$, one has $S = S'/(1 + T)$. Thus, $N = T^2 J(S, T) = \Delta d/2h_1^2$ can be regarded as a function of S' and T. Since h_1, Δ, and d determine N and S', the problem of determining $h_2(h_1, \Delta, R)$ is equivalent to solving N(S', T) for T. A graphical solution of N(S', T) is available in Fishback[42]

Another method for determining $h_2(h_1, \Delta, R)$ has been derived by McCracken.[43] Substituting $h_2 = \sum_{n=0}^{\infty} a_n a^{-n}$ into (106) and evaluating the coefficients a_n, one obtains the approximation

$$h_2 = \frac{r\Delta}{2h_1}\left[1 + \frac{r^2}{2a\left(h_1 + \frac{r\Delta}{2h_1}\right)} + \frac{h_1^2 r^4}{4a^2\left(h_1 + \frac{r\Delta}{2h_1}\right)^4}\right] . \qquad (113)$$

For a more comprehensive discussion of spherical-earth formulas, the reader is referred to the report by Durlach, et al.[44] This report contains additional exact equations, additional approximations, detailed graphical comparisons of the approximations with the exact equations, and finally, a large number of graphs computed by use of the exact equations.

ACKNOWLEDGMENT

In writing this report, the author has received the help of many people. In particular, the writer wishes to express his thanks to E.J. Kelly, Jr., of Lincoln Laboratory for the many hours spent in discussing various topics covered in this report and for his help in clarifying many of the important ideas. Useful conversations were also had with F.C. Macdonald of the Naval Research Laboratory; R. Manasse of the MITRE Corporation; M.A. Herlin, D.H. Lyons, J.W. McGinn, E.W. Pike, and J.A. Sheahan of Lincoln Laboratory. Considerable assistance was also obtained from Mrs. A.M. Carpenter, Miss J.H. Dinsmore, and Mrs. D.A. Hallé of Lincoln Laboratory in the preparation of figures and in the collection of source material.

REFERENCES

1. H.R. Reed and C.M. Russell, Ultra High Frequency Propagation (Wiley, New York, 1953).
2. J.A. Stratton, Electromagnetic Theory (McGraw-Hill, New York, 1941).
3. H. Bremmer, Terrestrial Radio Waves (Elsevier, New York, 1949).
4. S.A. Schelkunoff and H.T. Friis, Antennas: Theory and Practice (Wiley, New York, 1952).
5. P. Beckmann, "A New Approach to the Problem of Reflection from a Rough Surface," Acta Technica, No. 4, 311 (1957).
6. M. Katzin, E.A. Wolff and J.C. Katzin, "Investigations of Ground Clutter and Ground Scattering," Final Report ERC-CRC-5198-4, Electromagnetic Research Corporation, Washington, D.C. (15 March 1960).
7. S. Applebaum and P.W. Howells, "Waveform Design for Tomorrows Radars," Space/Aeronautics 32, 186 (October 1959).
8. E.C. Westerfield, R.H. Prager and J.L. Stewart, "Processing Gains Against Reverberation (Clutter) Using Matched Filters," Trans. IRE IT-6, 342 (June 1960).
9. E.N. Fowle, E.J. Kelly, Jr., and J.A. Sheehan, "Radar System Performance in a Dense-Target Environment," IRE Internat. Conv. Record 9, Part 4, 136 (March 1961).
10. B.M. Dwork, "Detection of a Pulse Superimposed on Fluctuation Noise," Proc. IRE 38, 771 (July 1950).
11. H. Urkowitz, "Filters for Detection of Small Radar Signals in Clutter," J. Appl. Phys. 24, No. 8, 1024 (August 1953).
12. R. Manasse, "The Use of Pulse Coding to Discriminate Against Clutter," G-Report 312-12 (Rev. 1), Lincoln Laboratory, M.I.T. (7 June 1961), DDC 260230, H-320.
13. See, for example, H. Lamb, Hydrodynamics (Cambridge University Press, London, 1932); "Gravity Waves," U.S. National Bureau of Standards Circular 521, (1952); "Manual on Amphibious Oceanography," Waves Investigations Group, Institute of Engineering Research, University of California (1952); U.S. Navy Hydrographic Office Publications, Nos. 601, 603, and 604; Journals of Opt. Soc. Am., Marine Res., Geophys. Res., and Fluid Mech.; Proceedings of the Conference on Ocean Wave Spectra (Prentice-Hall, New Jersey, 1963), conference sponsored by the Natl. Acad. of Sci. (1961).
14. D.E. Kerr, ed., Propagation of Short Radio Waves, Radiation Laboratory Series, M.I.T. (McGraw-Hill, New York, 1951), Vol. 13.
15. H. Goldstein, "Frequency Dependence of the Properties of Sea Echo," Phys. Rev. 70, 938 (December 1946).
16. _____, "A Primer of Sea Echo," Report 157, U.S. Naval Electronics Laboratory, San Diego, California (August 1950).
17. Unpublished data at Lincoln Laboratory.
18. T. Gold and W. Renwick, "Wave-Clutter Experiments, Seaford," A.S.E. Technical Note RXC9/46/8, Admiralty Surface Weapons Establishment, England (August 1946).
19. G.J.R. MacLusky and H. Davies, "The Dependence of Sea Clutter on Angle of Elevation Together with a Brief Note on the Rates of Fluctuation," TRE-T-1956, M/107/HD, Telecommunications Research Establishment, Malvern, England (26 November 1945).
20. F.C. Macdonald, "The Correlation of Radar Sea Clutter on Vertical and Horizontal Polarization with Wave Height and Slope," IRE Conv. Record 4, Part 1, 29 (1956).
21. J.G. Boring, E.R. Flynt, M.W. Long and V.R. Widerquist, "Sea Return Study," Final Report, Project No. 157-96, Engineering Experiment Station, Georgia Institute of Technology (August 1957).

22. H. Davies and G.G. Macfarlane, "Radar Echoes from the Sea Surface at Centimeter Wave-Lengths," Proc. Phys. Soc. 58, No. 11, 717 (November 1946).

23. M. Katzin, "On the Mechanisms of Radar Sea Clutter," Proc. IRE 45, 44 (January 1957).

24. C.R. Grant and B.S. Yaplee, "Back-Scattering from Water and Land at Centimeter and Millimeter Wavelengths," Proc. IRE 45, 976 (July 1957).

25. J.C. Wiltse, S.P. Schlesinger and C.M. Johnson, "Back-Scattering Characteristics of the Sea in the Region from 10 to 50 KMC," Proc. IRE 45, 220 (February 1957).

26. J.J. Kovaly, G.S. Newell, W.C. Prothe and C.W. Sherwin, "Sea Clutter Studies Using Airborne Coherent Radar II," Report R-37, Coordinated Science Laboratory, University of Illinois (June 1953).

27. B.L. Hicks, N. Knable, J.J. Kovaly, G.S. Newell, J.P. Ruina and C.W. Sherwin, "The Spectrum of X-Band Radiation Backscattered from the Sea Surface," J. Geophys. Res. 65, 825 (March 1960).

28. W.S. Ament, J.A. Burkett, F.C. Macdonald and D.L. Ringwalt, "Characteristics of Sea Clutter: Observations at 220 MC," NRL Report 5218, U.S. Naval Research Laboratory, Washington, D.C. (November 1958).

29. F.C. Macdonald, "Characteristics of Radar Sea Clutter: Part I – Persistent Target-Like Echoes in Sea Clutter," NRL Report 4902, U.S. Naval Research Laboratory, Washington, D.C. (March 1957).

30. J.L. Lawson and G.E. Uhlenbeck, eds., Threshold Signals, Radiation Laboratory Series, M.I.T. (McGraw-Hill, New York, 1950), Vol. 24.

31. E.J. Kelly and E.C. Lerner, "A Mathematical Model for the Radar Echo from a Random Collection of Scatterers," Technical Report 123, Lincoln Laboratory, M.I.T. (15 June 1956), DDC 120260.

32. J.W. McGinn and W.E. Pike, "A Study of Sea Clutter Spectra," in Statistical Methods in Radio Wave Propagation, W.C. Hoffman, ed. (Pergamon Press, London, 1960).

33. H. Cramér, Mathematical Methods of Statistics (Princeton University Press, Princeton, N.J., 1951).

34. W.B. Davenport, Jr., and W.L. Root, An Introduction to the Theory of Random Signals and Noise, Lincoln Laboratory Publications (McGraw-Hill, New York, 1958).

35. J.S. Bendat, Principles and Applications of Random Noise Theory (Wiley, New York, 1958).

36. D.D. Crombie, "Doppler Spectrum of Sea Echo at 13.56 Mc/s," Nature 175, 681 (April 1955).

37. C.A. Stutt, S.J. Fricker, R.P. Ingalls and M.L. Stone, "Preliminary Report on Ground-Wave-Radar Sea Clutter," Technical Report 134, Lincoln Laboratory, M.I.T. (21 September 1956), DDC 110004.

38. A.H. Schooley, "Relationship between Surface Slope, Average Facet Size, and Flatness Tolerance of a Wind-Disturbed Water Surface," J. Geophys. Res. 66, 157 (January 1961); and "Upwind-Downwind Ratio of Radar Return Calculated from Facet Size Statistics of a Wind-Disturbed Water Surface," Proc. IRE 50, No. 4, Part 1, 456 (April 1962).

39. I. Ranzi, "Experiments on Backscatter of H.F. Radiowaves from Open and Coastal Sea," Scientific Note No. 3 (1 March 1961), and "Doppler Frequency Shift of H.F. to S.H.F. Radio Waves Returned from the Sea," Technical Note No. 6 (15 September 1961), Contract AF 61(052)-139, Centro Radioelettrico Sperimentale "G. Marconi," Rome, Italy.

40. C.I. Beard, "Coherent and Incoherent Scattering of Microwaves from the Ocean," Trans. IRE AP-9, No. 5, 470 (September 1961).

41. C.R. Burrows and S.S. Attwood, Eds., Radio Wave Propagation, Consolidated Summary of the Committee on Propagation of the National Defense Research Committee (Academic Press, New York, 1949).

42. W.T. Fishback, "Simplified Methods of Field Intensity Calculations in the Interference Region," Report 461, Radiation Laboratory, M.I.T. (December 1943).

43. L.G. McCracken, "Height-Finding Radars Based on the Image Principle," Parts II and III, NRL Reports 5062 and 5063, U.S. Naval Research Laboratory, Washington, D.C. (January 1958).

44. N. Durlach, A. Carpenter and M.A. Herlin, "Curved-Earth Computations for Airborne Early Warning and Control," Technical Report 194, Lincoln Laboratory, M.I.T. (13 January 1959), DDC 210005.

DOCUMENT CONTROL DATA - R&D

(Security classification of title, body of abstract and indexing annotation must be entered when the overall report is classified)

1. ORIGINATING ACTIVITY (Corporate author) Lincoln Laboratory, M.I.T.	2a. REPORT SECURITY CLASSIFICATION Unclassified 2b. GROUP None

3. REPORT TITLE

Influence of the Earth's Surface on Radar

4. DESCRIPTIVE NOTES (Type of report and inclusive dates)

Technical Report

5. AUTHOR(S) (Last name, first name, initial)

Durlach, Nathaniel I.

6. REPORT DATE	7a. TOTAL NO. OF PAGES	7b. NO. OF REFS
18 January 1965	76	44

8a. CONTRACT OR GRANT NO. AF 19(628)-500 b. PROJECT NO. 649L c. d.	9a. ORIGINATOR'S REPORT NUMBER(S) Technical Report 373 9b. OTHER REPORT NO(S) (Any other numbers that may be assigned this report) ESD-TDR-65-32

10. AVAILABILITY/LIMITATION NOTICES

None

11. SUPPLEMENTARY NOTES	12. SPONSORING MILITARY ACTIVITY
None	Air Force Systems Command, USAF

13. ABSTRACT

This report provides radar designers with background information on how the idealized free-space radar theory must be modified to take account of reflections from the earth's surface. It is primarily concerned with problems that arise in designing systems that are airborne and contains discussions of the following topics: effects of reflections from the earth on the signal received from an elevated target, implications of these effects for detection and parameter estimation, effects of surface roughness, techniques for the reduction of clutter, scattering from the ocean, and spherical-earth geometry.

14. KEY WORDS

airborne-radar design
clutter rejection
earth reflections
geometry